Title
Effects of Design Factors and Microenvironment on Mesenchymal Stem Cells and Nucleus Pulposus Cells for Intervertebral Disc Tissue Engineering

Author
Ouyang, Ann

Publication Date
2017

Peer reviewed|Thesis/dissertation

Effects of Design Factors and Microenvironment on Mesenchymal Stem Cells and Nucleus Pulposus Cells for Intervertebral Disc Tissue Engineering

by

Ann Ouyang

DISSERTATION

Submitted in partial satisfaction of the requirements for the degree of

DOCTOR OF PHILOSOPHY

in

Bioengineering

in the

GRADUATE DIVISION

of the

UNIVERSITY OF CALIFORNIA, SAN FRANCISCO

AND

UNIVERSITY OF CALIFORNIA, BERKELEY

Acknowledgements

I would like to thank everyone who contributed to this work and my graduate school (and life!) experience. First and foremost is my advisor Jeffrey Lotz, who created a welcoming lab environment, provided encouragement and guidance, and helped me to become a more independent scientist. Jeff's support for scientific exploration and new ideas helped me to take my research in unexpected and interesting directions.

Thanks also to my other committee members, including Grace O'Connell, who always has excellent scientific and life advice, Ralph Marcucio, whose curiosity is irresistibly contagious, Zev Gartner, who is a master of scientific storytelling, and Tamara Alliston, who always makes time for even the most minor questions and is an all-around amazing role model. I would especially like to thank Tamara and Rich Schneider, other members of our small Orthosurg research pod, for their dedication to helping the lab run smoothly and for being there when equipment and experiments needed their expert advice. I'd also like to thank Aaron Fields, who has been an inspiring mentor and collaborator, and SarahJane Taylor, who has made the administrative wheels run smoothly for many years.

Of course, a major part of day-to-day research life hinges upon everyone else in the lab, so I'd also like to acknowledge all of my current and past labmates and collaborators who have made the work environment fun and supportive, including Alec, who always made experiments exciting, Joanna, Stephanie, and Chris, whose dark humor made everything better, Kate, Jennifer, and Zuzka, who are excellent beer and falafel companions, Jeannie, an unforgettable friend and conference buddy, Mark, whose presentations and experiments were highly entertaining, Xinyan, whose optimism and energy amaze me, Ellen, who always helps me gain perspective, and Devante, who is a great new addition to the lab. In addition, I'd like to thank

Rachel for being an incredibly patient teacher and cell culture buddy – I'm so lucky that you were the first person I met when I joined the lab. Thanks also to Britta for going on all kinds of lab and non-lab adventures with me – I'm glad we had the chance to go through so much of the grad school process together!

Another important part of my grad school life has been my bioengineering and non-bioengineering friends, who have all provided advice, encouragement, and support. Special thanks go to Elena, Martha, Jen, and Shea, who provided a sounding board and community, both Harrisons, who excel at friendship in completely different ways, Victoria, who always believes in me more than I believed in myself, and Gloria, Jet, Marie, Alex, Hong, and Brad, who should maybe actually be in the next section because they're more like family than friends.

Finally, I'd like to thank my family, especially my parents, my sister Alicia, my cousin Jack, and my grandparents, for all the big and little things they've done over the years that contributed to who and where I am today. Although we're on opposite coasts, their visits and phone calls have been invaluable during my grad school experience. In addition, my parents-in-law and sister-in-law Yi-Chin have also been a great source of support and a wonderful addition to the family. And last but not least, I'd like to thank my husband Wei, whose importance I can't even begin to explain, so I won't. Thank you all for everything – grad school has been almost nothing like I initially imagined, but the experience has been enriched by all the amazing people who've been part of it.

Abstract

Effects of Design Factors and Microenvironment on Mesenchymal Stem Cells and Nucleus Pulposus Cells for Intervertebral Disc Tissue Engineering

By

Ann Ouyang

Doctor of Philosophy in Bioengineering

University of California, San Francisco

And

University of California, Berkeley

Professor Jeffrey C. Lotz, Chair

Intervertebral disc degeneration is a common and significant health concern that often leads to low back pain and worker disability. Disc degeneration is often irreversible, and current treatments do not adequately restore cell health or biomechanical function. Tissue engineering strategies are a possible solution to regenerate disc matrix, but one challenge for regenerating tissue is the degenerative disc microenvironment, which is characterized by inflammation, hypoxia, low glucose, low pH, and high osmolality. This research focuses on the effect of design factors on tissue-engineered constructs in the context of the disc microenvironment.

To evaluate the effects of cell type and configuration on anabolic and catabolic performance, we compared MSC-only, NPC-only, and 50:50 coculture groups in individual cell and micropellet configurations in basal and degenerative (hypoxic and inflammatory) media conditions. NPC and coculture groups had the most anabolic gene expression and GAG synthesis, but inflammatory media conditions dramatically reduced anabolic activity in all groups. Inflammatory and hypoxic media also led to upregulation in catabolic gene expression in

NPC-only groups, but MSC-only and coculture groups were more resistant to this upregulation. A micropellet configuration, which provides more direct cell-cell contact, also reduced catabolic induction, and the group combining a cocultured cell type with a micropellet configuration had the lowest catabolic gene expression, suggesting that both design factors contribute to the response to inflammation. The coculture micropellet group also self-organized into a bilayered pellet, which may mimic a structure and mechanical environment present during development.

In the latter part of this research, we evaluated the effect of cell type and hypoxic preconditioning in a diffusion chamber we created to simulate nutrient limitations in the disc microenvironment. We limited diffusion within an agarose gel, and tested NPC-only, MSC-only, and 50:50 coculture groups, along with MSC-only and coculture groups that included MSCs expanded in hypoxia. Within the diffusion-limited system, cell type affected viability. Surprisingly, NPCs had the lowest viability and MSCs had the highest. Viability of the coculture group was close to the mean of its component groups, suggesting that there was no synergistic benefit. Hypoxic preconditioning of MSCs also did not significantly affect viability.

Our results emphasize the importance of considering the microenvironmental context when evaluating cell therapies. In addition, improved understanding of the effects of various design factors can improve the performance of tissue-engineered constructs.

Table of Contents

Chapter 1: Introduction……...1

1.1 Clinical Motivations……1

1.2 Intervertebral Disc Structure and Function Overview……1

1.2.1 Intervertebral Disc Development……1

1.2.2 Intervertebral Disc Structure and Biomechanics……2

1.2.2.1 Annulus Fibrosus……3

1.2.2.2 Nucleus Pulposus……3

1.2.2.3 Cartilage Endplate……4

1.2.3 Cellular Structure and Function……5

1.2.3.1 Annulus Fibrosus Cells……5

1.2.3.2 Endplate Chondrocytes……5

1.2.3.3 Nucleus Pulposus Cells……6

1.3 Intervertebral Disc Degeneration……7

1.3.1 Etiology and Diagnosis……7

1.3.2 Structural and Biomechanical Changes and the Degenerative Microenvironment……9

1.3.3 Cellular Changes……10

1.4 Intervertebral Disc Tissue Engineering……11

1.4.1 NPCs for IVD Tissue Engineering……12

1.4.2 Mesenchymal Stem Cells in IVD Tissue Engineering……13

1.4.2.1 Definition……13

1.4.2.2 *In vitro* and animal studies with MSCs……14

1.4.2.3 Clinical studies with MSCs……..15

1.4.3 Coculture of MSCs and NPCs……...……16

1.5 Objectives…….....……21

1.6 References……...……...……22

Chapter 2: Effects of cell type and configuration on cocultured MSC and NPC constructs…….46

2.1 Introduction……46

2.2 Methods……..48

Experimental Design……..48

Cell type effects……..49

Configuration effects……..49

Cell culture……49

NPC phenotype stability……....50

Micropellet formation……51

Gene expression analysis……...52

DNA and Dimethylmethylene Blue assays for glycosaminoglycan quantification……53

Histological analysis……..54

Observation of micropellet structure and intracellular cohesivity assay……..54

2.3 Results……55

Cell type effects……..55

Configuration effects……...57

Extracellular matrix deposition……60

Self-organization of cocultured cells in micropellets……63

2.4 Discussion……..65

2.5 References……..70

Chapter 3: Effects of cell type and hypoxic preconditioning on cell viability in a diffusion-limited microenvironment……...79

3.1 Introduction……79

3.2 Methods……..82

Cell expansion……82

Cell type groups…….83

Diffusion chamber materials……..83

Diffusion chamber formation…….84

Viable distance measurement……84

Cell density estimate……..85

Statistics…….85

3.3 Results……85

3.4 Discussion……..89

3.5 References…….93

Chapter 4: Conclusions and Future Directions……..…….…...102

4.1 Research Summary…….….102

4.2 Future Directions…….104

4.2.1 Mechanisms of cell-cell communication in coculture systems…….…..104

4.2.1.1 Role of soluble factors and direct cell-cell contact in MSC:NPC coculture..104

4.2.1.2 MSC Roles in Coculture: Differentiation versus Trophic Effects……107

4.2.2 Self-organization in coculture systems……...108

4.2.3. Mechanisms of hypoxia response……..109

4.2.4 Effect of individual differences on cell viability……109

4.3 References……110

Appendix A: Micropellet formation parameters……116

Appendix B: Effects of NPC donor variation on cell viability in a diffusion-limited system……..122

Appendix C: Effects of hypoxia, configuration, and inflammatory media on NPC synthetic and catabolic activity……124

Appendix D: Cell fate tracking in coculture……131

Appendix E: RNA extraction from agarose diffusion chamber constructs for gene expression analysis……138

List of Tables

Table 2.1 Primer sequences for gene expression analysis……53

Table B.2 Number of replicates available for diffusion chambers from different bovine individual donors……122

Table C.1 Significant associations with synthetic and catabolic gene expression levels……...127

Table D.1 Species-specific primer sequences……132

List of Figures

Figure 2.1 Cell type and configuration groups…….49

Figure 2.2 Methods for forming cell micropellets……52

Figure 2.3 Effect of cell type in individually encapsulated cell constructs……..57

Figure 2.4 Anabolic and catabolic gene expression in a micropellet configuration…….59

Figure 2.5 Coculture and micropellet configurations exhibit reduced catabolic induction……..60

Figure 2.6 Glycosaminoglycan content and distribution varies with cell type and configuration……..62

Figure 2.7 Differential adhesion of MSCs and NPCs leads to a bilaminar self-organization in coculture micropellets……64

Figure 3.1 Diffusion chamber manufacturing……...84

Figure 3.2 Representative viable distance images……86

Figure 3.3 Viable distance model fit with estimated cell density and cell types……..87

Figure 3.4 Live cell estimate of different cell type groups……...88

Figure 3.5 Live cell estimate of coculture comparison groups, with and without hypoxia preconditioning……..89

Figure A.1 Agarose microwells of various diameters immediately following cell loading…...119

Figure A.2 Agarose microwells of various diameters 48 hours following cell loading…….120

Figure A.3 Fibrin microwells 29 hours after cell loading……...121

Figure B.1 Viable distance and live cell number variation in NPCs from three different donors……..…….123

Figure C.1 Diagrams and histology images of configurations of individual cells, micropellets, and large pellets……...125

Figure C.2 Gene expression of chondrogenic and catabolic markers in NPC constructs after 21 days…….127

Figure C.3 GAG and DNA content of large pellets and individual cell and micropellet configurations……..128

Figure D.1 NPC:MSC ratios calculated from species-specific GAPDH mRNA measurements……..133

Figure D.2 Cocultured micropellet with live/dead stain and membrane dye after 24 hours of culture……..134

Figure D.3 Coculture diffusion chamber section with live/dead stain and membrane dye……136

Figure E.1 Diffusion chamber harvesting diagram…….139

Figure E.2 qPCR results for NPC, MSC, and coculture diffusion chambers divided into regions……..142

Chapter 1: Introduction

Sections of the chapter were also written by A. O. in a submitted chapter in Stem Cell and Tissue Engineering. *The reference is as follows: Ouyang, A., Allon, A.A., Buser, Z., Berven, S., Lotz, J.C. "Stem Cells for Disc Repair." In Stem Cell and Tissue Engineering, edited by Song Li, Nicolas L'Heureux, and Jennifer Elisseeff, World Scientific Publishers. Submitted update to 2011 edition.*

1.1 Clinical Motivations

Low back pain affects up to 80% of adults at some point during their lives and costs the United States hundreds of billions of dollars per year in medical costs and lost worker productivity (*1*, *2*). Intervertebral disc degeneration is strongly implicated as a cause of lower back pain, but degeneration itself is complex and correlated with a variety of causes including genetics, mechanical injury, age, and diabetes (*3*–*7*). Current treatments focus on pain management, muscular stabilization, and eventual surgery. However, surgery does not restore disc function, limits mobility, and may increase risk of degeneration in adjacent discs (*3*). Artificial disc replacements aim to simulate physiological mechanical functions, but do not perfectly mimic natural discs and still carry a risk of adjacent-level degeneration (*3*, *8*).

More effective and minimally-invasive treatments are needed to address intervertebral disc degeneration. In particular, cell-based therapies that might regenerate disc tissue are promising (*9*). Investigating the effect of microenvironmental factors on success of these therapies is the main focus of this research.

1.2 Intervertebral Disc Structure and Function Overview

1.2.1 Intervertebral Disc Development

The intervertebral disc consists of a soft nucleus pulposus center surrounded by the stiffer annulus fibrosus, which forms a ring around the nucleus. In the vertebral column, this structure is located between adjacent bony vertebrae, with thin cartilage endplates between the disc and the bone (*10*). The vertebral column forms from mesodermal tissue, including the notochord, which also serves as a signaling center during development and eventually differentiates into nucleus pulposus tissue (*3*). The annulus fibrosus, endplate, and vertebrae form from sclerotomal cells in the paraxial somites, which are located in pairs next to the notochord. During development, cells migrate from the somites and condense around the notochord, eventually dividing into AF and vertebral body regions. Some of these cells also differentiate to form the bony and cartilage endplates, which cover the surface of the vertebral growth plate (*3, 11*).

Meanwhile, cells in the notochord undergo involution and form the NP region inside the migrated AF cells. Eventually, notochordal condensations disappear in the vertebral regions (*3, 12*). The notochordal condensation process is similar to mesenchymal condensations that form cartilage tissues in other areas of the body, and the resulting nucleus pulposus and cartilage tissues also have similar biochemical and mechanical properties (*13*). Therefore, a more detailed understanding of the development of cartilage and intervertebral disc tissues can further inform regeneration strategies.

1.2.2 Intervertebral Disc Structure and Biomechanics

Intervertebral discs experience both compression and tension during normal spine loading, and they provide flexibility in the spinal structure while connecting adjacent vertebral bodies (*14–16*). The various regions within intervertebral disc, the annulus fibrosus (AF), nucleus pulposus (NP), and the adjacent cartilage endplate (CEP), play specific biomechanical roles, which are closely related to their structures.

1.2.2.1 Annulus Fibrosus

The annulus fibrosus has an angle-ply lamellar structure made of highly organized collagen fibers (*3*). The fibers form concentric lamellae (layers of parallel fibers) at about a +/- 60° angle to the spine's axis. Adjacent lamellae, which add up to approximately 25 rings in total, have alternating fiber directions (*17, 18*). This alternating arrangement helps the disc withstand bending and twisting forces within the spine (*19*). The lamellae also experience circumferential tension when the NP expands under axial compressive loading (*20*).

The AF is further divided into outer and inner annulus regions, which have slightly different mechanical and biochemical structures. The outer annulus is more fibrous and ligamentous, with many collagen I fibers. The inner annulus is a fibrocartilaginous zone between the outer annulus and the nucleus pulposus – like the outer annulus, it is still composed of lamellae with aligned fibers, but like the NP, it has increased proteoglycan and collagen II content (*15*), and subsequently a lower tensile modulus and failure stress (*21*).

1.2.2.2 Nucleus Pulposus

The nucleus pulposus (NP) extracellular matrix is similar to that of cartilage, primarily consisting of proteoglycans, collagen, and elastin. Unlike collagen fibers in the annulus, the collagen fibers in the nucleus are randomly organized, while the elastin fibers are radially oriented (*22*). Unlike the AF, the NP is rich in type II collagen, with smaller amounts of other collagen types, including I, VI, IX, and X (*23, 24*). The proteoglycans, the most common of which is aggrecan, contain dozens of sulfated glycosaminoglycan (GAG) chains that are negatively charged, attracting water to the tissue (*25*). The high water content of healthy discs (80-88%) helps to resist compression during physiologic loading: during normal loading, the NP experiences pressures in the range of 0.4 – 2.3 MPa (*12, 21*). Some of this pressure is transferred

to the annulus around the NP circumference and to the cartilage endplates above and below, which help distribute the load and constrain the pressurized NP (*12, 20*). As water content decreases with age and degeneration, the NP begins to experience abnormal biomechanical loading (*26*).

At a macro level NP tissue appears similar to articular and endplate hyaline cartilage, but its composition and mechanical properties have key differences. The NP has a proteoglycan:collagen ratio > 20 in varying species, which is much higher than that of cartilage, meniscus, and AF tissue (*1, 23, 27*). The ratio difference may be attributed to lower collagen II gene expression at the cellular level (*28*). The composition affects mechanical properties: collagen-rich cartilage behaves similar to a viscoelastic solid, while the proteoglycan-rich NP can behave as either a viscoelastic solid or a fluid, depending on loading conditions (*29*).

1.2.2.3 Cartilage Endplate

The intervertebral disc is bordered inferiorly and superiorly by thin endplates, which are divided into cartilage and bony regions. The bony endplate region is calcified at the adjacent vertebral body interface, and is similar to the vertebral cortex (*30, 31*). The CEP, which borders the NP and inner annulus, is primarily composed of avascular hyaline cartilage. The structure mainly consists of collagen I, collagen II, and proteoglycans, with sparsely seeded chondrocytes. The collagen fibers in the CEP are more aligned than in other types of hyaline cartilage because they are roughly parallel to the ends of the vertebrae, but the tissue also lacks the distinct zones of articular cartilage (*12*). Although both have a high water content, CEP cartilage has a higher collagen:proteoglycan ratio than the NP tissue (*18*).

As previously mentioned, the endplate helps to distribute pressure from the NP onto the vertebrae and constrains the pressurized nucleus. The constraining force causes the endplate to

stretch, generating tensile stress. The likelihood of endplate failure is influenced by structural factors such as thickness, porosity, and curvature, which change with age and degeneration (*12*). CEP permeability also impacts disc cell health because it is the primary transport pathway between the NP and the vertebral capillaries. Blood vessels are limited in the endplate and AF and do not penetrate into the NP or CEP, so nutrients must diffuse through these avascular regions to reach cells in the center of the disc (*18, 32*).

1.2.3 Cellular Structure and Function

In concert with their unique biomechanical roles, disc tissues also contain specialized cell types that contribute to the structure and function of each tissue. The primary focus of this dissertation is nucleus pulposus cells (NPCs).

1.2.3.1 Annulus Fibrosus Cells

Annulus fibrosus cells (AFCs) are found in the AF with an estimated density of $9x10^3$ cells/mm^3 (*33*). They are similar to fibroblasts in both shape and collagen I synthesis capability (*34*). During development, they align with each other to form lamellae. The cells' aligned organization is facilitated by stress fibers made of cytoskeletal actin filaments (*3*). Cell phenotypes are correlated with the structural gradient from the outer to inner annulus: cells in the outer annulus are more fibroblastic, while AFCs in the inner annulus are more chondrocyte-like (*26, 33*). In general, AFCs can be distinguished from NPCs by a higher collagen I: collagen II gene expression ratio, a higher collagen II: aggrecan ratio, and expression of collagen V (*34*).

1.2.3.2 Endplate Chondrocytes

Endplate chondrocytes are found in the CEP with a density of approximately $15x10^3$ cells/mm^3, similar to chondrocyte density in articular cartilage (*35*). They are morphologically similar to articular chondrocytes, with a rounded phenotype, and also synthesize collagen II and

proteoglycans (*36*). Although nucleus pulposus cells are also chondrocyte-like, endplate chondrocytes have a slightly different expression profile, including different levels of procollagen I, procollagen II, and aggrecan chondroitin sulfate throughout aging, as well as lower KRT-19, LAM-5, PAX1, and FOXF1 protein levels (*35*, *37*). Further transcriptome studies are needed to better characterize CEP-specific markers (*38*).

1.2.3.3 Nucleus Pulposus Cells

Nucleus pulposus cells (NPCs) are often described as chondrocyte-like due to their spherical shape and expression of aggrecan and collagen II (*34*). They are more sparsely distributed than AFCs, with an average cell density of 4000 cells/mm^3 (*3*). For many years the NPC phenotype was not clearly defined or differentiated from chondrocyte phenotypes, but a recent Spine Research Interest Group meeting identified several primary and secondary makers for young, healthy NPCs (*1*). Primary markers include stabilized HIF1-2α, GLUT-1, Shh, Brachyury, carbonic anhydrase 3/12, CD24, and cytokeratins 8, 18, and 19. Secondary markers have also been identified through microarray and proteomics studies, but are less validated, and may vary with species. In particular, cytokeratin 19, glypican 3, PAX1, and FOXF1 are markers that have been shown to distinguish NPCs from articular chondrocytes (*22*, *37*), as well as differences in aggrecan:collagen expression ratios and glycoprofiles (*22*, *23*, *34*, *39*).

In adult humans the nucleus pulposus primarily contains NPCs, but in other species notochordal cells are also often present in skeletally mature animals (*40*). Notochordal cells are identified by their size (30-40 μm in diameter) and large vacuoles, which may serve as storage for additional GAGs (*3*). In humans, NP tissue initially contains notochordal cells, but the population becomes more chondrocyte-like with age. The exact mechanism for this transition is still unknown: early notochordal cells may turn into NPCs, or they may undergo cell death and

be replaced by chondrocyte-like NPCs that migrate from disc endplates (*41*). The age-related loss of notochordal cells in humans and several other species, such as chondrodystrophoid dogs, may be connected to disc degeneration (*22*). The presence and function of notochordal cells are important to consider when choosing animal models to study disc degeneration and regeneration.

1.3 Intervertebral Disc Degeneration

1.3.1 Etiology and Diagnosis

Disc degeneration is a cascade of changes in cells, extracellular matrix, and biomechanics that form a "degenerative circle" (*42*). Etiology of degeneration is complex and multi-factorial. Aging is highly associated with degeneration, and many age-related changes in disc structure, such as decreased cell nutrition, cell senescence, matrix disorganization, and increased catabolism, are also associated with pathologic degeneration (*6*, *33*, *43*). Other risk factors, such as diabetes, obesity, physical injury, smoking, gender, and genetics are also associated with degeneration, but studies disagree on the extent of contribution of individual factors (*44–51*).

Lumbar degeneration can be diagnosed in patients through noninvasive imaging methods. Magnetic resonance imaging (MRI) is the current gold standard. Traditional T1- and T2-weighted MRIs show anatomical details clearly, allowing for accurate diagnosis of disc bulges and various types of disc herniation (*52*). T1-and T2- weighted MRIs are also used to detect advanced disc degeneration, which is characterized by hypointensive NP regions (due to loss of water content), decreased disc height, annular disruptions, modic changes, and changes in vascularity, fat content, and bone density of vertebral endplates (*53–55*). Discs are often graded for degeneration on the Pfirrmann scale, which has good intra- and interobserver reliability (*56*).

Although degeneration is strongly correlated with low-back pain, many asymptomatic patients also show degenerative changes in imaging studies, and prevalence of degenerative discs

in asymptomatic patients increases with age (*57*). By age 60, 92% of asymptomatic patients have at least one degenerative disc visible on MRI (*53*). To better distinguish painful and non-painful degeneration, advanced imaging methods detect biochemical changes that occur earlier in degeneration, as well as evidence of inflammatory reactions that may contribute to pain.

Many advanced imaging techniques build on existing MRI protocols. For example, calculating relaxation times captured during T2 imaging may improve detection of early degeneration because relaxation times correlate with disc hydration, proteoglycan and collagen content, as well as mechanical properties (*53*, *58*, *59*). In addition, T2 and T2* mapping offers more information about spatial variation in the disc, which is correlated with early degenerative changes (*60–62*). T2* imaging with short echo times and ultrashort time-to-echo (UTE) imaging can also be used to visualize degenerative changes in CEPs, which normally are not visible due to their lower water content (*63*, *64*). $T_{1\rho}$ MRI imaging is also more sensitive to changes in proteoglycan (PG) content and AF degeneration, and when combined with disc height measurements, could be used to create a more accurate predictive model of degeneration (*65–68*). Older imaging techniques such as PET (positron emission tomography) could also be useful to assess disc inflammation or cell senescence, but more research is needed to validate their accuracy (*53*, *69*).

Other experimental disc imaging techniques include sodium MRI, which can be used to measure PG content in cartilage and discs (*70*, *71*), ultrahigh-field strength MRI, which improves visualization of structural details (*72*), and MR spectroscopy, which can measure metabolites associated with inflammation and pain (*53*). Dynamic imaging and kinetic MRIs assess changes in degenerative or herniated discs under different postural loading conditions, which is useful for biomechanical assessments (*52*, *73*). In addition, MRI imaging of diffusion of contrast agents can

provide useful information about nutrient diffusion through the CEP, as well as highlight annular tears (*52, 53, 74–77*). However, the high negative fixed charged density in the NP can interfere with charged contrast agents (*65*).

Another, more invasive, diagnostic technique for disc degeneration is discography, which involves injecting a contrast agent into the disc during radiographic imaging. Although low pressure discography is standard for diagnosis of discogenic pain, it is controversial due to questions about the sensitivity and subjectivity of the test, as well as possible increased degeneration risk (*53, 78–80*).

Finally, recent advances in sequencing and screening technology have also inspired research into molecular biomarkers of disc degeneration. Studies have identified microRNAs (miRNAs) and long noncoding RNAs (lncRNAs) associated with degeneration (*81, 82*), and other "-omics" studies aim to identify additional biomarkers of chronic low back pain (*83, 84*). Diagnosis of degeneration through biomarkers would also be relatively non-invasive, since sequencing requires minimal tissue samples, and analysis of peripheral blood, particularly of cytokines and chemokines, can also predict disc degeneration and chronic low back pain (*85–87*). Identifying additional biomarkers of degeneration will also provide clues into the molecular processes involved.

1.3.2 Structural and Biomechanical Changes and the Degenerative Microenvironment

Matrix changes are a critical factor contributing to the degenerative cascade. During degeneration, the NP experiences loss of proteoglycan and collagen II, along with an increase in collagen I as the tissue becomes more fibrotic (*42*). Loss of proteoglycan changes the osmolality of the NP, leading to reduced water content and consequently, changes in mechanical properties. If the NP does not distribute mechanical loading forces optimally, other disc tissues are often

damaged during loading (*88*). Like the NP, the AF also becomes more fibrotic and disorganized, and biomechanical stresses lead to inward and outward buckling of its fibers (*42*).

The CEP also changes with age and degeneration, often becoming less permeable and more susceptible to damage. Endplate disruptions also affect loading patterns, contributing to the cycle of mechanical stress and matrix instability. Furthermore, loss of permeability limits nutrient delivery to the NP, which increases cellular stress (*3, 12, 32*).

Changes in the degenerative disc microenvironment accompany structural and biochemical changes in the matrix. The NP normally has a high osmolality, in the range of 400 to 550 mOsm, which decreases in degeneration due to GAG loss (*89–91*). Hypoxic and low-glucose conditions are also exacerbated by decreased permeability, resulting in 0.5 – 5% oxygen and <5 mmol/L glucose concentrations in the disc (*92, 93*). Anaerobic glycolysis also increases in hypoxic conditions, generating lactic acid as a byproduct. With limited transport into and out of the disc, the lactic acid accumulates and lowers disc pH to <6.8, or as low as 5.7 in severe degeneration. This reduces cell viability and increases matrix degradation (*92, 94*). In addition, the degenerative disc microenvironment has a high concentration of proinflammatory cytokines and imbalanced reactive oxygen species (ROS), which further impairs regenerative potential and affects cell health (*3, 95*). Finally, limited transport combined with ECM destruction results in buildup of matrix degradation fragments, which promotes more inflammation, contributing to the degenerative cascade (*96*). The influence of these factors is not necessarily independent: for example, hypoxia may support NPC survival during cellular stress and mediates responses to changes in pH and growth factor concentrations (*92, 97, 98*).

1.3.3 Cellular Changes

The stresses of the degenerative microenvironment affect NPC phenotype and gene expression. Proinflammatory cytokines, such as IL-1α, IL-1β, TNF-α, and IL-6 are upregulated during degeneration, and can stimulate NPCs to release additional inflammatory molecules such as IL-4, IL-10 (which may also play an anti-inflammatory role in some conditions), IFN-γ, CSF2, and chemokines CCL2, CZCL1, CXCL8, CCL7, CCL3, CCL4, CCL5, CXCL9, CXCL10 (*43*, *99*, *100*). Inflammatory cytokines can increase pain and downregulate new ECM synthesis, inhibiting regeneration (*3*, *99*). Perhaps most importantly, they also upregulate catabolic genes that break down the matrix, namely matrix metalloproteinases (MMPs-1, -2, -3, -7, -8, -9, -10, -12, -13, and -14) and disintegrins and metalloproteinases with thrombospondin motifs (ADAMTSs-1, -4, -15, and possibly -5) (*43*, *101*, *102*). ECM degradation by these proteases compromises mechanical stability of the disc and continues the "vicious circle" of degeneration (*42*). Some cytokines, such as IL-1 and TNF-α, also upregulate anti-inflammatory and anti-catabolic genes like IL-1 receptor antagonist (IL-1ra) and tissue inhibitors of metalloproteinases (TIMPs), but these are usually insufficient to counter the high levels of inflammation already present (*43*, *101*). Although the nucleus pulposus is normally immune-privileged, immune cells may also infiltrate the disc during degeneration (*103*, *104*).

In addition, the degenerative microenvironment also increases NPC cell death and senescence (*97*, *105*, *106*). Since cell density is low even in the healthy NP, these changes make it difficult for NPCs to regenerate disc tissue without outside intervention (*107*).

1.4 Intervertebral Disc Tissue Engineering

IVD tissue engineering aims to restore disc matrix structure and function by delivering some combination of biomaterials, cells, and growth factors that are able to replace and/or regenerate ECM. Optimal tissue engineering constructs might vary with extent of degeneration – for

example, mildly degenerative discs with a viable cell population might be treatable with biomolecules or gene therapy, while more severely degenerated discs might require a cell injection to replace unhealthy or senescent cells. Even more severely degenerated discs might have lost so much of their basic structure that they should be completely replaced with a pre-cultured construct the size of a whole disc (Moriguchi et al., 2016). Many advances have been made in biomaterials (*108*) and growth factor and gene therapy-based regeneration strategies (*109*), including those using breakthrough CRISPR-Cas technology (*110*), but this dissertation focuses on cell-based therapies. Common sources for cell-based therapies include autologous NPCs, mesenchymal stem cells, and cocultures. Other cell sources that are also under investigation include notochodral cells (*111*, *112*), "disc stem cells" that may be isolated or derived from from adult discs (*113*), induced-pluripotent stem cells (iPSCs), and others (*114*).

1.4.1 NPCs for IVD Tissue Engineering

NPCs are a good candidate for IVD tissue engineering because they already have adaptations to survive hypoxia and nutrient stress in the disc environment (*115*). Isolated NPCs are able to synthesize proteoglycan and express chondrogenic genes *in vitro*, especially with growth factor supplementation (*116*). *In vivo*, injected NPCs are able survive for up to 1 year in the disc (*117*), and treatment with NPCs or NP tissue slowed degeneration in animal models (*118–123*). The EuroDISC study found evidence of proteoglycan synthesis in animal models of autologous disc chondrocyte transplantation, and reduction of low back pain in patients (*124–126*). Both autologous and allogenic NPCs were tested, without any signs of graft-versus-host disease, most likely because the NP is considered immunoprivileged (*127*). Autologous NPCs are also the feature of an ongoing clinical study for treatment of herniated and degenerative discs (clinicaltrials.gov identifier NCT01640457).

Although NPCs are well adapted for the disc environment, their use in tissue engineering applications also has some challenges. First, only a small number of autologous cells can be harvested from a patient, and could induce degeneration, resulting in donor site morbidity. NPCs could be harvested from discs that are already degenerated to minimize overall damage, but cells from degenerative or aged discs may not have the same proliferation and synthesis capacity as healthy cells. Similarly, sourcing healthy discs for allogenic NPCs is difficult, considering that most organ donors are older, and 90% of people over 50 are likely to have experienced disc degeneration (*128*, *129*). In addition, the small number of harvested NPCs will need to be expanded *in vitro* for clinical applications, increasing the risk of de-differentiation. One way to "activate" and improve the viability of harvested NPCs might be to coculture with stem cells prior to transplantation, a therapy that is being evaluated clinically (*130*).

1.4.2 Mesenchymal Stem Cells in IVD Tissue Engineering

1.4.2.1 Definition

Mesenchymal stem cells (MSCs) are adult stem cells with self-renewal properties that can differentiate into multiple mesenchymal-derived cell types, including osteoblasts, chondrocytes, and adipocytes (*131*). MSCs are generally characterized by key surface markers, including CD105, CD73, CD166, CD29, CD44, CD90, and STRO-1, and the absence of CD34, CD45, and HLA-DR (*132*). However, because MSCs can be isolated from a variety of tissues including synovial fluid, adipose tissue, umbilical cord blood, and others, characterization methods are still incomplete and isolated MSCs may have some heterogeneity (*133*). Surface markers and tissue of origin may also influence the proliferation, differentiation and immunomodulatory potential of MSCs (*133–135*). In our studies we used bone-marrow-derived MSCs because they were the first to be isolated, and are the most well characterized.

1.4.2.2 *In vitro* and animal studies with MSCs

By definition, MSCs can be differentiated towards chondrogenic phenotypes like NPCs, but instructive signals are required both *in vitro* and *in vivo*. Optimal conditions *in vitro* include a three-dimensional (3D) culture system, such as pellet culture or culture in a hydrogel, and chondrogenic differentiation media with transforming growth factor β (TGF-β) and dexamethasone (*26, 136, 137*). MSCs have been shown to produce NP and cartilage-like ECM *in vitro* (*138–140*). In some culture systems, they also appear phenotypically similar to NPCs and express NPC-like surface markers (*141*). However, one challenge of growth-factor-induced chondrogenic differentiation is the risk of hypertrophy (*142, 143*).

In vivo animal studies of MSC cell therapy for disc degeneration have mixed results, both in terms of cell survival and matrix improvement. This is most likely due to the wide variety of experimental conditions, carriers, and animal models used. MSCs have been tested in many animal models, including rats, rabbits, dogs, mice, and pigs (*26, 128*). In some studies, MSCs appeared to survive up to 6 months and showed evidence of differentiation towards an NPC phenotype (*26, 144–146*). However, in other cases MSCs did not appear to survive the disc microenvironment: only 20% of injected MSCs survived in a bovine disc in organ culture (*147*), injected MSCs were only detectable up to 2 weeks in a rat model (*148*), and no evidence of viable MSCs was seen at 3, 6, or 12 months after injection in a porcine model (*149*). In some cases, the MSC population later recovered after high initial cell death (*150*).

In most animal studies, MSCs improved disc height and water content and inhibited degeneration. However, the effects may decrease after 6 weeks, suggesting only a short-term benefit (*151*). Positive results also seem more common in smaller animal models, while studies in larger animals were less likely to observe viable MSCs or proteoglycan synthesis. This

difference may be due to greater nutrient restrictions in a larger-sized disc, and may also have implications for human applications (*127, 152*). When compared with other cell therapy sources, MSCs also did not have any chondrogenic advantages over NPCs in a rabbit model (*121*), and had poor viability and produced a more fibrous scar tissue than juvenile chondrocytes in a porcine model (*149*).

In vivo experiments have been performed with allogenic and xenogenic MSCs without eliciting an immune response, which may be due to the avascular NP being an immune-privileged tissue (*127*). MSCs have also been characterized as immunoprivileged, but may actually be "immune evasive" and immunosuppressive (*153*). Their immunosuppressive properties may also be beneficial in the inflammatory degenerative disc microenvironment, as well as other trophic effects of MSCs (*154*).

1.4.2.3 Clinical studies with MSCs

In recent years, various clinical studies have also investigated MSC cell therapy for cartilage and IVD repair (*155*). A small study showed that MSCs implanted in discs with a collagen sponge improved water content, disc stability, and back and leg pain, but no improvement in disc height was reported (*156*). Similarly, Orozco *et al.* observed significant improvement in pain and disability and improved water content, but no significant change in disc height after 12 months (*157*). This pilot study led to another clinical trial, which recently finished but has not yet reported results (clinicaltrials.gov identifier NCT01860417). In a slightly larger study, Pettine *at al.* also recorded durable reduction in pain and disability scores through 2 years, but only 8/20 patients had improved Pfirrmann grades on MRI after 1 year (*158, 159*)/ Currently, several other trials are in progress or recently completed (clinicaltrials.gov identifiers NCT02338271, NCT01860417, NCT01643681, NCT02097862), including one phase 3 allogenic hMSC trial by

Mesoblast, Ltd. (clinicaltrials.gov identifier NCT02412735), which follows a phase 2 study completed in 2016 (clinicaltrials.gov identifier NCT01290367). This study found that a single injection of the proprietary allogenic mesenchymal precursor cell (MPC) production improved pain scores in 48% of patients after 24 months. However, 13% of the control group, patients treated with saline only, also had a successful pain score improvement (*160*). Similar to *in vitro* and animal studies, clinical trials have also revealed additional MSC effects that were unrelated to differentiation, suggesting that MSCs played trophic or immunomodulatory roles (*100*, *134*). To provide more substantial evidence of MSC efficacy, more careful examination of control groups and evidence of survival of injected cells are needed.

MSCs are a popular choice for clinical studies in many other tissues besides the IVD, with an approximately 3-fold increase in the number of MSC-based product submissions to the FDA between 2006 and 2012 (*161*). However, regulatory approval of these therapies has been challenging. The FDA classifies cultured MSCs as more than "minimal manipulation," and therefore requiring similar steps as mass-produced drugs (*162*). In addition, MSC products have a great deal of manufacturing diversity, are isolated from an increasing variety of tissues, and lack consistent nomenclature and definition of surface markers (*161*). MSCs expanded at a clinical scale may also undergo phenotypic changes that are not present in laboratory experiments – in particular, clinical scale expansion lowers differentiation capacity and the ability to inhibit T-cell proliferation (*163*). An improved understanding of MSC mechanisms of action in different systems, as well as more consistent nomenclature and isolation protocols, will expedite their translation into the clinic.

1.4.3 Coculture of MSCs and NPCs

Coculture was originally used to explore interactions between implanted stem cells and host cells, but synergistic effects were observed, suggesting potential therapeutic applications. Currently, coculture of MSCs with mature instructive cells has been shown to improve regeneration of many tissue types, including neural, cardiovascular, hepatic, renal, and musculoskeletal, and has been used in some clinical studies (*130*, *164*).

Many studies have explored coculture of MSCs with NPCs as well as with a similar cell type, articular chondrocytes. Experimental conditions such as cell density, cell type ratios, media conditions, culture time, and culture configurations vary widely among different studies, but many find common benefits of coculture. These benefits include improved chondrogenesis and ECM production (*165–173*), improved mechanical properties (*169*), increased cell proliferation (*88*, *167*, *168*, *171*), reduced hypertrophy (*174*, *175*), and increased resilience to inflammation (*176*, *177*). Furthermore, *in vivo* studies have verified coculture effects in a more complex environment (*172*, *178*, *179*). However, observations from these studies have raised two key questions: first, whether benefits of coculture are mediated by direct cell-cell contact or by released soluble factors, and second, whether MSCs play a synthetic or trophic role in tissue regeneration.

To determine if coculture benefits are mediated by direct contact or soluble factors, various groups have experimented with direct and indirect coculture systems. Watanabe *et al.* found that MSCs and NPCs in direct contact had increased proliferation and proteoglycan synthesis compared to cells that were cultured in the same well without direct contact (*171*), which was similar to results observed with chondrocytes (*167*, *168*, *170*). Possible mechanisms suggested for cell-cell communication in direct cocultures include spontaneous cell fusion, exchange of membrane components, and gap junctions (*170*, *180*, *181*).

On the other hand, indirect coculture systems and conditioned media also have the ability to increase cell proliferation and chondrogenesis (*88, 179, 182–184*). Paracrine signaling in indirect cocultures may be mediated by soluble growth factors: TGF-β-1,-3, FGF-1,-4,-6, IGF-1, BMP-2, EGF, and PDGF have all been shown to increase in coculture (*168, 179, 185, 186*).

Direct contact and soluble factors may also not be mutually exclusive mechanisms of interaction. Yamamoto *et al.* found that growth factor concentrations increased with both indirect and direct coculture, but were higher in groups with direct contact (*185*). Other studies found that closer proximity of cocultured cell types increases matrix production (*169, 187*). Optimal tissue engineering outcomes may rely on a combination of contact mediated mechanisms and improved paracrine signaling.

3D pellets have been identified as a particular direct coculture configuration that may enhance chondrogenesis, perhaps by creating extracellular cues that can alter cell behavior and phenotypes (*188*). Pellet culture is commonly used to promote chondrogenic differentiation *in vitro* (*189*). Even in single-cell-type cultures, direct cell-cell contact between MSCs increases chondrogenesis (*190, 191*). While most coculture pellets are formed from randomly mixed cells, a structured coculture pellet may provide additional advantages and more closely mimic developmental processes. The bilaminar cell pellet (BCP) is a coculture pellet composed of an inner sphere of MSC enclosed in an outer shell of NPC, allowing for homotypic interactions between cells of the same type within the layer and for heterotypic interactions between different cell types across a defined interface. This organization mimics the developmental processes of condensation, where cell aggregates form, and induction, where a mature layer of tissue directs the differentiation of a naïve one. The two cell types provide one another with stimulatory signaling, which allows for enhanced chondrogenesis, and increased cell proliferation (*192, 193*).

A similar bilaminar pellet with cocultured MSCs and articular chondrocytes also exhibited less hypertrophy than MSC-only pellets, and maintained proteoglycan synthesis under inflammatory conditions (*175*).

One interesting phenomenon observed in cocultured pellets is self-organization. Both randomly-organized and bilaminar pellets experienced budding of satellite pellets, and all satellite pellets had a bilayered structure with an MSC core and NPC outer layer, regardless of origin (*192*). Self-organization with an MSC core was also observed in cocultured pellets containing randomly mixed MSCs and primary chondrocytes (*167*). Cell type ratio may also influence the orientation of the organization (*173*).

Another question that arises from recent coculture studies is whether MSCs play a synthetic or trophic role in tissue regeneration. The traditional theory is that NPCs provide biochemical and/or physical cues to direct MSC differentiation into a chondrogenic phenotype. This is supported by upregulation of chondrogenic gene expression without hypertrophy in MSCs after coculture (*193–195*), and chondrogenic phenotypes of MSCs injected into an *in vivo* disc environment (*196*). Immunostaining in coculture BCPs also suggests that while NPCs initially produce the majority of collagen II and aggrecan in the pellet, over time MSCs in the center of the pellets also synthesize ECM (*175*, *193*). In coculture with chondrocytes, MSCs express chondrogenic markers and proteins, synthesize ECM, and exhibit chondrocyte-like morphology and surface markers (*169*, *178*, *179*, *182*, *197*, *198*).

However, researchers are increasingly questioning the theory of MSC differentiation because MSCs often have a beneficial effect without detectable engraftment or differentiation (*199, 200*). In animal studies targeting IVD and cartilage regeneration, MSCs are retained well in subcutaneous studies (*178*, *179*), but disappear or migrate to other regions when injected *in situ*

(*173*, *201*). Many *in vitro* studies have also observed a decrease in MSC:chondrocyte ratios over time with relatively constant overall cell numbers, suggesting that MSCs undergo cell death and are replaced by chondrocytes (*165*, *167*, *168*, *170*). In addition, several studies were unable to detect chondrogenic gene expression by MSCs, indicating that they did not play a synthetic role in the coculture (*142*, *166*, *167*).

Even though MSCs do not appear to persist and differentiate in the above examples, their initial presence still leads to increased matrix production and other benefits, suggesting that they have a trophic effect and provide stimulatory signals to cocultured cells. In recent years, MSCs have been proposed to influence regeneration with bioactive factors rather than differentiation in many different tissues and organ systems (*154*, *202*). Yang *et al.* theorized that MSCs injected into a mouse degenerative disc disease model stimulated endogenous notochordal cells to prevent cell death and increase matrix production (*196*). Other groups also found that MSCs induced cell proliferation of NPCs and chondrocytes in coculture, possibly by secreting the growth factor FGF-1 (*167*, *185*, *186*).

Another trophic role of MSCs, downmodulating inflammatory responses, has particular significance in therapeutic settings (*100*). MSC suppression of lymphocytes is well-documented and thought to be mediated by cell-cell contact and secreted anti-inflammatory molecules such as prostaglandin E2 (PGE-2), TGF-β, and IL-10 (*134*, *203*). MSCs have also been shown to modulate degenerative cascades in osteoarthritic chondrocytes by downregulating gene expression of inflammatory and catabolic factors (*176*, *183*). When cocultured with NPCs, they maintained a similar gene expression profile to single-cell-type controls (assayed by microarray), while NPCs experienced upregulation of collagen II and downregulation of inflammatory and catabolic genes (*151*). When cocultured with IVD fragments and lymphocytes, MSCs also

reduced lymphocyte activation and proliferation in a donor-dependent manner (*204*). As previously mentioned, secretion of anti-inflammatory PGE-2 and TGF-β were identified as possible mechanisms (*176*, *204*). Cocultured bilaminar cell pellets (BCPs) also demonstrated resilience in an inflammatory environment, in a rat degeneration model, and in a similar study with chondrocytes (*172*, *175*, *177*).

As with direct contact and soluble factor signaling, MSC differentiation and trophic effects may not be mutually exclusive. Several studies saw evidence of both (*168*, *175*, *193*, *196*). Additionally, environmental factors such as growth factors, preconditioning, and mechanical stimuli can influence cell behavior and are difficult to standardize among studies. A clearer understanding of these complex variables is crucial towards developing an optimal strategy for disc repair.

1.5 Objectives

The overall goal of this dissertation was to identify effects of microenvironmental and design factors on IVD tissue engineering constructs, using fabrication techniques to create specific culture conditions. First, we varied the design factors of cell type and cell configuration, using a microwell mold to create cocultured micopellets. We investigated MSCs and NPCs performed in a 3D culture system that simulated hypoxia and inflammation that is present in the degenerative microenvironment. We also simulated diffusion constraints of the microenvironment using a diffusion chamber system, and investigated the effects of cell type and hypoxic preconditioning on cell viability.

Specific Aims:

1. Identify the effects of both cell type and cell configuration on anabolic and catabolic gene expression of MSCs and NPCs *in vitro.*

a. Chapter 2 describes the anabolic and catabolic gene expression changes we observed in coculture and single-cell-type groups with individual-cell and micropellet configurations, in basal and hypoxic and inflammatory microenvironments, as well as self-organization behavior we observed in coculture micropellets.

2. Identify the effects of cell type and hypoxic preconditioning on cell viability in a diffusion-limited *in vitro* environment.

    a. Chapter 3 describes the diffusion chambers we manufactured and viable distance changes we observed in different cell type groups, which included cocultures as well as MSCs that were expanded in hypoxia.

Chapter 4 summarizes the conclusions of this thesis and suggests areas for future work. In particular, identifying more mechanisms behind cell-cell communication and adaptation to the degenerative microenvironment can motivate design improvements in tissue engineering.

1.6 References

1. M. V Risbud *et al.*, Defining the phenotype of young healthy nucleus pulposus cells: recommendations of the Spine Research Interest Group at the 2014 annual ORS meeting. *J. Orthop. Res.* **33**, 283–93 (2015).
2. J. N. Katz, Lumbar disc disorders and low-back pain: socioeconomic factors and consequences. *J. Bone Joint Surg. Am.* **88 Suppl 2**, 21–4 (2006).
3. L. J. Smith, N. L. Nerurkar, K.-S. Choi, B. D. Harfe, D. M. Elliott, Degeneration and regeneration of the intervertebral disc: lessons from development. *Dis. Model. Mech.* **4**, 31–41 (2011).

4. J. E. Mayer *et al.*, Genetic polymorphisms associated with intervertebral disc degeneration. *Spine J.* **13**, 299–317 (2013).

5. B. Alkhatib *et al.*, Acute mechanical injury of the human intervertebral disc: link to degeneration and pain. *Eur. Cell. Mater.* **28**, 98-110–1 (2014).

6. F. Wang, F. Cai, R. Shi, X.-H. Wang, X.-T. Wu, Aging and age related stresses: a senescence mechanism of intervertebral disc degeneration. *Osteoarthr. Cartil.* **24**, 398–408 (2016).

7. M. C. Battié, T. Videman, Lumbar disc degeneration: epidemiology and genetics. *J. Bone Jt. Surg.* **88 Suppl 2**, 3–9 (2006).

8. J. J. Costi, B. J. Freeman, D. M. Elliott, Intervertebral disc properties: challenges for biodevices. *Expert Rev. Med. Devices*. **8**, 357–376 (2011).

9. H. B. Henriksson, H. Brisby, Development and regeneration potential of the mammalian intervertebral disc. *Cells. Tissues. Organs*. **197**, 1–13 (2013).

10. V. Sivakamasundari, T. Lufkin, Bridging the Gap: Understanding Embryonic Intervertebral Disc Development. *Cell Dev. Biol.* **1** (2012).

11. C. L. Dahia, E. J. Mahoney, A. A. Durrani, C. Wylie, Postnatal growth, differentiation, and aging of the mouse intervertebral disc. *Spine (Phila. Pa. 1976).* **34**, 447–55 (2009).

12. J. C. Lotz, A. J. Fields, E. C. Liebenberg, The role of the vertebral end plate in low back pain. *Glob. Spine J.* **3**, 153–64 (2013).

13. V. Lefebvre, P. Bhattaram, Vertebrate skeletogenesis. *Curr. Top. Dev. Biol.* **90**, 291–317 (2010).

14. T. R. Oegema, Biochemistry of the intervertebral disc. *Clin. Sports Med.* **12**, 419–39 (1993).

15. J. A. Buckwalter, Aging and degeneration of the human intervertebral disc. *Spine (Phila. Pa. 1976).* **20** (1995), pp. 1307–14.

16. S. Holm, A. Nachemson, Variations in the nutrition of the canine intervertebral disc induced by motion. *Spine (Phila. Pa. 1976).* **8**, 866–74.

17. F. Marchand, A. M. Ahmed, Investigation of the laminate structure of lumbar disc anulus fibrosus. *Spine (Phila. Pa. 1976).* **15** (1990), pp. 402–410.

18. S. Roberts, Disc morphology in health and disease. *Biochem. Soc. Trans.* **30**, 864–9 (2002).

19. P. J. Roughley, Biology of intervertebral disc aging and degeneration: involvement of the extracellular matrix. *Spine (Phila. Pa. 1976).* **29**, 2691–9 (2004).

20. J. M. Cloyd *et al.*, Material properties in unconfined compression of human nucleus pulposus, injectable hyaluronic acid-based hydrogels and tissue engineering scaffolds. *Eur. Spine J.* **16**, 1892–1898 (2007).

21. D. L. Skaggs, M. Weidenbaum, J. C. Iatridis, A. Ratcliffe, V. C. Mow, Regional variation in tensile properties and biochemical composition of the human lumbar anulus fibrosus. *Spine (Phila. Pa. 1976).* **19** (1994), pp. 1310–1319.

22. C. R. Lee *et al.*, A phenotypic comparison of intervertebral disc and articular cartilage cells in the rat. *Eur. Spine J.* **16**, 2174–2185 (2007).

23. L. A. Vonk *et al.*, Caprine articular, meniscus and intervertebral disc cartilage: An integral analysis of collagen network and chondrocytes. *Matrix Biol.* **29**, 209–218 (2010).

24. M. T. Bayliss, B. Johnstone, in *The Lumbar Spine and Back Pain* (Churchill Livingstone, ed. 4, 1992), pp. 111–127.

25. A. J. Freemont, The cellular pathobiology of the degenerate intervertebral disc and

discogenic back pain. *Rheumatology*. **48**, 5–10 (2009).

26. A. Wei, B. Shen, L. Williams, A. Diwan, Mesenchymal stem cells: potential application in intervertebral disc regeneration. *Transl. Pediatr.* **3**, 71–90 (2014).

27. F. Mwale, P. Roughley, J. Antoniou, Distinction between the extracellular matrix of the nucleus pulposus and hyaline cartilage: a requisite for tissue engineering of intervertebral disc. *Eur. Cell. Mater.* **8**, 58-63–4 (2004).

28. S. Poiraudeau *et al.*, Phenotypic characteristics of rabbit intervertebral disc cells. Comparison with cartilage cells from the same animals. *Spine (Phila. Pa. 1976).* **24**, 837–44 (1999).

29. J. C. Iatridis, M. Weidenbaum, L. A. Setton, V. C. Mow, Is the nucleus pulposus a solid or a fluid? Mechanical behaviors of the nucleus pulposus of the human intervertebral disc. *Spine (Phila. Pa. 1976).* **21**, 1174–84 (1996).

30. A. J. Fields, F. Sahli, A. G. Rodriguez, J. C. Lotz, Seeing double: a comparison of microstructure, biomechanical function, and adjacent disc health between double- and single-layer vertebral endplates. *Spine (Phila. Pa. 1976).* **37**, E1310-7 (2012).

31. S. Roberts, J. Menage, J. P. Urban, Biochemical and structural properties of the cartilage end-plate and its relation to the intervertebral disc. *Spine (Phila. Pa. 1976).* **14**, 166–74 (1989).

32. H. Li, C. Z. Liang, Q. X. Chen, Regulatory role of hypoxia inducible factor in the biological behavior of nucleus pulposus cells. *Yonsei Med. J.* **54**, 807–812 (2013).

33. S. Roberts, H. Evans, Histology and Pathology of the human intervertebral disc. *J. Bone Jt. Surg.*, 2000 (2006).

34. J. Clouet *et al.*, Identification of phenotypic discriminating markers for intervertebral disc

cells and articular chondrocytes. *Rheumatology (Oxford).* **48**, 1447–1450 (2009).

35. G. Pattappa *et al.*, Diversity of intervertebral disc cells: phenotype and function. *J. Anat.* **221**, 480–496 (2012).

36. K. Chen *et al.*, Autophagy Is a Protective Response to the Oxidative Damage to Endplate Chondrocytes in Intervertebral Disc: Implications for the Treatment of Degenerative Lumbar Disc. *Oxid. Med. Cell. Longev.* **2017**, 1–9 (2017).

37. A. A. Thorpe, A. L. A. Binch, L. B. Creemers, C. Sammon, C. L. Le Maitre, Nucleus pulposus phenotypic markers to determine stem cell differentiation: fact or fiction? *Oncotarget*. **7**, 2189–200 (2016).

38. G. J. Kerr, M. A. Veras, M. K. M. Kim, C. A. Séguin, Decoding the intervertebral disc: Unravelling the complexities of cell phenotypes and pathways associated with degeneration and mechanotransduction. *Semin. Cell Dev. Biol.* **62**, 94–103 (2017).

39. E. C. Collin *et al.*, Unique glycosignature for intervertebral disc and articular cartilage cells and tissues in immaturity and maturity. *Sci. Rep.* **6**, 23062 (2016).

40. J. C. Lotz, A. H. Hsieh, in *The Intervertebral Disc* (Springer Vienna, Vienna, 2014), vol. 21, pp. 109–124.

41. R. Rodrigues-Pinto, S. M. Richardson, J. A. Hoyland, An understanding of intervertebral disc development, maturation and cell phenotype provides clues to direct cell-based tissue regeneration therapies for disc degeneration. *Eur. Spine J.* **23**, 1803–1814 (2014).

42. P. P. A. Vergroesen *et al.*, Mechanics and biology in intervertebral disc degeneration: A vicious circle. *Osteoarthr. Cartil.* **23**, 1057–1070 (2015).

43. N. V. Vo *et al.*, Expression and regulation of metalloproteinases and their inhibitors in intervertebral disc aging and degeneration. *Spine J.* **13**, 331–341 (2013).

44. A. J. Fields *et al.*, Alterations in intervertebral disc composition, matrix homeostasis and biomechanical behavior in the UCD-T2DM rat model of type 2 diabetes. *J. Orthop. Res.* **33**, 738–46 (2015).

45. S. M. Fabiane, K. J. Ward, J. C. Iatridis, F. M. K. Williams, Does type 2 diabetes mellitus promote intervertebral disc degeneration? *Eur. Spine J.* **25**, 2716–2720 (2016).

46. D. Samartzis, J. Karppinen, D. Chan, K. D. K. Luk, K. M. C. Cheung, The association of lumbar intervertebral disc degeneration on magnetic resonance imaging with body mass index in overweight and obese adults: a population-based study. *Arthritis Rheum.* **64**, 1488–96 (2012).

47. K. Luoma *et al.*, Lumbar disc degeneration in relation to occupation. *Scand. J. Work. Environ. Health.* **24**, 358–66 (1998).

48. P. N. Sambrook, A. J. MacGregor, T. D. Spector, Genetic influences on cervical and lumbar disc degeneration: a magnetic resonance imaging study in twins. *Arthritis Rheum.* **42**, 366–72 (1999).

49. M. Teraguchi *et al.*, Progression, incidence, and risk factors for intervertebral disc degeneration in a longitudinal population-based cohort: the Wakayama Spine Study. *Osteoarthr. Cartil.* (2017), doi:10.1016/j.joca.2017.01.001.

50. G. Hassett, D. J. Hart, N. J. Manek, D. V Doyle, T. D. Spector, Risk factors for progression of lumbar spine disc degeneration: the Chingford Study. *Arthritis Rheum.* **48**, 3112–7 (2003).

51. M. Teraguchi *et al.*, Prevalence and distribution of intervertebral disc degeneration over the entire spine in a population-based cohort: the Wakayama Spine Study. *Osteoarthr. Cartil.* **22**, 104–110 (2014).

52. M. Ghannam *et al.*, Surgical anatomy, radiological features, and molecular biology of the lumbar intervertebral discs. *Clin. Anat.* **30**, 251–266 (2017).

53. J. C. Lotz *et al.*, New treatments and imaging strategies in degenerative disease of the intervertebral disks. *Radiology*. **264**, 6–19 (2012).

54. Y.-H. Zhang, C.-Q. Zhao, L.-S. Jiang, X.-D. Chen, L.-Y. Dai, Modic changes: a systematic review of the literature. *Eur. Spine J.* **17**, 1289–1299 (2008).

55. I. Ract *et al.*, A review of the value of MRI signs in low back pain. *Diagn. Interv. Imaging*. **96**, 239–249 (2015).

56. C. W. Pfirrmann, A. Metzdorf, M. Zanetti, J. Hodler, N. Boos, Magnetic resonance classification of lumbar intervertebral disc degeneration. *Spine (Phila. Pa. 1976).* **26**, 1873–8 (2001).

57. W. Brinjikji *et al.*, Systematic Literature Review of Imaging Features of Spinal Degeneration in Asymptomatic Populations. *Am. J. Neuroradiol.* **36**, 811–816 (2015).

58. N. L. Marinelli, V. M. Haughton, A. Muñoz, P. A. Anderson, T2 relaxation times of intervertebral disc tissue correlated with water content and proteoglycan content. *Spine (Phila. Pa. 1976).* **34**, 520–4 (2009).

59. A. M. Ellingson, T. M. Nagel, D. W. Polly, J. Ellermann, D. J. Nuckley, Quantitative T2* (T2 star) relaxation times predict site specific proteoglycan content and residual mechanics of the intervertebral disc throughout degeneration. *J. Orthop. Res.* **32**, 1083–1089 (2014).

60. S. Trattnig *et al.*, Lumbar intervertebral disc abnormalities: comparison of quantitative T2 mapping with conventional MR at 3.0 T. *Eur. Radiol.* **20**, 2715–22 (2010).

61. G. H. Welsch *et al.*, Parametric T2 and T2* mapping techniques to visualize intervertebral

disc degeneration in patients with low back pain: initial results on the clinical use of 3.0 Tesla MRI. *Skeletal Radiol.* **40**, 543–551 (2011).

62. S. Hoppe *et al.*, Axial T2* mapping in intervertebral discs: a new technique for assessment of intervertebral disc degeneration. *Eur. Radiol.* **22**, 2013–2019 (2012).

63. A. J. Fields, M. Han, R. Krug, J. C. Lotz, Cartilaginous end plates: Quantitative MR imaging with very short echo times-orientation dependence and correlation with biochemical composition. *Radiology*. **274**, 482–9 (2015).

64. W. C. Bae *et al.*, Morphology of the cartilaginous endplates in human intervertebral disks with ultrashort echo time MR imaging. *Radiology*. **266**, 564–74 (2013).

65. A. Borthakur *et al.*, T1ρ magnetic resonance imaging and discography pressure as novel biomarkers for disc degeneration and low back pain. *Spine (Phila. Pa. 1976).* **36**, 2190–6 (2011).

66. J. D. Auerbach *et al.*, In vivo quantification of human lumbar disc degeneration using T(1rho)-weighted magnetic resonance imaging. *Eur. Spine J.* **15 Suppl 3**, S338-44 (2006).

67. M. Fenty *et al.*, Novel imaging of the intervertebral disk and pain. *Glob. Spine J.* **3**, 127–32 (2013).

68. Y.-X. J. Wáng *et al.*, T1ρ magnetic resonance: basic physics principles and applications in knee and intervertebral disc imaging. *Quant. Imaging Med. Surg.* **5**, 858–85 (2015).

69. S. Basu *et al.*, Novel Quantitative Techniques for Assessing Regional and Global Function and Structure Based on Modern Imaging Modalities: Implications for Normal Variation, Aging and Diseased States. *Semin. Nucl. Med.* **37**, 223–239 (2007).

70. R. Reddy *et al.*, Sodium MRI of human articular cartilage in vivo. *Magn. Reson. Med.* **39**, 697–701 (1998).

71. C. Wang *et al.*, Validation of Sodium Magnetic Resonance Imaging of Intervertebral Disc. *Spine (Phila. Pa. 1976).* **35**, 505–510 (2010).

72. V. N. Wijayathunga *et al.*, A Nondestructive Method to Distinguish the Internal Constituent Architecture of the Intervertebral Discs Using 9.4 Tesla Magnetic Resonance Imaging. *Spine (Phila. Pa. 1976).* **40**, E1315-22 (2015).

73. L. feng Lao, G. bin Zhong, Q. yi Li, Z. de Liu, Kinetic magnetic resonance imaging analysis of spinal degeneration: a systematic review. *Orthop. Surg.* **6**, 294–299 (2014).

74. M. A. Ibrahim, A. Jesmanowicz, J. S. Hyde, L. Estkowski, V. M. Haughton, Contrast enhancement of normal intervertebral disks: time and dose dependence. *AJNR. Am. J. Neuroradiol.* **15**, 419–23 (1994).

75. R. Arun *et al.*, 2009 ISSLS Prize Winner: What influence does sustained mechanical load have on diffusion in the human intervertebral disc?: an in vivo study using serial postcontrast magnetic resonance imaging. *Spine (Phila. Pa. 1976).* **34**, 2324–37 (2009).

76. S. Rajasekaran *et al.*, ISSLS prize winner: A study of diffusion in human lumbar discs: a serial magnetic resonance imaging study documenting the influence of the endplate on diffusion in normal and degenerate discs. *Spine (Phila. Pa. 1976).* **29**, 2654–67 (2004).

77. J. S. Ross, M. T. Modic, T. J. Masaryk, Tears of the anulus fibrosus: assessment with Gd-DTPA-enhanced MR imaging. *Am. J. Roentgenol.* **154**, 159–162 (1990).

78. E. J. Carragee, T. F. Alamin, Discography: A review. *Spine J.* **1**, 364–372 (2001).

79. E. J. Carragee *et al.*, 2009 ISSLS Prize Winner: Does discography cause accelerated progression of degeneration changes in the lumbar disc: a ten-year matched cohort study. *Spine (Phila. Pa. 1976).* **34**, 2338–45 (2009).

80. J. Tehranzadeh, Discography 2000. *Radiol. Clin. North Am.* **36**, 463–95 (1998).

81. X. Zhou *et al.*, The roles and perspectives of microRNAs as biomarkers for intervertebral disc degeneration. *J. Tissue Eng. Regen. Med.* (2017), doi:10.1002/term.2261.

82. B. Zhao, M. Lu, D. Wang, H. Li, X. He, Genome-Wide Identification of Long Noncoding RNAs in Human Intervertebral Disc Degeneration by RNA Sequencing. *Biomed Res. Int.* **2016**, 3684875 (2016).

83. C. Dagostino *et al.*, Validation of standard operating procedures in a multicenter retrospective study to identify -omics biomarkers for chronic low back pain. *PLoS One*. **12**, e0176372 (2017).

84. M. Allegri *et al.*, "Omics" biomarkers associated with chronic low back pain: protocol of a retrospective longitudinal study. *BMJ Open*. **6**, e012070 (2016).

85. S. Grad *et al.*, Systemic blood plasma CCL5 and CXCL6: Potential biomarkers for human lumbar disc degeneration. *Eur. Cells Mater.* **31**, 1–10 (2016).

86. G. Lippi *et al.*, The serum concentrations of leptin and MCP-1 independently predict low back pain duration. *Clin. Chem. Lab. Med.* (2017), doi:10.1515/cclm-2016-0942.

87. Y. Li, J. Liu, Z.-Z. Liu, D.-P. Duan, Inflammation in low back pain may be detected from the peripheral blood: suggestions for biomarker. *Biosci. Rep.* **36** (2016), doi:10.1042/BSR20160187.

88. S. Yang, C.-C. Wu, T. T.-F. Shih, Y.-H. Sun, F.-H. Lin, In vitro study on interaction between human nucleus pulposus cells and mesenchymal stem cells through paracrine stimulation. *Spine (Phila. Pa. 1976).* **33**, 1951–7 (2008).

89. J. Kraemer, D. Kolditz, R. Gowin, Water and electrolyte content of human intervertebral discs under variable load. *Spine (Phila. Pa. 1976).* **10**, 69–71 (1985).

90. G. D. O'Connell, I. B. Newman, M. A. Carapezza, Effect of Long-Term Osmotic Loading

Culture on Matrix Synthesis from Intervertebral Disc Cells. *Biores. Open Access*. **3**, 242–249 (2014).

91. K. Wuertz, K. E. Godburn, C. Neidlinger-Wilke, J. Urban, J. C. Iatridis, Behavior of mesenchymal stem cellsin the chemical microenvironment of the intervertebral disc. *Spine (Phila. Pa. 1976).* **33**, 1843–1849 (2008).

92. S. M. Naqvi, C. T. Buckley, Bone Marrow Stem Cells in Response to Intervertebral Disc-Like Matrix Acidity and Oxygen Concentration. *Spine (Phila. Pa. 1976).* **41**, 743–750 (2016).

93. J. W. Stairmand, S. Holm, J. P. Urban, Factors influencing oxygen concentration gradients in the intervertebral disc. A theoretical analysis. *Spine (Phila. Pa. 1976).* **16**, 444–449 (1991).

94. H. a Horner, J. P. Urban, 2001 Volvo Award Winner in Basic Science Studies: Effect of nutrient supply on the viability of cells from the nucleus pulposus of the intervertebral disc. *Spine (Phila. Pa. 1976).* **26**, 2543–9 (2001).

95. C. Feng *et al.*, ROS: Crucial Intermediators in the Pathogenesis of Intervertebral Disc Degeneration. *Oxid. Med. Cell. Longev.* **2017**, 1–12 (2017).

96. M. Molinos *et al.*, Inflammation in intervertebral disc degeneration and regeneration. *J. R. Soc. Interface*. **12**, 20141191–20141191 (2015).

97. W. E. B. Johnson, S. Stephan, S. Roberts, The influence of serum, glucose and oxygen on intervertebral disc cell growth in vitro: implications for degenerative disc disease. *Arthritis Res. Ther.* **10**, R46 (2008).

98. J. Chiche *et al.*, Hypoxia-Inducible Carbonic Anhydrase IX and XII Promote Tumor Cell Growth by Counteracting Acidosis through the Regulation of the Intracellular pH. *Cancer*

Res. **69**, 358–368 (2009).

99. K. L. E. Phillips *et al.*, Potential roles of cytokines and chemokines in human intervertebral disc degeneration: interleukin-1 is a master regulator of catabolic processes. *Osteoarthritis Cartilage.* **23**, 1165–77 (2015).

100. N. G. Singer, A. I. Caplan, Mesenchymal stem cells: mechanisms of inflammation. *Annu. Rev. Pathol.* **6**, 457–478 (2011).

101. S. J. Millward-Sadler, P. W. Costello, A. J. Freemont, J. A. Hoyland, Regulation of catabolic gene expression in normal and degenerate human intervertebral disc cells: implications for the pathogenesis of intervertebral disc degeneration. *Arthritis Res. Ther.* **11**, R65 (2009).

102. Y. C. Huang, V. Y. L. Leung, W. W. Lu, K. D. K. Luk, The effects of microenvironment in mesenchymal stem cell-based regeneration of intervertebral disc. *Spine J.* **13**, 352–362 (2013).

103. Z. Sun *et al.*, Immune cascades in human intervertebral disc: the pros and cons. *Int. J. Clin. Exp. Pathol.* **6**, 1009–14 (2013).

104. M. V Risbud, I. M. Shapiro, Role of cytokines in intervertebral disc degeneration: pain and disc content. *Nat. Rev. Rheumatol.* **10**, 44–56 (2014).

105. H. E. Gruber, J. A. Ingram, H. J. Norton, E. N. Hanley, Senescence in cells of the aging and degenerating intervertebral disc: immunolocalization of senescence-associated beta-galactosidase in human and sand rat discs. *Spine (Phila. Pa. 1976).* **32**, 321–7 (2007).

106. P. Li *et al.*, The inflammatory cytokine TNF-α promotes the premature senescence of rat nucleus pulposus cells via the PI3K/Akt signaling pathway. *Sci. Rep.* **7**, 42938 (2017).

107. X. Li, J. P. Lee, G. Balian, D. Greg Anderson, Modulation of chondrocytic properties of

fat-derived mesenchymal cells in co-cultures with nucleus pulposus. *Connect. Tissue Res.* **46**, 75–82 (2005).

108. R. D. Bowles, L. A. Setton, Biomaterials for intervertebral disc regeneration and repair. *Biomaterials*. **129**, 54–67 (2017).

109. K. Masuda, T. R. Oegema, H. S. An, Growth factors and treatment of intervertebral disc degeneration. *Spine (Phila. Pa. 1976).* **29**, 2757–69 (2004).

110. N. Farhang *et al.*, *Tissue Eng. Part A*, in press, doi:10.1089/ten.tea.2016.0441.

111. I. T. M. Arkesteijn, E. Potier, K. Ito, The Regenerative Potential of Notochordal Cells in a Nucleus Pulposus Explant. *Glob. Spine J.* **7**, 14–20 (2017).

112. C. J. Hunter, J. R. Matyas, N. a Duncan, The notochordal cell in the nucleus pulposus: a review in the context of tissue engineering. *Tissue Eng.* **9**, 667–77 (2003).

113. H. Wang *et al.*, Utilization of stem cells in alginate for nucleus pulposus tissue engineering. *Tissue Eng. Part A.* **20**, 908–20 (2014).

114. G. Vadalà, F. Russo, L. Ambrosio, M. Loppini, V. Denaro, Stem cells sources for intervertebral disc regeneration. *World J. Stem Cells*. **8**, 185–201 (2016).

115. M. V Risbud *et al.*, Nucleus pulposus cells express HIF-1 alpha under normoxic culture conditions: a metabolic adaptation to the intervertebral disc microenvironment. *J. Cell. Biochem.* **98**, 152–9 (2006).

116. K.-I. Lee *et al.*, Tissue engineering of the intervertebral disc with cultured nucleus pulposus cells using atelocollagen scaffold and growth factors. *Spine (Phila. Pa. 1976).* **37**, 452–8 (2012).

117. T. Ganey *et al.*, Disc chondrocyte transplantation in a canine model: a treatment for degenerated or damaged intervertebral disc. *Spine (Phila. Pa. 1976).* **28**, 2609–20 (2003).

118. K. Nishimura, J. Mochida, Percutaneous reinsertion of the nucleus pulposus. An experimental study. *Spine (Phila. Pa. 1976).* **23**, 1531–8; discussion 1539 (1998).

119. M. Okuma, J. Mochida, K. Nishimura, K. Sakabe, K. Seiki, Reinsertion of stimulated nucleus pulposus cells retards intervertebral disc degeneration: Anin vitro andin vivo experimental study. *J. Orthop. Res.* **18**, 988–997 (2000).

120. T. Nomura, J. Mochida, M. Okuma, K. Nishimura, K. Sakabe, Nucleus pulposus allograft retards intervertebral disc degeneration. *Clin. Orthop. Relat. Res.*, 94–101 (2001).

121. G. Feng *et al.*, Transplantation of mesenchymal stem cells and nucleus pulposus cells in a degenerative disc model in rabbits: a comparison of 2 cell types as potential candidates for disc regeneration. *J. Neurosurg. Spine*. **14**, 322–329 (2011).

122. B. Huang, Y. Zhuang, C.-Q. Li, L.-T. Liu, Y. Zhou, Regeneration of the intervertebral disc with nucleus pulposus cell-seeded collagen II/hyaluronan/chondroitin-6-sulfate tri-copolymer constructs in a rabbit disc degeneration model. *Spine (Phila. Pa. 1976).* **36**, 2252–9 (2011).

123. H. E. Gruber *et al.*, Autologous intervertebral disc cell implantation: a model using Psammomys obesus, the sand rat. *Spine (Phila. Pa. 1976).* **27**, 1626–33 (2002).

124. H. J. Meisel *et al.*, Clinical experience in cell-based therapeutics: Disc chondrocyte transplantation. *Biomol. Eng.* **24**, 5–21 (2007).

125. C. Hohaus, T. M. Ganey, Y. Minkus, H. J. Meisel, Cell transplantation in lumbar spine disc degeneration disease. *Eur. Spine J.* **17**, 492–503 (2008).

126. H. J. Meisel *et al.*, Clinical experience in cell-based therapeutics: intervention and outcome. *Eur. Spine J.* **15**, 397–405 (2006).

127. D. Drazin, J. Rosner, P. Avalos, F. Acosta, Stem Cell Therapy for Degenerative Disc

Disease. *Adv. Orthop.* **2012**, 1–8 (2012).

128. Y. Moriguchi *et al.*, Biological Treatment Approaches for Degenerative Disk Disease: A Literature Review of In Vivo Animal and Clinical Data. *Glob. Spine J.* **6**, 497–518 (2016).

129. N. Kregar Velikonja *et al.*, Cell sources for nucleus pulposus regeneration. *Eur. Spine J.* **23**, 364–374 (2014).

130. J. Mochida *et al.*, Intervertebral disc repair with activated nucleus pulposus cell transplantation: a three-year, prospective clinical study of its safety. *Eur. Cell. Mater.* **29**, 202–12; discussion 212 (2015).

131. M. Dominici *et al.*, Minimal criteria for defining multipotent mesenchymal stromal cells. The International Society for Cellular Therapy position statement. *Cytotherapy*. **8**, 315–7 (2006).

132. H.-J. Bühring *et al.*, Novel markers for the prospective isolation of human MSC. *Ann. N. Y. Acad. Sci.* **1106**, 262–71 (2007).

133. R. J. MacFarlane *et al.*, Anti-inflammatory role and immunomodulation of mesenchymal stem cells in systemic joint diseases: potential for treatment. *Expert Opin. Ther. Targets*. **17**, 243–54 (2013).

134. A. I. Caplan, D. Correa, The MSC: an injury drugstore. *Cell Stem Cell*. **9**, 11–5 (2011).

135. P. Anderson, A. B. Carrillo-Gálvez, A. García-Pérez, M. Cobo, F. Martín, CD105 (endoglin)-negative murine mesenchymal stromal cells define a new multipotent subpopulation with distinct differentiation and immunomodulatory capacities. *PLoS One*. **8**, e76979 (2013).

136. N. S. Hwang, S. Varghese, C. Puleo, Z. Zhang, J. Elisseeff, Morphogenetic signals from chondrocytes promote chondrogenic and osteogenic differentiation of mesenchymal stem

cells. *J. Cell. Physiol.* **212**, 281–284 (2007).

137. S. Giovannini *et al.*, Micromass co-culture of human articular chondrocytes and human bone marrow mesenchymal stem cells to investigate stable neocartilage tissue formation in vitro. *Eur. Cell. Mater.* **20**, 245–259 (2010).

138. I. Sekiya, J. T. Vuoristo, B. L. Larson, D. J. Prockop, In vitro cartilage formation by human adult stem cells from bone marrow stroma defines the sequence of cellular and molecular events during chondrogenesis. *Proc. Natl. Acad. Sci. U. S. A.* **99**, 4397–402 (2002).

139. R. L. Mauck, X. Yuan, R. S. Tuan, Chondrogenic differentiation and functional maturation of bovine mesenchymal stem cells in long-term agarose culture. *Osteoarthritis Cartilage*. **14**, 179–89 (2006).

140. S. M. Richardson, N. Hughes, J. a Hunt, A. J. Freemont, J. a Hoyland, Human mesenchymal stem cell differentiation to NP-like cells in chitosan-glycerophosphate hydrogels. *Biomaterials*. **29**, 85–93 (2008).

141. J. V Stoyanov *et al.*, Role of hypoxia and growth and differentiation factor-5 on differentiation of human mesenchymal stem cells towards intervertebral nucleus pulposus-like cells. *Eur. Cells Mater.* **21**, 533–47 (2011).

142. X. Mo *et al.*, Variations in the ratios of co-cultured mesenchymal stem cells and chondrocytes regulate the expression of cartilaginous and osseous phenotype in alginate constructs. *Bone*. **45**, 42–51 (2009).

143. S. M. Richardson *et al.*, Mesenchymal stem cells in regenerative medicine: Focus on articular cartilage and intervertebral disc regeneration. *Methods*. **99**, 69–80 (2015).

144. D. Sakai *et al.*, Differentiation of mesenchymal stem cells transplanted to a rabbit

degenerative disc model: potential and limitations for stem cell therapy in disc regeneration. *Spine (Phila. Pa. 1976).* **30**, 2379–2387 (2005).

145. A. Wei *et al.*, The fate of transplanted xenogeneic bone marrow-derived stem cells in rat intervertebral discs. *J. Orthop. Res.* **27**, 374–379 (2009).

146. Y.-G. Zhang, X. Guo, P. Xu, L.-L. Kang, J. Li, Bone mesenchymal stem cells transplanted into rabbit intervertebral discs can increase proteoglycans. *Clin. Orthop. Relat. Res.*, 219–26 (2005).

147. S. C. W. Chan *et al.*, Cryopreserved intervertebral disc with injected bone marrow–derived stromal cells: a feasibility study using organ culture. *Spine J.* **10**, 486–496 (2010).

148. J. H. Jeong *et al.*, Human mesenchymal stem cells implantation into the degenerated coccygeal disc of the rat. *Cytotechnology*. **59**, 55–64 (2009).

149. F. L. Acosta *et al.*, Porcine Intervertebral Disc Repair Using Allogeneic Juvenile Articular Chondrocytes or Mesenchymal Stem Cells. *Tissue Eng. Part A.* **17**, 3045–3055 (2011).

150. G. Crevensten *et al.*, Intervertebral disc cell therapy for regeneration: mesenchymal stem cell implantation in rat intervertebral discs. *Ann. Biomed. Eng.* **32**, 430–4 (2004).

151. T. Miyamoto *et al.*, Intradiscal transplantation of synovial mesenchymal stem cells prevents intervertebral disc degeneration through suppression of matrix metalloproteinase-related genes in nucleus pulposus cells in rabbits. *Arthritis Res. Ther.* **12**, R206 (2010).

152. R. L.-H. Yim *et al.*, A Systematic Review of the Safety and Efficacy of Mesenchymal Stem Cells for Disc Degeneration: Insights and Future Directions for Regenerative Therapeutics. *Stem Cells Dev.* **23**, 2553–2567 (2014).

153. J. A. Ankrum, J. F. Ong, J. M. Karp, Mesenchymal stem cells: immune evasive, not immune privileged. *Nat. Biotechnol.* **32**, 252–60 (2014).

154. A. I. Caplan, J. E. Dennis, Mesenchymal stem cells as trophic mediators. *J. Cell. Biochem.* **98**, 1076–84 (2006).

155. S. Vedicherla, C. T. Buckley, Cell-based therapies for intervertebral disc and cartilage regeneration— Current concepts, parallels, and perspectives. *J. Orthop. Res.* **35**, 8–22 (2017).

156. T. Yoshikawa, Y. Ueda, K. Miyazaki, M. Koizumi, Y. Takakura, Disc regeneration therapy using marrow mesenchymal cell transplantation: a report of two case studies. *Spine (Phila. Pa. 1976).* **35**, E475–E480 (2010).

157. L. Orozco *et al.*, Intervertebral Disc Repair by Autologous Mesenchymal Bone Marrow Cells: A Pilot Study. *Transplantation*. **92**, 822–828 (2011).

158. K. A. Pettine, M. B. Murphy, R. K. Suzuki, T. T. Sand, Percutaneous injection of autologous bone marrow concentrate cells significantly reduces lumbar discogenic pain through 12 months. *Stem Cells*. **33**, 146–156 (2015).

159. K. Pettine, R. Suzuki, T. Sand, M. Murphy, Treatment of discogenic back pain with autologous bone marrow concentrate injection with minimum two year follow-up. *Int. Orthop.* **40**, 135–140 (2016).

160. Mesoblast, Trial Results: MPC-06-ID Phase 2 Chronic Low Back Pain Due to Disc Degeneration Clinical Trial (2015), (available at http://www.mesoblast.com/clinical-trial-results/mpc-06-id-phase-2).

161. M. Mendicino, A. M. Bailey, K. Wonnacott, R. K. Puri, S. R. Bauer, MSC-Based Product Characterization for Clinical Trials: An FDA Perspective. *Cell Stem Cell*. **14**, 141–145 (2014).

162. J. Zeckser, M. Wolff, J. Tucker, J. Goodwin, Multipotent Mesenchymal Stem Cell

Treatment for Discogenic Low Back Pain and Disc Degeneration. *Stem Cells Int.* **2016**, 1–13 (2016).

163. G. R. Fajardo-Orduña *et al.*, Bone Marrow Mesenchymal Stromal Cells from Clinical Scale Culture: In Vitro Evaluation of Their Differentiation, Hematopoietic Support, and Immunosuppressive Capacities. *Stem Cells Dev.* **25**, 1299–1310 (2016).

164. N. K. Paschos, W. E. Brown, R. Eswaramoorthy, J. C. Hu, K. A. Athanasiou, Advances in tissue engineering through stem cell-based co-culture. *J. Tissue Eng. Regen. Med.* **9**, 488–503 (2015).

165. V. V Meretoja, R. L. Dahlin, F. K. Kasper, A. G. Mikos, Enhanced chondrogenesis in co-cultures with articular chondrocytes and mesenchymal stem cells. *Biomaterials*. **33**, 6362–9 (2012).

166. K. Tsuchiya, G. Chen, T. Ushida, T. Matsuno, T. Tateishi, The effect of coculture of chondrocytes with mesenchymal stem cells on their cartilaginous phenotype in vitro. *Mater. Sci. Eng. C.* **24**, 391–396 (2004).

167. L. Wu *et al.*, Trophic effects of mesenchymal stem cells increase chondrocyte proliferation and matrix formation. *Tissue Eng. Part A.* **17**, 1425–36 (2011).

168. C. Acharya *et al.*, Enhanced chondrocyte proliferation and mesenchymal stromal cells chondrogenesis in coculture pellets mediate improved cartilage formation. *J. Cell. Physiol.* **227**, 88–97 (2012).

169. L. Bian, D. Y. Zhai, R. L. Mauck, J. A. Burdick, Coculture of human mesenchymal stem cells and articular chondrocytes reduces hypertrophy and enhances functional properties of engineered cartilage. *Tissue Eng. Part A.* **17**, 1137–45 (2011).

170. T. S. de Windt *et al.*, Direct Cell–Cell Contact with Chondrocytes Is a Key Mechanism in

Multipotent Mesenchymal Stromal Cell-Mediated Chondrogenesis. *Tissue Eng. Part A.* **21**, 2536–2547 (2015).

171. T. Watanabe *et al.*, Human nucleus pulposus cells significantly enhanced biological properties in a coculture system with direct cell-to-cell contact with autologous mesenchymal stem cells. *J. Orthop. Res.* **28**, 623–30 (2010).

172. A. a Allon *et al.*, Structured coculture of stem cells and disc cells prevent disc degeneration in a rat model. *Spine J.* **10**, 1089–97 (2010).

173. S. Sobajima *et al.*, Feasibility of a stem cell therapy for intervertebral disc degeneration. *Spine J.* **8**, 888–896 (2008).

174. J. Fischer, A. Dickhut, M. Rickert, W. Richter, Human articular chondrocytes secrete parathyroid hormone-related protein and inhibit hypertrophy of mesenchymal stem cells in coculture during chondrogenesis. *Arthritis Rheum.* **62**, 2696–706 (2010).

175. M. E. Cooke *et al.*, Structured three-dimensional co-culture of mesenchymal stem cells with chondrocytes promotes chondrogenic differentiation without hypertrophy. *Osteoarthritis Cartilage.* **19**, 1210–8 (2011).

176. C. Manferdini *et al.*, Adipose-derived mesenchymal stem cells exert antiinflammatory effects on chondrocytes and synoviocytes from osteoarthritis patients through prostaglandin E2. *Arthritis Rheum.* **65**, 1271–81 (2013).

177. A. A. Allon, K. Butcher, R. A. Schneider, J. C. Lotz, Structured bilaminar coculture outperforms stem cells and disc cells in a simulated degenerate disc environment. *Spine (Phila. Pa. 1976).* **37**, 813–8 (2012).

178. H. N. Yang *et al.*, The use of green fluorescence gene (GFP)-modified rabbit mesenchymal stem cells (rMSCs) co-cultured with chondrocytes in hydrogel constructs to

reveal the chondrogenesis of MSCs. *Biomaterials*. **30**, 6374–85 (2009).

179. X. Liu *et al.*, In vivo ectopic chondrogenesis of BMSCs directed by mature chondrocytes. *Biomaterials*. **31**, 9406–14 (2010).

180. C.-C. Niu, L.-J. Yuan, S.-S. Lin, L.-H. Chen, W.-J. Chen, Mesenchymal stem cell and nucleus pulposus cell coculture modulates cell profile. *Clin. Orthop. Relat. Res.* **467**, 3263–72 (2009).

181. S. Strassburg, N. W. Hodson, P. I. Hill, S. M. Richardson, J. a Hoyland, Bi-directional exchange of membrane components occurs during co-culture of mesenchymal stem cells and nucleus pulposus cells. *PLoS One*. **7**, e33739 (2012).

182. A. Aung, G. Gupta, G. Majid, S. Varghese, Osteoarthritic chondrocyte-secreted morphogens induce chondrogenic differentiation of human mesenchymal stem cells. *Arthritis Rheum.* **63**, 148–58 (2011).

183. J. Platas *et al.*, Conditioned media from adipose-tissue-derived mesenchymal stem cells downregulate degradative mediators induced by interleukin-1 β in osteoarthritic chondrocytes. *Mediators Inflamm.* **2013** (2013), doi:10.1155/2013/357014.

184. D. H. Kim *et al.*, Enhanced differentiation of mesenchymal stem cells into NP-like cells via 3D co-culturing with mechanical stimulation. *J. Biosci. Bioeng.* **108**, 63–7 (2009).

185. Y. Yamamoto *et al.*, Upregulation of the viability of nucleus pulposus cells by bone marrow-derived stromal cells: significance of direct cell-to-cell contact in coculture system. *Spine (Phila. Pa. 1976).* **29**, 1508–1514 (2004).

186. L. Wu, J. Leijten, C. a van Blitterswijk, M. Karperien, Fibroblast growth factor-1 is a mesenchymal stromal cell-secreted factor stimulating proliferation of osteoarthritic chondrocytes in co-culture. *Stem Cells Dev.* **22**, 2356–67 (2013).

187. J. H. Lai, G. Kajiyama, R. L. Smith, W. Maloney, F. Yang, Stem cells catalyze cartilage formation by neonatal articular chondrocytes in 3D biomimetic hydrogels. *Sci. Rep.* **3**, 3553 (2013).

188. D. R. Albrecht, G. H. Underhill, T. B. Wassermann, R. L. Sah, S. N. Bhatia, Probing the role of multicellular organization in three-dimensional microenvironments. *Nat. Methods*. **3**, 369–75 (2006).

189. X. Tang, L. Fan, M. Pei, L. Zeng, Z. Ge, Evolving concepts of chondrogenic differentiation: history, state-of-the-art and future perspectives. *Eur. Cell. Mater.* **30**, 12–27 (2015).

190. B. Cao, Z. Li, R. Peng, J. Ding, Effects of cell–cell contact and oxygen tension on chondrogenic differentiation of stem cells. *Biomaterials*. **64**, 21–32 (2015).

191. L. Xie, M. Mao, L. Zhou, B. Jiang, Spheroid Mesenchymal Stem Cells and Mesenchymal Stem Cell-Derived Microvesicles: Two Potential Therapeutic Strategies. *Stem Cells Dev.* **25**, 203–213 (2016).

192. A. Allon, R. Schneider, J. Lotz, Co-culture of adult mesenchymal stem cells and nucleus pulposus cells in bilaminar pellets for intervertebral disc regeneration. *SAS J.* **3**, 41–49 (2009).

193. A. A. Allon, K. Butcher, R. A. Schneider, J. C. Lotz, Structured coculture of mesenchymal stem cells and disc cells enhances differentiation and proliferation. *Cells Tissues Organs*. **196**, 99–106 (2012).

194. S. M. Richardson *et al.*, Intervertebral disc cell-mediated mesenchymal stem cell differentiation. *Stem Cells*. **24**, 707–16 (2006).

195. G. Vadalà *et al.*, Coculture of bone marrow mesenchymal stem cells and nucleus pulposus

cells modulate gene expression profile without cell fusion. *Spine (Phila. Pa. 1976).* **33**, 870–6 (2008).

196. F. Yang, V. Y. L. Leung, K. D. K. Luk, D. Chan, K. M. C. Cheung, Mesenchymal stem cells arrest intervertebral disc degeneration through chondrocytic differentiation and stimulation of endogenous cells. *Mol. Ther.* **17**, 1959–66 (2009).

197. W. H. Chen *et al.*, In vitro stage-specific chondrogenesis of mesenchymal stem cells committed to chondrocytes. *Arthritis Rheum.* **60**, 450–459 (2009).

198. Y.-H. Yang, A. J. Lee, G. a Barabino, Coculture-driven mesenchymal stem cell-differentiated articular chondrocyte-like cells support neocartilage development. *Stem Cells Transl. Med.* **1**, 843–54 (2012).

199. D. J. Prockop, "Stemness" does not explain the repair of many tissues by mesenchymal stem/multipotent stromal cells (MSCs). *Clin. Pharmacol. Ther.* **82**, 241–3 (2007).

200. E. M. Horwitz, W. R. Prather, Cytokines as the major mechanism of mesenchymal stem cell clinical activity: expanding the spectrum of cell therapy. *Isr. Med. Assoc. J.* **11**, 209–11 (2009).

201. N. Ozeki *et al.*, Not single but periodic injections of synovial mesenchymal stem cells maintain viable cells in knees and inhibit osteoarthritis progression in rats. *Osteoarthr. Cartil.* **24**, 1061–1070 (2015).

202. P. R. Baraniak, T. C. McDevitt, Stem cell paracrine actions and tissue regeneration. *Regen. Med.* **5**, 121–43 (2010).

203. L. D. S. Meirelles, A. M. Fontes, D. T. Covas, A. I. Caplan, Mechanisms involved in the therapeutic properties of mesenchymal stem cells. *Cytokine Growth Factor Rev.* **20**, 419–27 (2009).

204. A. Bertolo *et al.*, Human mesenchymal stem cell co-culture modulates the immunological properties of human intervertebral disc tissue fragments in vitro. *Eur. Spine J.* **20**, 592–603 (2011).

Chapter 2: Effects of cell type and configuration on cocultured MSC and NPC constructs.

This chapter is published as a manuscript in JOR with the following citation: Ouyang, A., Cerchiari, A., Tang, X., Liebenberg, E., Gartner, Z.J., Alliston, T., Lotz, J.C. "Effects of cell type and configuration on anabolic and catabolic gene expression in a 3-dimensional IVD tissue engineering construct," Journal of Orthopaedic Research. (2017). 35(1): 61-73.

2.1 Introduction

Low back pain is a leading cause of disability worldwide and is most often associated with intervertebral disc degeneration (*1*). Degeneration is irreversible due to the low cellularity and low regenerative capacity of nucleus pulposus tissue, which has raised interest in cell-based tissue engineering therapies that could be injected into the NP space to restore mechanical and biochemical properties. However, degenerative IVDs have a hypoxic and inflammatory microenvironment, which inhibits cell survival and proliferation. Inflammatory cytokines also upregulate catabolic factors such as matrix metalloproteinases, which further exacerbate degeneration (*2–4*). Therefore, a better understanding of how tissue-engineering constructs respond to a degenerative microenvironment is needed to evaluate their regeneration potential.

Tissue-engineering constructs can be designed with many different parameters in mind, including choices of biomaterial, cell types, and exogenous growth factors. Furthermore, the 3D cell configuration within a construct is an inherent design factor that controls the availability and intensity of mechanical and biochemical signals (*5*). In this study, we measure the effects of cell type and 3D configuration in IVD tissue engineering constructs. We focus on both anabolic and catabolic gene expression to more comprehensively assess regenerative potential in a degenerative context.

Many cell types are potential candidates for IVD tissue engineering, including autologous nucleus pulposus cells (NPCs), progenitor cells (such as mesenchymal stem cells, or MSCs), or combinations of multiple cell types (*6*). NPCs, which are native to the disc space, are able to produce disc matrix components even after being expanded and cultivated *in vitro.* When injected into the IVD in animal studies, NPCs in conjunction with carrier materials or scaffolds improve disc height and material properties (*6, 7*). However, these methods pose some clinical challenges, due to the dilemma of donor cell availability (*8*).

An alternative cell source, MSCs, resolves some of these clinical issues because autologous MSCs can be isolated from bone marrow without causing disc damage. MSCs have the potential to differentiate into chondrogenic lineages, and are able to modulate inflammatory responses in some environments (*9, 10*). However, chondrogenic differentiation of MSCs requires specific inductive cues (such as addition of exogenous growth factors), and is difficult to regulate due to hypertrophy and calcification in later differentiation stages (*8, 11*).Combining NPCs and MSCs in coculture may be a way to simultaneously address the challenges of NPCs' limited availability (fewer NPCs are needed) and MSCs' dependence on an instructive microenvironment (NPCs can provide differentiation cues)(*12*). Previously observed benefits of coculturing MSCs with articular chondrocytes or NPCs include increased cell proliferation, upregulated proteoglycan (PG) synthesis, and reduced hypertrophy (*13, 14*).

Another potentially important design consideration for tissue-engineering constructs is 3D cell configuration, a structural variable that alters the physical, spatial, and biochemical cues that cells perceive (*15*). Structural factors such as cell density, homotypic and heterotypic cell type proximity, and presence of direct contact affect cell proliferation and chondrogenic potential, but the relative importance of these factors is controversial and unclear (*14, 16–18*).One particular

3D configuration that externally controls cell proximity and contact is cell micropellets or microaggregates (*19*). Pellet culture is commonly used to promote chondrogenic differentiation *in vitro*, possibly because contact between cells mimics a mesenchymal condensation structure (*20–22*). Direct contact in smaller cell clusters can also improve GAG deposition by articular chondrocytes, and chondrogenic differentiation of MSCs (*19*, *23*), so micropellets most likely provide similar contact-associated benefits. Furthermore, micropellets have fewer diffusion limitations than traditional, larger cell pellets, and can be injectable for clinical applications (*24*)**.**

We hypothesized that both cell type and 3D configuration affect synthetic and catabolic activity, and investigated the extent of these effects by comparing individual-cell and micropellet constructs. We fabricated nucleus pulposus tissue-engineering constructs consisting of MSCs and NPCs encapsulated in alginate hydrogels, evaluating both anabolic and catabolic performance to assess the ability of implanted constructs to synthesize matrix while surviving in degenerative environments (simulated by hypoxic and inflammatory media). We first compared anabolic and catabolic performance of cocultured constructs with that of single-cell-type constructs to more clearly define the benefits of coculture in our system. Next, we formed micropellets with single cell types and cocultured cells to determine the effect of cell configuration on anabolic and catabolic gene expression. We observed that the cocultured micropellets self-organized into a bilayered structure, and investigated whether this self-organization might be attributed to differences in intracellular cohesivity in MSCs and NPCs.

2.2 Methods

Experimental Design: To determine the effects of cell type and cell configuration, we varied these parameters through two sets of experiments.

Cell type effects: To more clearly define the effect of cell type in nucleus pulposus tissue engineering constructs, we compared a 50:50 coculture of MSC and NPC with single-cell-type cultures (Figure 2.1A-C). MSCs, NPCs, and coculture groups were all encapsulated in alginate beads as individual cells and cultured as described below, with n=3 for each experimental condition.

Configuration effects: We also wanted to study the effect of 3D configuration, particularly in the context of direct cell-cell contact, on cell behavior. Therefore, we formed micropellets of MSCs, NPCs, and a 50:50 coculture, which we also encapsulated in alginate beads for long-term culture (Figure 2.1 D-F) (n=3).

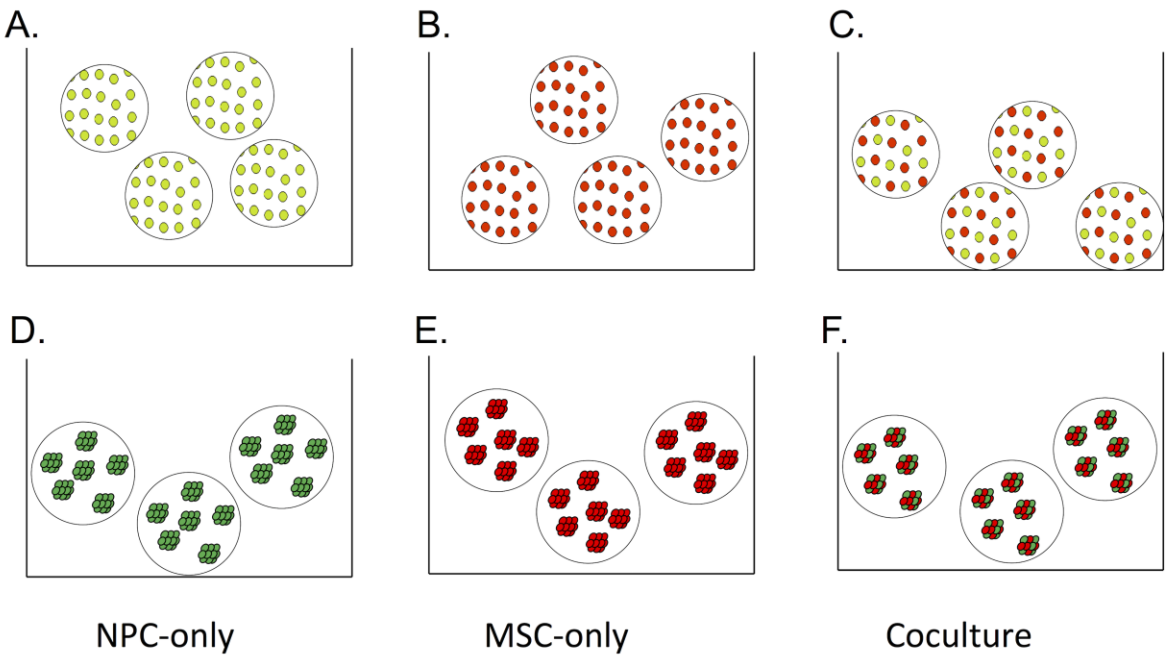

Figure 2.1 Cell type and configuration groups. Individual cell (A-C) and micropellet (D-F) groups of NPCs (A, D), MSCs (B, E), and cocultured (C, F) cells allow us to compare the effects of cell type and cell configuration. NPCs are shown in green and MSCs are shown in red.

Cell culture: Human MSCs (passage 5, purchased from EMD Millipore, CA) were cultured in MSC growth media (low-glucose DMEM with 10% FBS and 1% antibiotic/antimycotic). Bovine NPCs (passage 4, harvested from caudal discs from a local slaughterhouse, as previously

described (*25*)) were cultured in standard disc media (low-glucose DMEM with 5% FBS, 1% antibiotic/antimycotic, 1% non-essential amino acids, and 1.5% osmolarity salt solution containing 5M NaCl and 0.4M KCl). Human MSCs were acquired from a single donor, and bovine NPCs were from a pooled expansion of 3 simultaneously harvested tails.

All experimental groups were suspended in alginate beads, which were formed by resuspending cells in 1.2% sodium alginate (FMC BioPolymer) in D-PBS at a concentration of 1 x 10^6 cells/mL. We expelled the alginate-cell mixture dropwise through a 22-gauge needle into a 102 mmol/L $CaCl_2$ solution and allowed the beads to crosslink for 10 minutes before washing with PBS and media. The groups were cultured in basal media (MSC growth media, described above) or inflammatory and hypoxic media (MSC growth media with 10 ng/ml of IL-1β and 10 ng/ml of TNF-α, 2% O_2) to simulate normal and degenerative disc environments. All groups were cultured for 21 days, with media changes 3 times per week.

MSC growth media was used instead of differentiation media because the addition of TGF-β in differentiation media often leads to hypertrophic differentiation and expression of collagen X (*26*), and previous studies suggest that cocultured MSCs and ACs in growth media induce chondrogenic gene and protein expression (*27*). Cells were encapsulated in alginate beads to provide a non-fouling 3D environment with rounded cell morphology, simulating native conditions in the NP (*28*). We suspended cells with a density of 1M cells per mL to minimize accidental direct contact between neighboring individual cells, as shown in the individual-cell group histology sections in Figure 2.6C.

NPC phenotype stability: To assess the phenotype stability of NPCs in coculture, we measured the gene expression of bovine CD24, a marker of healthy NPCs (*29*), in NPC-only and coculture groups at 21 days. Gene expression analysis was performed as described later in this section,

with bovine GAPDH as the housekeeping gene (primer sequences are shown in Table 2.1). There were no significant differences in CD24 gene expression associated with coculture conditions, cell configurations, or media conditions.

Micropellet formation: Micropellets with 100 µm diameters were formed in molds generated by soft lithography (Figure 2.2). Molds were formed by creating a silicon master with 100 µm diameter wells. The master was made with SU-8 2035 photoresist (MicroCheM) and crosslinked under a photo-mask (*30*). A polydimethylsiloxane (PDMS) "stamp" was molded from these masters with the negative image: posts with diameter 100 µm. Finally, these PDMS stamps were inserted into a 3.5% agarose solution (Low gelling agarose type VII-A, Sigma-Aldrich), which, after gelling, formed 100 µm diameter wells. MSCs and NPCs were loaded into the wells at a 50:50 ratio and total concentration of 1M cells/mL. They condensed into micropellets over 12 hours in MSC growth media. The micropellets, which contain approximately 100 cells each, were released from wells with a D-PBS wash before alginate encapsulation at a density of 10,000 micropellets per mL, or 1x 10^6 cells/mL. Additional micropellet formation parameters are described in Appendix A.

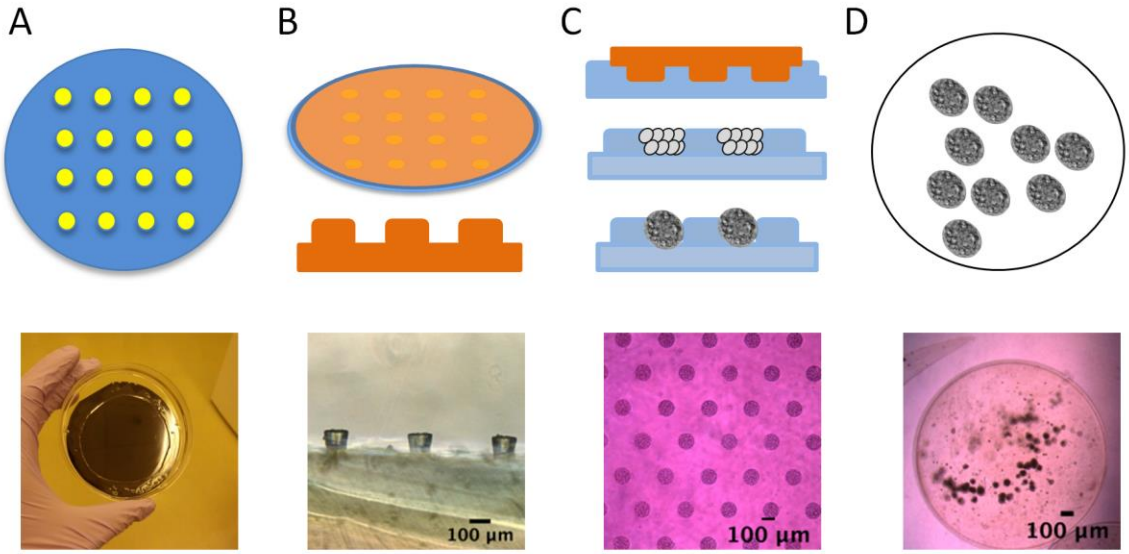

Figure 2.2. Methods for forming cell micropellets. A. Create 100-µm wells in a silicon wafer with photolithography. B. Cover the wafer with PDMS, and peel off to form posts. C. Use the PDMS as a "stamp" to form agarose wells. Load the wells with cells, which condense in 12-24 hours. D. Release condensed pellets from the wells by washing with D-PBS, and resuspend in alginate.

Gene expression analysis: After 21 days of culture, the alginate beads were dissolved in 55 mM sodium citrate, and cell pellets were isolated by centrifugation. Total RNA was extracted from all groups using QIAShredder and RNeasy mini kits (Qiagen) and was converted to cDNA using iScript reverse transcriptase (BioRad). Gene expression was measured using quantitative reverse transcription PCR with SYBR green master mix (BioRad) using the BioRad CFX96 RealTime Thermal Cycler.

Gene expression was measured for aggrecan and collagen 2A1 (anabolic chondrogenic markers), and MMP-1, MMP-9, MMP-13, and ADAMTS5 (catabolic factors present in disc degeneration (*31*)) using primers that amplified homologous regions in human and bovine transcripts (Table 2.1). Fold changes were calculated using the ΔΔCt method (*32*) and normalized to GAPDH. Results were compared using a one-way ANOVA test (among cell-type

groups) and multiple t-tests (between groups in basal and inflammatory media conditions) with a Tukey HSD correction for multiple hypotheses. P values < 0.05 were considered significant.

	Human ref	Bovine ref	Forward	Reverse
GAPDH	NM_002046	NM_001034034	AGC TCA CTG GCA TGG CCT TC	CGC CTG CTT CAC CAC CTT CT
Aggrecan	NM_001135	NM_173981	AGG AGC AGG AGT TTG TCA AC	AGT TGT CAG GCT GGT TGG
Collagen 2A1	NM_001844	NM_001001135	AGG AAT TCG GTG TGG ACA TAG	TCA GGT CAG CCA TTC AGT G
MMP-1	NM_002421 and NM_001145938	NM_174112	CTT GCT CAT GCT TTT CAA CCA GG	GCT GAA CAT CAC CAC TGA AGG T
MMP-9	NM_004994	NM_174744	CTA CAC CCA GGA CGG CAA TG	GTC GTA GTT GGC GGT GGT
MMP-13	NM_002427	NM_174389	TGA AAC CTG GAC AAG TAG TTC C	ATG AGT GCT CCT GGG TCC TT
ADAMTS5	NM_007038	NM_001166515	GCG CTT AAT GTC TTC CAT CCT	CGT GGT AGG TCC AGC AAA CA
Bovine GAPDH	Sequences from Wu et al., 2011(*33*)		GCC ATC ACT GCC ACC CAG AA	GCG GCA GGT CAG ATC CAC AA
Bovine CD24	N/A	XM_002690126 and XM_015464783	TCT GGC GCT GCT CTT ACC TA	GCA GGT GAG GTA GTC TGG GA

Table 2.1. Primer sequences for gene expression analysis. All amplify homologous regions of the human and bovine genes of interest, except the species-specific bovine GAPDH and CD24 primers, which were used to measure NPC phenotype markers.

DNA and Dimethylmethylene Blue assays for glycosaminoglycan quantification: After dissolving the alginate beads in 55 mM sodium citrate, we digested the supernatant in 0.56U/ml papain (Sigma-Aldrich) at 60°C overnight. Media samples of 1 mL volume were collected at the time of harvest, but did not go through the digest step. DNA content was assayed with a Quant-iTPicoGreen kit (ThermoFisher) and measured on a microplate reader (Molecular Devices) with

excitation at 488 nm and absorption at 525 nm. GAG content was analyzed using a dimethylmethylene blue (DMMB) assay with modifications for alginate (*34*) and media(*35*) measurements and normalized by DNA content. Statistics on normalized total GAG content were calculated using a one-way ANOVA test and multiple t-tests, as described in the previous section.

Histological analysis: Alginate beads were fixed in 10% formalin for 20 minutes, dehydrated with ethanol washes, embedded in paraffin, and sectioned at 7 micron thickness. Immunohistochemistry was performed following manufacturer instructions for the DAB substrate kit (Vector Laboratories, Inc., CA) with a 1:100 dilution of the primary mouse anti-aggrecan antibody (12/21/1-C-6, Developmental Studies Hybridoma Bank, University of Iowa). The slides were counterstained with hematoxylin. The figures show representative images out of three replicates.

Observation of micropellet structure and intracellular cohesivity assay: To visualize micropellet organization, we labeled cell populations with Vybrant DiI and DiO cell membrane dyes (5 µl/1x10^6 cells) (Life Technologies). The micropellets were imaged using inverted epifluoresent microscopes (Zeiss Axiovert 200M running SlideBook software and Leica DMi8 running LAS X).

The coculture micropellets contain two different cell types that might vary in cohesivity, which could affect their adhesion-forming behavior. To quantify the intracellular cohesivity, we allowed 100% NPC and 100% MSC populations to interact overnight in agarose microwells and analyzed the contours of the resulting 100% NPC or 100% MSC micropellets. We measured circularity of the contours using FIJI's built-in circularity measurement tool as previously described (*30*). Briefly, circularity is a measure of the ratio of a micropellet's area to the square

of its perimeter, where $C = 4\pi * \text{area}/\text{perimeter}^2$. Higher circularity scores are correlated with smoother micropellet contours, which result from higher intracellular cohesivity.

2.3 Results

Cell type effects:

To determine the role of cell type in synthetic activity and responses to inflammation, we compared NPC-only and MSC-only seeded alginate beads with beads containing a 50:50 mix of both cell types (Figure 2.1 A-C in methods).

Anabolic performance:

To analyze the anabolic performance of the different cell types, we measured aggrecan and collagen 2A1 gene expression. Under basal media conditions, the MSC-only group exhibited very low anabolic gene expression: for both aggrecan and collagen 2A1, MSC-only levels were significantly lower than those of NPC-only and coculture groups (Figure 2.3A, B). Although the NPC-only and coculture groups did not show a significant difference in aggrecan or collagen 2A1 gene expression, the NPC-only group had a trend of higher anabolic gene expression levels.

We also evaluated changes in anabolic gene expression when cells were cultured in an inflammatory and hypoxic microenvironment (Figure 2.3A, B). In this environment, anabolic gene expression remained low for MSCs and decreased for the NPC-only and coculture groups. Similar to the basal media condition, the aggrecan and collagen 2A1 gene expression of the MSC-only group was significantly lower than that of the NPC-only and coculture groups. The NPC-only and coculture groups did not have a significant difference in aggrecan expression, but the NPC-only group had significantly higher collagen 2A1 expression than the coculture group. Collagen 2A1 expression decreased significantly in NPC-only and coculture groups ($p < 0.05$),

while aggrecan expression decreased significantly in the NPC-only group and showed a decreasing trend in the coculture group ($p < 0.05$ prior to a multiple hypothesis correction).

Catabolic performance:

To measure the groups' catabolic response to a hypoxic and inflammatory microenvironment, we measured gene expression of MMP-1, MMP-9, MMP-13, and ADAMTS5 (Figure 2.3C-F). The basal expression levels of these genes varied: the MSC-only group exhibited significantly lower levels of MMP-1, MMP-13, and ADAMTS5, but had a high basal expression level of MMP-9. The coculture group exhibited significantly higher basal levels of MMP-1 and MMP-13 compared with the single-cell-type groups. In inflammatory and hypoxic conditions, the NPC-only group consistently exhibited a significant upregulation of all four catabolic factors, and the subsequent expression levels of MMP-1, MMP-13, and ADAMTS5 were higher in the NPC-only groups than in MSC-only and coculture groups. The MSC-only group did not show significant catabolic upregulation, and, in fact, exhibited a significant decrease in MMP-9 expression in the inflammatory and hypoxic condition. The coculture group exhibited significant catabolic upregulation in two of the genes, MMP-1 and ADAMTS5. However, in both these cases, the upregulated gene expression levels were still significantly lower than those of the NPC-only group.

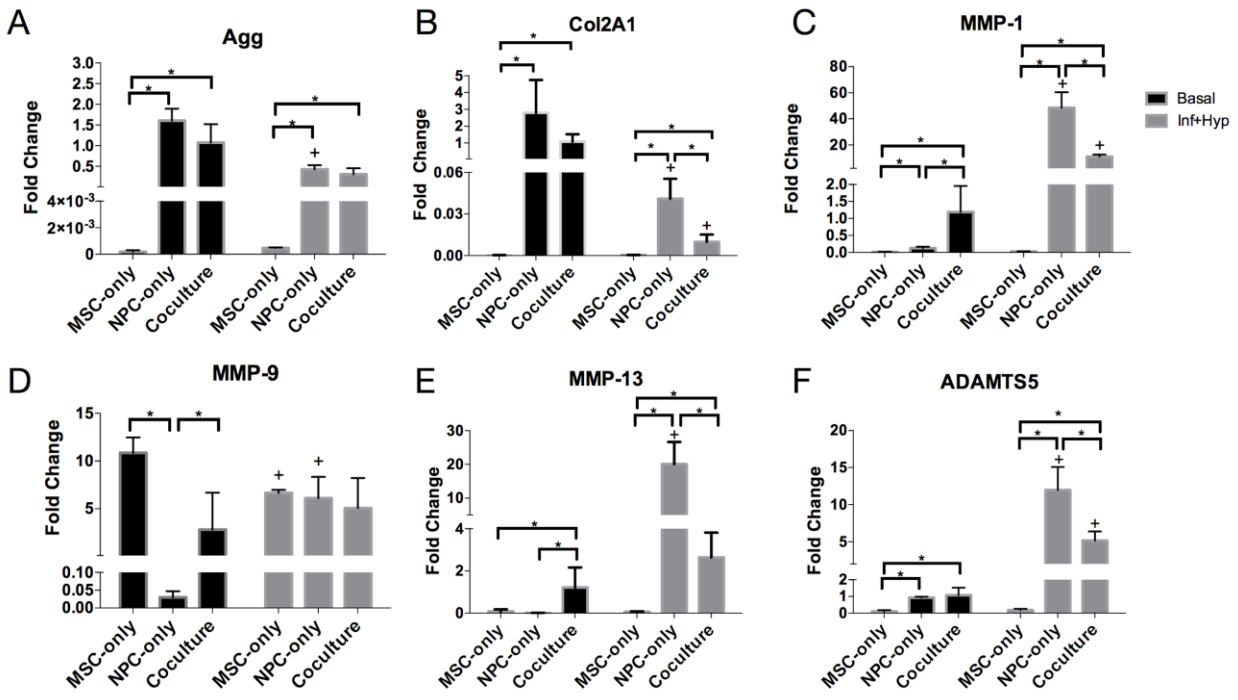

Figure 2.3: Effect of cell type in individually encapsulated cell constructs: NPCs maximize ECM synthesis while coculture provides protection against hypoxic and inflammatory conditions. Aggrecan (A), collagen 2A1 (B), MMP-1 (C), MMP-9 (D), MMP-13 (E), and ADAMTS5 (F) gene expression in MSC-only, NPC-only, and coculture groups after 21 days in basal or hypoxic and inflammatory media conditions. Fold changes were normalized to the coculture basal media group. The + symbol indicates a significant difference ($p<0.05$) within a cell type group for different media conditions, while the * symbol indicates a significant difference between different cell type groups under the same media conditions. Error bars represent standard deviation.

Configuration effects:

To explore the effects of 3D cell configuration, we formed NPC, MSC, and coculture micropellets, and compared them to each other and to the previous patterns we observed in individual cell groups. (Figure 2.1 D-F).

Anabolic performance:

The micropellet configuration did not significantly affect MSC anabolic gene expression patterns. Similar to the MSC-only individual cells, the MSC-only micropellet group also produced very low expression of aggrecan and collagen 2A1 mRNAs in both basal and

hypoxic/inflammatory media (Figure 2.4 A, B). The MSC micropellet aggrecan and collagen 2A1 expression was significantly lower than NPC and coculture micropellet gene expression in most conditions. In hypoxic and inflammatory media, the coculture micropellets experienced a significant downregulation of aggrecan gene expression, and their resulting aggrecan level was similar to that of the MSC micropellets (Figure 2.4A).

The micropellet configuration also did not affect the NPC and coculture groups' response to hypoxic and inflammatory media. Both groups had significantly lower aggrecan and collagen 2A1 gene expression in hypoxic and inflammatory media than in basal media.

In the individual-cells configuration (Figure 2.3A,B), the NPC-only group generally exhibited higher anabolic expression than the coculture group. In the micropellet configuration (Figure 2.4A, B) the NPC-only group maintained higher aggrecan expression in both media conditions, but the coculture micropellets exhibited a trend of higher collagen 2A1 expression, with a significantly higher expression of Col2A1 than NPCs in hypoxic and inflammatory media.

Catabolic performance:

Similar to the pattern observed in the individual cell constructs, the MSC-only micropellets exhibited a significantly higher basal level of MMP-9 and a significantly lower basal level of the other catabolic genes compared with NPC-only and coculture micropellets (Fig 2.4C-F). NPC-only and coculture micropellets had similar basal expression levels for all four genes. In inflammatory and hypoxic media conditions, the MSC-only micropellets did not display any significant changes in catabolic gene expression. NPC-only micropellets showed a significant upregulation of MMP-1 and MMP-9, but unlike in the NPC-only individual cell group, MMP-13 and ADAMTS5 expression did not significantly change. In the coculture micropellets, MMP-1 expression significantly increased in inflammatory and hypoxic media, but the increased levels

were still significantly lower than those in NPC-only micropellets (Fig 2.4C). MMP-9 expression did not significantly change in the coculture micropellets, and MMP-13 and ADAMTS5 expression actually showed a significant decrease in degenerative media conditions.

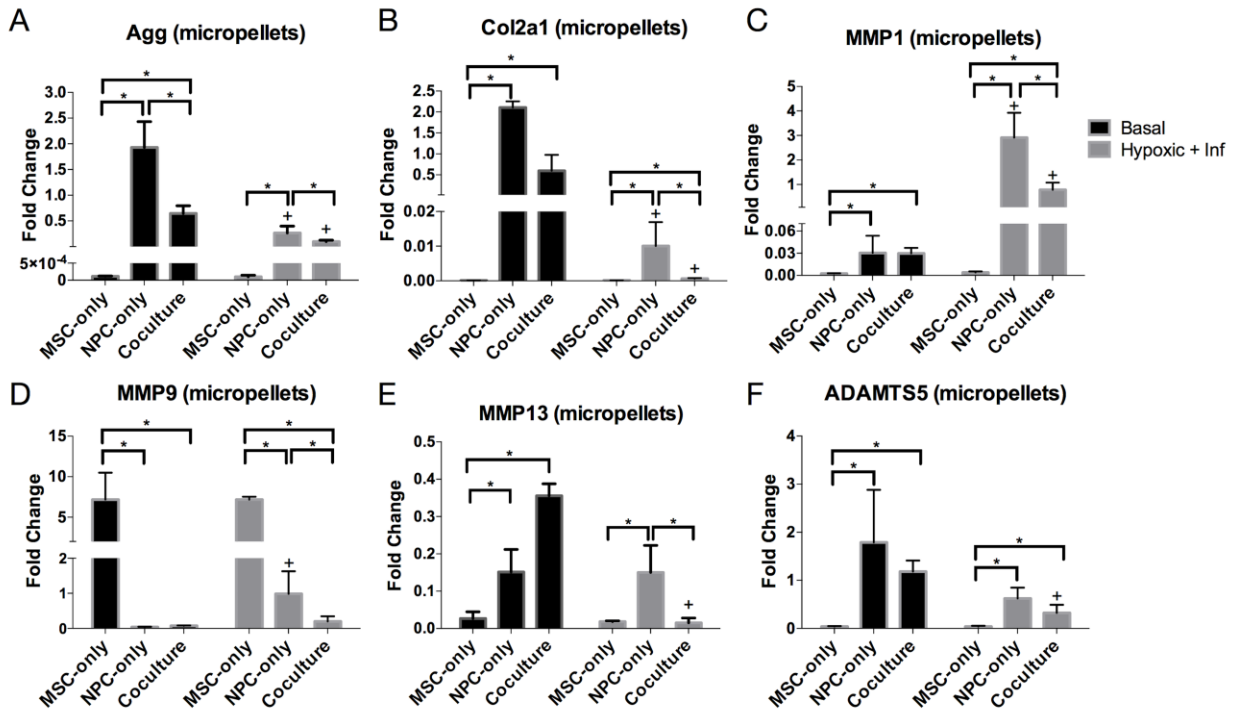

Figure 2.4. Anabolic and catabolic gene expression in a micropellet configuration: configuration and coculture reduce catabolic upregulation in inflammatory and hypoxic conditions. Aggrecan (A), collagen 2A1 (B), MMP-1 (C), MMP-9 (D), MMP-13 (E), and ADAMTS5 (F) gene expression in MSC-only, NPC-only, and coculture micropellet groups after 21 days in basal or hypoxic and inflammatory media conditions. Fold changes for each gene were normalized to the coculture individual cell basal media group, which is shown in Figure 2.3. The + symbol indicates a significant difference ($p < 0.05$) within a cell type group for different media conditions, while the * symbol indicates a significant difference between different cell type groups under the same media conditions. Error bars represent standard deviation.

To illustrate how cell type and configuration influenced the response to inflammation, we calculated fold induction for the four catabolic markers (fold change difference between basal and hypoxic/inflammatory levels; Figure 2.5). All MSC groups exhibited no significant catabolic induction, while the NPC-only individual cell group consistently exhibited the highest fold induction, with a greater-than-100-fold induction in all the MMPs that we tested (Figure 2.5 A-

C). Coculture groups generally exhibited lower induction levels, and even experienced a significant decrease in MMP-13 and ADAMTS5 (fold induction was <1) (Fig 2.5 C, D). Finally, micropellet configurations are associated with lower induction levels in both NPC-only and coculture groups.

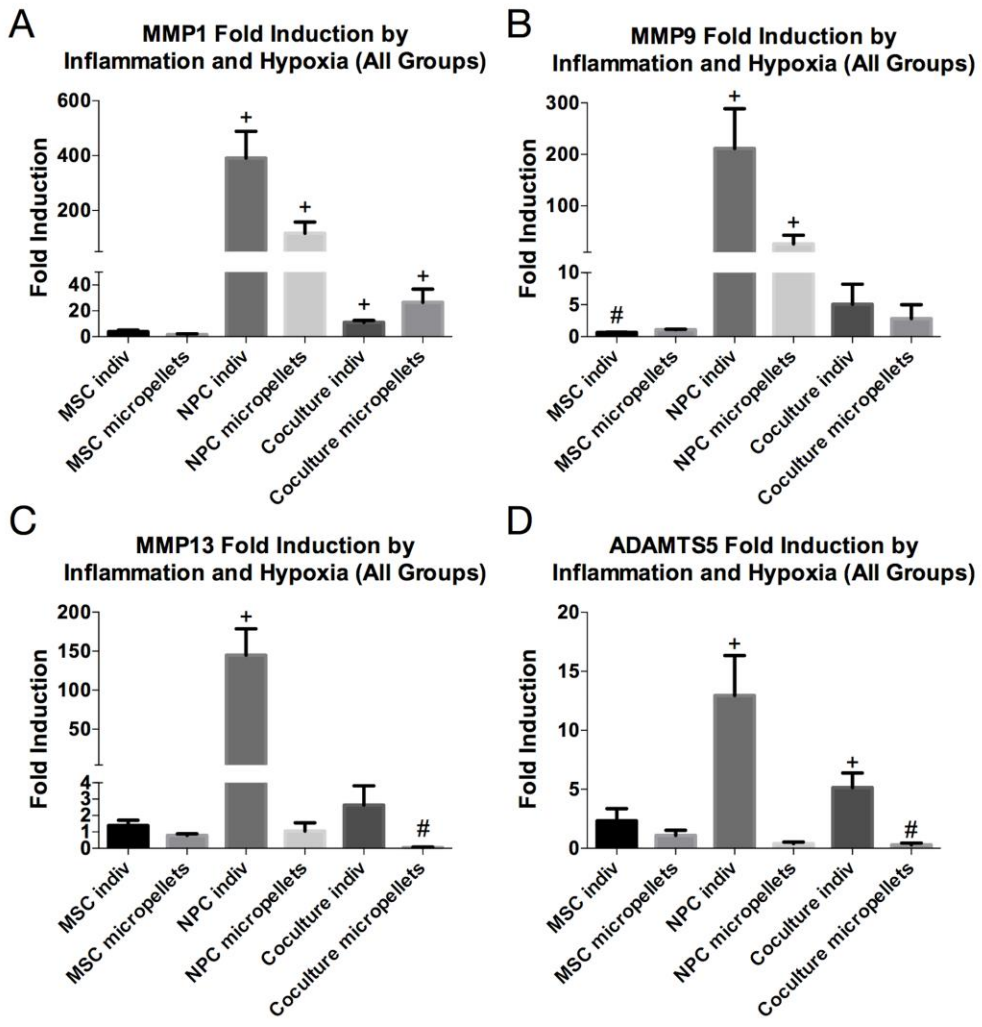

Figure 2.5: Coculture and micropellet configurations exhibit reduced catabolic induction. Fold induction of catabolic markers MMP-1 (A), MMP-9 (B), MMP-13 (C), and ADAMTS5 (D) represents the fold change between basal and hypoxic/inflammatory media conditions (normalized separately to the basal media condition for each group, which is not shown in the graph). The + and # symbols indicate a significant ($p<0.05$) increase and decrease, respectively, in expression in degenerative media conditions. Error bars represent standard deviation.

Extracellular matrix deposition:

To evaluate the effects of cell type and configuration on proteoglycan and glycosaminoglycan synthesis, we measured glycosaminoglycan (GAG) content in the alginate beads and media, and performed immunohistochemical staining for aggrecan.

GAG content:

MSC-only groups exhibited the lowest GAG content in both individual cell and micropellet configurations (Figure 2.6 A, B), but their GAG secretion was not significantly affected by degenerative media conditions. On the other hand, both NPC-only and coculture groups exhibited a significant decrease in total GAG content in inflammatory and hypoxic media, regardless of cell configuration. In basal media, NPC-only and coculture groups had similar GAG content levels, but in degenerative conditions the coculture group had significantly lower GAG content, also regardless of cell configuration. Overall, micropellet groups had lower total GAG content than individual cell groups.

Histological detection of aggrecan:

Aggrecan staining was clearly present in coculture basal groups, in both individual cell and micropellet configurations (Figure 2.6C). There was a smaller amount of aggrecan staining visible in the NPC-only individual cell basal media group, but the staining followed a similar pattern as the coculture groups, in which staining was most concentrated in the regions directly surrounding cells or pellets. Staining was very faint in inflammatory and hypoxic media condition groups and NPC-only micropellet groups, and was negative in MSC-only micropellet groups. MSC-only individual cell histology was unavailable due to processing problems, but is expected to be negative for aggrecan staining based on micropellet images and results from pilot experiments.

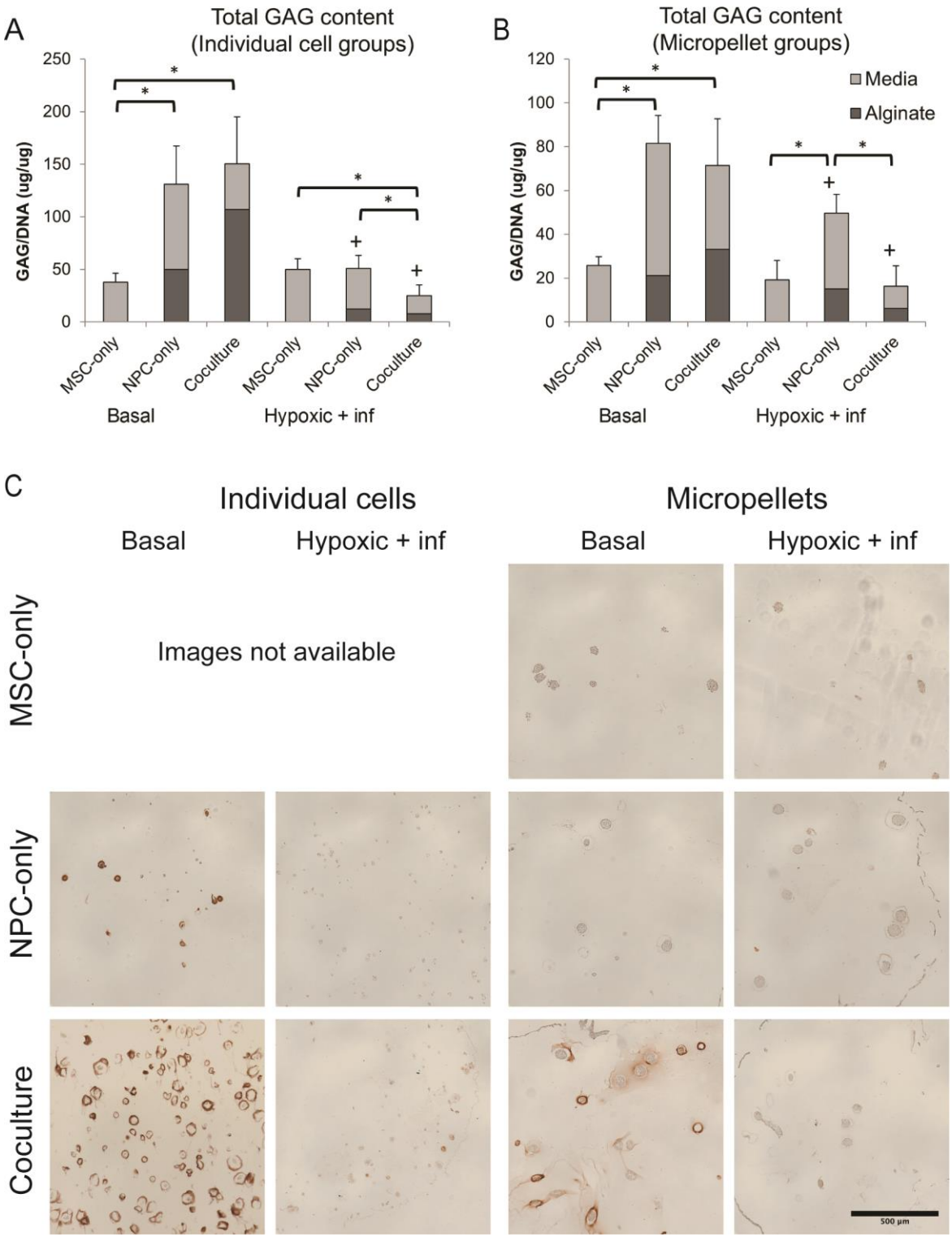

Figure 2.6 Glycosaminoglycan content and distribution varies with cell type and configuration. We calculated total GAG content of individual cell (A) and micropellet (B) groups as the sum of GAG concentration (normalized by DNA content) in alginate bead and media samples. The + symbol indicates a significant difference ($p<0.05$) within a cell type group for different media

conditions, while the * symbol indicates a significant difference between different cell type groups under the same media conditions. Error bars represent standard deviation of the total GAG, and statistics were performed on the total as described in the methods section. Panel (C) shows distribution of aggrecan in MSC-only, NPC-only and coculture individual cell and micropellet constructs after 21 days in basal or inflammatory and hypoxic media conditions. Aggrecan staining (with a hematoxylin counterstain) was visible in coculture basal media groups as well as the NPC-only individual cell basal media group, and was most concentrated in regions surrounding cells and micropellets. Scale bar: 500 μm.

Self-organization of cocultured cells in micropellets:

We investigated the nature of heterotypic cell-cell contact between MSCs and NPCs in coculture micropellets by labeling the MSCs and NPCs with membrane dyes. We observed that the two cell types spontaneously self-organized into a bilayered structure during pellet condensation.

The differential adhesion hypothesis suggests that differences in intercellular cohesivity can lead to changes in surface tension and subsequent cell segregation, which influences tissue morphologies in development (*11*). We hypothesized that the two cell types (MSCs and NPCs) in our coculture construct might have different adhesivity, leading to changes in the organization of the cocultured micropellets. Although two cell types were isolated from different species (human and bovine), previous work suggested that cross-species interactions did not significantly alter cell behavior or phenotypes (*36*). To more closely observe changes in micropellet organization over time, we used fluorescent membrane dyes to track MSCs and NPCs before and after the micropellets formed and condensed. Although MSCs and NPCs were randomly seeded in agarose microwells (Figure 2.7A), after condensation, the cocultured micropellets exhibited a unique bilayered structure with an MSC core and NPC outer layer (Figure 2.7B). This self-organization was evident across large batches of micropellets (Figure 2.7C).

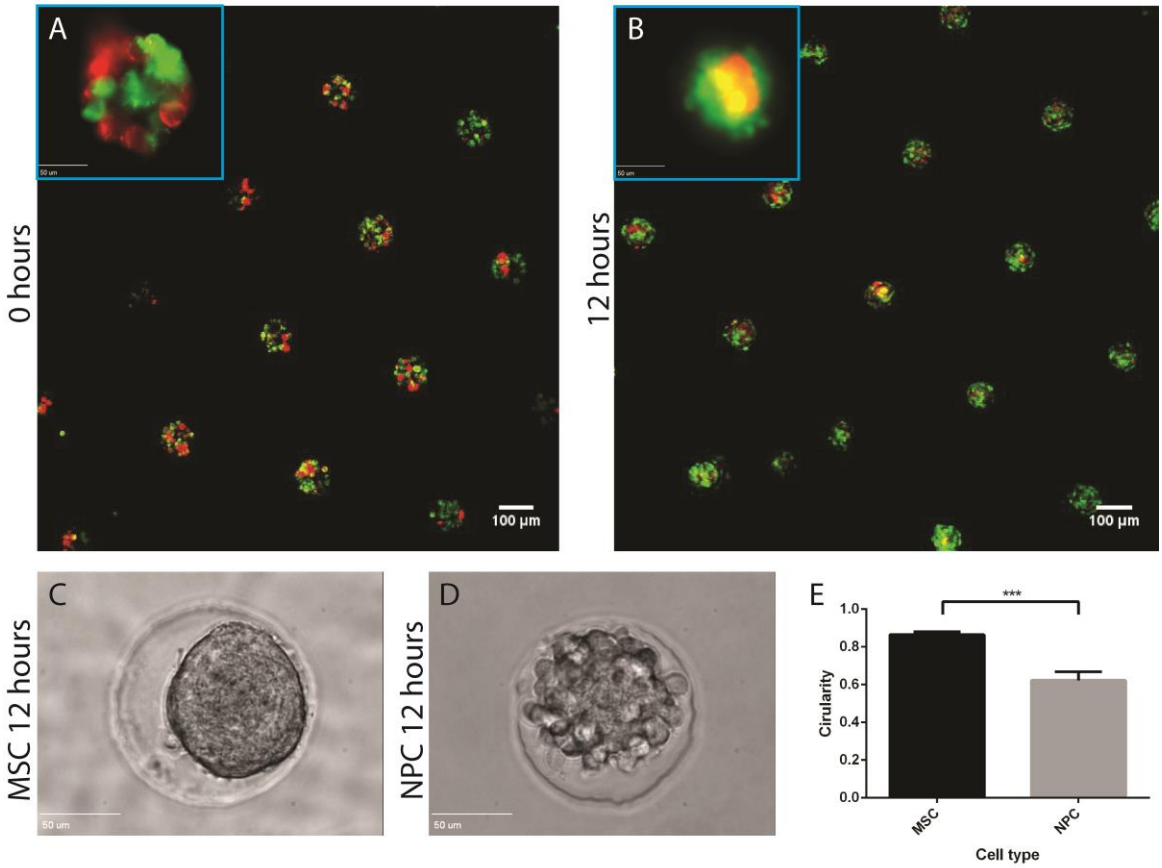

Figure 2.7. Differential adhesion of MSCs and NPCs leads to a bilaminar self-organization in coculture micropellets. MSCs (red) and NPCs (green) were labeled with DiI and DiO membrane dyes. Micropellets were seeded with a random 50:50 cell mixture (A), but condensed after 12 hours to form a bilaminar structure with an MSC core and NPC outer layer (B). To investigate whether the bilaminar self-organization was caused by differences in intracellular cohesivity, we assessed the circularity of MSCs and NPCs in single-cell micropellets. After a 12-hour condensation, MSCs (C) had a significantly higher circularity than NPCs (D, E). Scale bar for A and B = 100 µm (50 µm for the 40x inserts). Scale bar for C and D = 50 µm.

To determine if MSCs and NPCs exhibit differences in intracellular cohesivity, we measured the circularity of single-cell-type micropellets after 24 hours and determined that MSC micropellets had a significantly higher circularity, and therefore higher intercellular cohesivity (Figure 2.6D-F). This concurs with previous work predicting that due to minimization of free surface energy, cells with greater cohesivity tend to migrate towards the core of self-organized

micropellets (*30*, *37*). The observed bilaminar structure of the coculture micropellets may be related to the anabolic and catabolic differences we observed between coculture micropellets and cocultured individual cells.

2.4 Discussion

In this study, we varied cell type and configuration to elucidate the roles of these factors in synthesizing new matrix and adapting to a degenerative disc microenvironment. We measured anabolic and catabolic outcomes of the constructs in basal and degenerative culture conditions and found that both cell type and configuration influence cell behavior.

When comparing the anabolic activity of different cell types, we found that MSC-only groups had the lowest anabolic gene expression and proteoglycan content, which is consistent with previous studies in the literature, suggesting that non-induced MSC monocultures have low synthetic activity (*38*). NPC-only groups had the highest anabolic gene expression, but at the protein level, coculture and NPC-only groups had similar total GAG content in basal media conditions. Coculture groups also exhibited more positive aggrecan staining, so their synthetic activity may be comparable to that NPC-only groups despite their lower anabolic gene expression.

Micropellet configurations did not alter the anabolic gene expression trends we observed in individual cell groups. However, NPC-only and coculture micropellet groups exhibited lower overall GAG content and less aggrecan staining than the corresponding individual cell groups, which may indicate that micropellets were less effective at synthesizing matrix.

Overall, we only observed dense aggrecan staining in three of the histological samples, which suggests that immunohistochemistry was less sensitive than the DMMB assay, which was able to measure GAG content in all groups. Low aggrecan staining may be related to the low

starting cell density of $1x10^6$ cells/ml: in 2010, Watanabe *et al.* noted that even after 6 months of implantation in a mouse skin nodule, NPC cells that were sparsely arranged did not show much safranin-O staining (*14*). Furthermore, cartilage and NP tissue engineering studies use a wide variety of non-standardized cell densities, media compositions, and coculture ratios, which all can affect GAG content, chondrogenic gene expression, and cell proliferation (*11, 13, 39–41*). Differences in these experimental culture conditions between our study and previous works may account for differences in histological outcomes.

Inflammatory and hypoxic media conditions also influenced anabolic activity: regardless of configuration, NPC-only and coculture groups experienced significant decreases in anabolic gene expression, total GAG content, and aggrecan staining. Previous studies have suggested that coculture with MSCs increases NPCs' resilience to degenerative conditions(*42*), but we did not observe this phenomenon. As mentioned in the previous paragraph, differences in experimental culture conditions might account for this discrepancy.

In addition to matrix synthesis, matrix degradation is another important process that influences biochemical and mechanical properties of the IVD. Therefore, we investigated the effect of cell type and configuration on catabolic gene expression. Catabolic activity in hypoxic and inflammatory media conditions was strongly associated with cell type: NPC-only groups had much higher upregulation of catabolic gene expression than MSC-only and coculture groups. Other studies have also found that cocultures containing MSCs are able to modulate inflammatory responses (*43*, *44*). This effect is attributed to immunomodulatory properties of MSCs, which may involve trophic factors and/or contact-mediated signaling (*45*).

3D configuration also significantly affected cells' response to inflammatory and hypoxic stimuli. Arranging cells in a micropellet configuration reduced catabolic induction in both NPC-

only and coculture groups. Strikingly, MMP-13 and ADAMTS5 expression significantly decreased in coculture micropellets when subjected to the degenerative media conditions, possibly because a micropellet configuration enhances immunomodulatory properties of MSCs (*46*).

Our results motivate further investigation into the mechanisms behind benefits of coculture and micropellet configurations. The roles of the different cell types in coculture systems is still unclear. Some studies have found evidence of MSC differentiation(*11*, *12*, *47*), while others indicate that MSCs play a trophic role (*33*, *48*, *49*). To isolate and analyze MSC and NPC or chondrocyte contributions in coculture systems, previous studies have labeled MSCs with fluorescent markers and separated them with high-speed sorting(*12*), or used species-specific markers to analyze gene expression contributions of cells isolated from different species(*11*). Our xenogenic system is well suited to this second approach

The observed differences in micropellet and individual cell cultures may be related to cell-cell communication mechanisms such as soluble factors and contact-mediated signaling. Cells in micropellets are in close contact with each other, allowing them to experience higher soluble factor concentrations. Trophic factors secreted by MSCs such as IL-10 and PGE_2 may be involved in immunomodulatory mechanisms, and a decreased diffusion distance could increase their potency in the cocultured micropellets (*43*, *44*, *50*). Micropellets also allow cells to form direct contacts. Contact-mediated signaling, including formation of gap junctions (*51*) or exchange of membrane components (*52*), has been shown to influence anabolic and catabolic gene expression. In particular, previous studies have found that direct cell-cell contact regulates synthetic activity, growth factor secretion, and responses to inflammation in MSCs and coculture systems (*12*, *53*, *54*). In our system, we measured levels of the trophic factors FGF-1 and PGE_2

and the contact-associated gene N-cadherin, but preliminary data did not show strong associations with cell type or cell configuration changes, possibly because these factors have time-dependent expression changes, or because other factors are more influential in the system.

Applying a micropellet configuration to cocultured MSCs and NPCs altered structural factors beyond cell proximity and contact. Upon closer observation of the cocultured micropellets, we found that they self-organized during the condensation process to form a bilayered structure with an MSC core and NPC outer layer. The tendency of MSCs to gravitate towards the core in pellet culture with chondrocytes or NPCs has previously been observed in "satellite" pellets that budded from large cocultured pellets over time (*25*) and larger pellets that were initially formed without any specific structure (*33*). The differences we measured in intracellular cohesivity of MSCs and NPCs may also explain these earlier observations. However, in another study the core-outer layer organization was more heavily influenced by the coculture ratio (*55*). This self-organization behavior has been observed in both bovine-human and human-human NPC:MSC combinations, so the effects are not due to xenogenic differences (*25*, *56*).

The observed bilayered organization (with an MSC core and NPC or chondrocyte outer layer) has also been fabricated in larger cell pellets using multiple centrifugation steps instead of self-assembly (*25*, *27*, *57*). These Bilaminar Cell Pellets (BCPs) exhibited increased proliferation and chondrogenic gene expression, reduced hypertrophy, and modulated responses in inflammatory environments (*11*, *27*, *42*). Although the bilaminar organization minimizes heterotypic cell-cell contact, the MSC-core structure may be advantageous because it mimics condensations present in cartilage and IVD development (*52*, *58*). In this study, the micropellets did not sustain anabolic gene expression in inflammatory conditions to the extent observed in

larger pellets(*27*), but they showed similar reductions in catabolic responses, and their smaller diameter reduces transport barriers that are associated with larger pellets (*24*).

One limitation of the current study is the use of pooled bovine NPCs from three individuals and human MSCs from a single donor. Related experiments from our group suggest that individual variation among bovine NPC donors has only a minor effect (~ 3%) on catabolic induction by inflammatory cytokines, while human MSC donors showed a larger variation. However, when comparing human donors in coculture systems with the same NPC source, all MSC-only and coculture groups maintained significantly lower catabolic induction than NPC-only groups. Individual cells also exhibited increased catabolic induction compared with micropellets regardless of donor variability. These results are consistent with the cell type and configuration effects we observed in this study, but future studies with additional biological replicates are needed to confirm with more certainty whether these trends are consistent across a population.

Additional factors such as donor age, sex, and location of the MSC source may also influence cell phenotype of both NPCs and MSCs (*59–61*). In previous studies, bovine NPCs showed less individual-individual catabolic variation than human NPCs (*62*). MSCs also showed some individual variation in immunomodulatory activity (*60*), but induction with pro-inflammatory cytokines may reduce this variability (*63*). Additional studies of protein expression and ECM production are needed to ensure that inter-donor variability does not hinder the applicability of tissue engineering strategies. In addition, cocultures containing human NPCs harvested from surgical samples and human MSCs could also be used to test observations from our xenogenic model in a more clinically-relevant system. Both cell types could be isolated from the same

patients, which would illuminate the extent to which individual variability affects cell behavior in cocultured constructs.

Another limitation of our study that hindered matrix deposition was the use of growth culture conditions that were not optimized for chondrogenic synthesis. Therefore, a future step is to determine how our constructs perform in more optimized experimental conditions. For example, overall cell density, ratios of cocultured cell types, and addition of growth factors affect chondrogenesis and cell survival both *in vitro* and *in vivo* (*40*, *64*, *65*). Encapsulation materials also affect matrix synthesis and whether cells benefit from direct cell-cell contact (*38*). The cell type and configuration results from our initial study provide a template to which additional elements can be added to design a more effective NP tissue engineered construct.

Overall, our results indicate that both cell type and configuration influence cell performance in a degenerative microenvironment. Coculture and micropellet configurations had especially strong immunomodulatory effects on catabolic gene expression in inflammatory and hypoxic environments. Further investigations are needed to elucidate mechanisms behind these effects, and to optimize their benefits in an IVD tissue-engineering context.

2.5 References

1. A. Aung, G. Gupta, G. Majid, S. Varghese, Osteoarthritic chondrocyte-secreted morphogens induce chondrogenic differentiation of human mesenchymal stem cells., *Arthritis Rheum.* **63**, 148–58 (2011).
2. J. Fischer, A. Dickhut, M. Rickert, W. Richter, Human articular chondrocytes secrete parathyroid hormone-related protein and inhibit hypertrophy of mesenchymal stem cells in coculture during chondrogenesis., *Arthritis Rheum.* **62**, 2696–706 (2010).
3. M. P. Vincenti, C. E. Brinckerhoff, Transcriptional regulation of collagenase (MMP-1,

MMP-13) genes in arthritis: integration of complex signaling pathways for the recruitment of gene-specific transcription factors., *Arthritis Res.* **4**, 157–64 (2002).

4. S. J. Millward-Sadler, P. W. Costello, A. J. Freemont, J. A. Hoyland, Regulation of catabolic gene expression in normal and degenerate human intervertebral disc cells: implications for the pathogenesis of intervertebral disc degeneration., *Arthritis Res. Ther.* **11**, R65 (2009).
5. M. a Kinney, T. a Hookway, Y. Wang, T. C. McDevitt, Engineering Three-Dimensional Stem Cell Morphogenesis for the Development of Tissue Models and Scalable Regenerative Therapeutics., *Ann. Biomed. Eng.* **42**, 352–367 (2013).
6. G. Paesold, A. G. Nerlich, N. Boos, Biological treatment strategies for disc degeneration: potentials and shortcomings., *Eur. Spine J.* **16**, 447–68 (2007).
7. a Mehrkens, a M. Müller, V. Valderrabano, S. Schären, P. Vavken, Tissue engineering approaches to degenerative disc disease - A meta-analysis of controlled animal trials., *Osteoarthritis Cartilage* **20**, 1316–25 (2012).
8. S. M. Richardson *et al.*, Mesenchymal stem cells in regenerative medicine: Focus on articular cartilage and intervertebral disc regeneration., *Methods* **99**, 69–80 (2015).
9. H. N. Yang *et al.*, The use of green fluorescence gene (GFP)-modified rabbit mesenchymal stem cells (rMSCs) co-cultured with chondrocytes in hydrogel constructs to reveal the chondrogenesis of MSCs., *Biomaterials* **30**, 6374–85 (2009).
10. V. V Meretoja, R. L. Dahlin, F. K. Kasper, A. G. Mikos, Enhanced chondrogenesis in co-cultures with articular chondrocytes and mesenchymal stem cells., *Biomaterials* **33**, 6362–9 (2012).
11. X. Mo *et al.*, Variations in the ratios of co-cultured mesenchymal stem cells and

chondrocytes regulate the expression of cartilaginous and osseous phenotype in alginate constructs., *Bone* **45**, 42–51 (2009).

12. S. Strassburg, S. M. Richardson, A. J. Freemont, J. a Hoyland, Co-culture induces mesenchymal stem cell differentiation and modulation of the degenerate human nucleus pulposus cell phenotype., *Regen. Med.* **5**, 701–711 (2010).
13. K. Tsuchiya, G. Chen, T. Ushida, T. Matsuno, T. Tateishi, The effect of coculture of chondrocytes with mesenchymal stem cells on their cartilaginous phenotype in vitro, *Mater. Sci. Eng. C* **24**, 391–396 (2004).
14. T. Watanabe *et al.*, Human nucleus pulposus cells significantly enhanced biological properties in a coculture system with direct cell-to-cell contact with autologous mesenchymal stem cells., *J. Orthop. Res.* **28**, 623–30 (2010).
15. E. R. Shamir, A. J. Ewald, Three-dimensional organotypic culture: experimental models of mammalian biology and disease, *Nat. Rev. Mol. Cell Biol.* **15**, 647–664 (2014).
16. S. M. Richardson *et al.*, Intervertebral disc cell-mediated mesenchymal stem cell differentiation., *Stem Cells* **24**, 707–16 (2006).
17. T. Svanvik *et al.*, Human disk cells from degenerated disks and mesenchymal stem cells in co-culture result in increased matrix production., *Cells. Tissues. Organs* **191**, 2–11 (2010).
18. T. S. de Windt *et al.*, Concise review: unraveling stem cell cocultures in regenerative medicine: which cell interactions steer cartilage regeneration and how?, *Stem Cells Transl. Med.* **3**, 723–33 (2014).
19. D. R. Albrecht, G. H. Underhill, T. B. Wassermann, R. L. Sah, S. N. Bhatia, Probing the role of multicellular organization in three-dimensional microenvironments., *Nat. Methods*

3, 369–75 (2006).

20. L. Gao, R. McBeath, C. S. Chen, Stem cell shape regulates a chondrogenic versus myogenic fate through Rac1 and N-cadherin., *Stem Cells* **28**, 564–72 (2010).

21. X. Tang, L. Fan, M. Pei, L. Zeng, Z. Ge, Evolving concepts of chondrogenic differentiation: history, state-of-the-art and future perspectives., *Eur. Cell. Mater.* **30**, 12–27 (2015).

22. Z. F. Lu, B. Zandieh Doulabi, P. I. Wuisman, R. a Bank, M. N. Helder, Differentiation of adipose stem cells by nucleus pulposus cells: configuration effect., *Biochem. Biophys. Res. Commun.* **359**, 991–6 (2007).

23. B. Cao, Z. Li, R. Peng, J. Ding, Effects of cell–cell contact and oxygen tension on chondrogenic differentiation of stem cells, *Biomaterials* **64**, 21–32 (2015).

24. M. C. Goude, T. C. McDevitt, J. S. Temenoff, Chondroitin sulfate microparticles modulate transforming growth factor-β1-induced chondrogenesis of human mesenchymal stem cell spheroids., *Cells. Tissues. Organs* **199**, 117–30 (2014).

25. A. Allon, R. Schneider, J. Lotz, Co-culture of adult mesenchymal stem cells and nucleus pulposus cells in bilaminar pellets for intervertebral disc regeneration, *SAS J.* **3**, 41–49 (2009).

26. M. B. Mueller *et al.*, Hypertrophy in mesenchymal stem cell chondrogenesis: effect of TGF-beta isoforms and chondrogenic conditioning., *Cells. Tissues. Organs* **192**, 158–66 (2010).

27. M. E. Cooke *et al.*, Structured three-dimensional co-culture of mesenchymal stem cells with chondrocytes promotes chondrogenic differentiation without hypertrophy., *Osteoarthritis Cartilage* **19**, 1210–8 (2011).

28. T. Kluba, T. Niemeyer, C. Gaissmaier, T. Grunder, Human anulus fibrosis and nucleus pulposus cells of the intervertebral disc: effect of degeneration and culture system on cell phenotype, *Spine (Phila. Pa. 1976).* **30**, 2743–2748 (2005).

29. M. V Risbud *et al.*, Defining the phenotype of young healthy nucleus pulposus cells: recommendations of the Spine Research Interest Group at the 2014 annual ORS meeting., *J. Orthop. Res.* **33**, 283–93 (2015).

30. A. E. Cerchiari *et al.*, A strategy for tissue self-organization that is robust to cellular heterogeneity and plasticity, *Proc. Natl. Acad. Sci.* **112**, 2287–2292 (2015).

31. Y. C. Huang, V. Y. L. Leung, W. W. Lu, K. D. K. Luk, The effects of microenvironment in mesenchymal stem cell-based regeneration of intervertebral disc, *Spine J.* **13**, 352–362 (2013).

32. T. D. Schmittgen, K. J. Livak, Analyzing real-time PCR data by the comparative C(T) method., *Nat. Protoc.* **3**, 1101–1108 (2008).

33. L. Wu *et al.*, Trophic effects of mesenchymal stem cells increase chondrocyte proliferation and matrix formation., *Tissue Eng. Part A* **17**, 1425–36 (2011).

34. B. O. Enobakhare, D. L. Bader, D. A. Lee, Quantification of sulfated glycosaminoglycans in chondrocyte/alginate cultures, by use of 1,9-dimethylmethylene blue., *Anal. Biochem.* **243**, 189–91 (1996).

35. C. J. Billington, in *Matrix Metalloproteinase Protocols*, (Humana Press, New Jersey, 2000), pp. 451–456.

36. X. Liu *et al.*, In vivo ectopic chondrogenesis of BMSCs directed by mature chondrocytes., *Biomaterials* **31**, 9406–14 (2010).

37. M. S. STEINBERG, Reconstruction of tissues by dissociated cells. Some morphogenetic

tissue movements and the sorting out of embryonic cells may have a common explanation., *Science* **141**, 401–8 (1963).

38. T. S. de Windt *et al.*, Direct Cell–Cell Contact with Chondrocytes Is a Key Mechanism in Multipotent Mesenchymal Stromal Cell-Mediated Chondrogenesis, *Tissue Eng. Part A* **21**, 2536–2547 (2015).

39. L. Bian, D. Y. Zhai, R. L. Mauck, J. A. Burdick, Coculture of human mesenchymal stem cells and articular chondrocytes reduces hypertrophy and enhances functional properties of engineered cartilage., *Tissue Eng. Part A* **17**, 1137–45 (2011).

40. Y.-H. Yang, A. J. Lee, G. a Barabino, Coculture-driven mesenchymal stem cell-differentiated articular chondrocyte-like cells support neocartilage development., *Stem Cells Transl. Med.* **1**, 843–54 (2012).

41. R. L. Mauck, X. Yuan, R. S. Tuan, Chondrogenic differentiation and functional maturation of bovine mesenchymal stem cells in long-term agarose culture., *Osteoarthritis Cartilage* **14**, 179–89 (2006).

42. A. A. Allon, K. Butcher, R. A. Schneider, J. C. Lotz, Structured bilaminar coculture outperforms stem cells and disc cells in a simulated degenerate disc environment., *Spine (Phila. Pa. 1976).* **37**, 813–8 (2012).

43. C. Manferdini *et al.*, Adipose-derived mesenchymal stem cells exert antiinflammatory effects on chondrocytes and synoviocytes from osteoarthritis patients through prostaglandin E2., *Arthritis Rheum.* **65**, 1271–81 (2013).

44. A. Bertolo *et al.*, Human mesenchymal stem cell co-culture modulates the immunological properties of human intervertebral disc tissue fragments in vitro., *Eur. Spine J.* **20**, 592–603 (2011).

45. A. I. Caplan, D. Correa, The MSC: an injury drugstore., *Cell Stem Cell* **9**, 11–5 (2011).

46. J. a Zimmermann, T. C. McDevitt, Pre-conditioning mesenchymal stromal cell spheroids for immunomodulatory paracrine factor secretion., *Cytotherapy* **16**, 331–45 (2014).

47. A. Wei *et al.*, Differentiation of rodent bone marrow mesenchymal stem cells into intervertebral disc-like cells following coculture with rat disc tissue., *Tissue Eng. Part A* **15**, 2581–95 (2009).

48. D. J. Prockop, "Stemness" does not explain the repair of many tissues by mesenchymal stem/multipotent stromal cells (MSCs)., *Clin. Pharmacol. Ther.* **82**, 241–3 (2007).

49. L. Wu, H.-J. Prins, M. N. Helder, C. A. van Blitterswijk, M. Karperien, Trophic effects of mesenchymal stem cells in chondrocyte co-cultures are independent of culture conditions and cell sources., *Tissue Eng. Part A* **18**, 1542–51 (2012).

50. R. Yañez, A. Oviedo, M. Aldea, J. A. Bueren, M. L. Lamana, Prostaglandin E2 plays a key role in the immunosuppressive properties of adipose and bone marrow tissue-derived mesenchymal stromal cells., *Exp. Cell Res.* **316**, 3109–23 (2010).

51. W. Zhang, C. Green, N. S. Stott, Bone morphogenetic protein-2 modulation of chondrogenic differentiation in vitro involves gap junction-mediated intercellular communication., *J. Cell. Physiol.* **193**, 233–43 (2002).

52. S. Strassburg, N. W. Hodson, P. I. Hill, S. M. Richardson, J. a Hoyland, Bi-directional exchange of membrane components occurs during co-culture of mesenchymal stem cells and nucleus pulposus cells., *PLoS One* **7**, e33739 (2012).

53. C. Acharya *et al.*, Enhanced chondrocyte proliferation and mesenchymal stromal cells chondrogenesis in coculture pellets mediate improved cartilage formation., *J. Cell. Physiol.* **227**, 88–97 (2012).

54. R. J. MacFarlane *et al.*, Anti-inflammatory role and immunomodulation of mesenchymal stem cells in systemic joint diseases: potential for treatment., *Expert Opin. Ther. Targets* **17**, 243–54 (2013).

55. S. Sobajima *et al.*, Feasibility of a stem cell therapy for intervertebral disc degeneration, *Spine J.* **8**, 888–896 (2008).

56. L. Wu, J. Leijten, C. a van Blitterswijk, M. Karperien, Fibroblast growth factor-1 is a mesenchymal stromal cell-secreted factor stimulating proliferation of osteoarthritic chondrocytes in co-culture., *Stem Cells Dev.* **22**, 2356–67 (2013).

57. A. A. Allon, K. Butcher, R. A. Schneider, J. C. Lotz, Structured coculture of mesenchymal stem cells and disc cells enhances differentiation and proliferation., *Cells Tissues Organs* **196**, 99–106 (2012).

58. L. J. Smith, N. L. Nerurkar, K.-S. Choi, B. D. Harfe, D. M. Elliott, Degeneration and regeneration of the intervertebral disc: lessons from development., *Dis. Model. Mech.* **4**, 31–41 (2011).

59. J. Rutges *et al.*, Variations in gene and protein expression in human nucleus pulposus in comparison with annulus fibrosus and cartilage cells: potential associations with aging and degeneration, *Osteoarthr. Cartil.* **18**, 416–423 (2010).

60. G. Siegel *et al.*, Phenotype, donor age and gender affect function of human bone marrow-derived mesenchymal stromal cells, *BMC Med.* **11**, 146 (2013).

61. A. Reinisch *et al.*, Epigenetic and in vivo comparison of diverse MSC sources reveals an endochondral signature for human hematopoietic niche formation, *Blood* **125**, 249–260 (2015).

62. C. Neidlinger-Wilke *et al.*, Regulation of gene expression in intervertebral disc cells by

low and high hydrostatic pressure., *Eur. Spine J.* **15 Suppl 3**, S372-8 (2006).

63. E. Szabó *et al.*, Licensing by Inflammatory Cytokines Abolishes Heterogeneity of Immunosuppressive Function of Mesenchymal Stem Cell Population, *Stem Cells Dev.* **24**, 2171–2180 (2015).

64. P. Bernstein *et al.*, Sox9 expression of alginate-encapsulated chondrocytes is stimulated by low cell density., *J. Biomed. Mater. Res. A* **91**, 910–8 (2009).

65. K. Serigano *et al.*, Effect of cell number on mesenchymal stem cell transplantation in a canine disc degeneration model., *J. Orthop. Res.* **28**, 1267–75 (2010).

Chapter 3: Effects of cell type and hypoxic preconditioning on cell viability in a diffusion-limited microenvironment.

3.1 Introduction

Intervertebral disc degeneration is a major cause of low back pain, and occurs in 90% of the population over 50 years of age. Current treatments for degeneration, which may include fusion surgery or artificial disc replacements, fail to restore the disc's biochemical and biomechanical properties. Therefore, tissue engineering with biomaterials, cells, or growth factors is a promising solution to regenerate disc structure and better restore function (*1*).

One major research area within intervertebral disc (IVD) tissue engineering is cell therapy, in which healthy cells are injected into a degenerative disc to increase matrix synthesis and repopulate the nucleus pulposus (NP) (*2*). However, cells introduced into the nucleus will have to cope with unique environmental challenges, including low glucose, low oxygen, pressure, low pH, and high osmolality (*3*, *4*). Nutrition is a primary limiting factor, because the disc is avascular, cells in the center may be up to 8 mm from a blood vessel, and the endplates become less permeable with age and degeneration (*5*, *6*). Endplate damage during disc degeneration often exacerbates these conditions by further limiting diffusion of nutrients and waste products. The degenerative microenvironment also contains inflammatory cytokines and matrix fragments, which impede cell survival, downregulate chondrogenesis, and upregulate catabolic activity, thus contributing to the degenerative cascade and further impairing cell viability (*7*, *8*). When developing and evaluating cell therapies, it is crucial to consider how implanted cells might survive in the disc microenvironment, as well as the impact on host nucleus pulposus cells (NPCs).

NPCs have an advantage as a cell therapy because they have already adapted for survival in the disc microenvironment (*9*). However, sources of healthy NPCs are limited, and harvesting them may cause donor site morbidity (*1*). Mesenchymal stem cells (MSCs), which are often used in other areas of tissue engineering, can be isolated from various tissues in the body and can differentiate to multiple lineages, including chondrogenic (*10*). NPCs and MSCs are both promising cell therapy candidates for IVD tissue engineering, but they may respond differently to the limitations of the disc environment, so it is important to consider how each reacts (*11*).

One important characteristic of the disc microenvironment caused by diffusion limitations is low glucose. Low glucose may stimulate chondrogenic gene expression in MSCs (*3*, *12*), but in some studies it decreased matrix production and deposition (*13*, *14*). NPCs appeared to be less sensitive than MSCs to changes in glucose concentration (*11*). Glucose also has a controversial effect on proliferation: increased proliferation was associated with low glucose levels in MSCs (*3*, *13*), but decreased cell viability was observed in both MSCs and NPCs (*12*, *15–17*). Results may depend on the severity of glucose deprivation (*11*) or cell seeding density (*17*) and the combination of low glucose with other stresses in the environment, such as low pH (*16*).

The disc microenvironment is often acidic due to buildup of lactic acid waste. In severe degeneration, the pH of the disc can be as low as 5.7 (*18*). Acidity appears to inhibit chondrogenesis and decrease cell proliferation and viability in MSCs while upregulating the expression of catabolic factors (*3*, *4*, *12*, *19*, *20*). In one study NPCs maintained proteoglycan (PG) synthesis in slightly acidic conditions (pH 6.6) (*21*), but in another increased acidity promoted a catabolic and inflammatory phenotype in NPCs, as well as reduced proliferation and viability (*18*).

Due to the high fixed negative charge in the NP, normal disc osmolality is also higher than other tissues, with a range of 400-550 mOsm/kg (*22*). While NPCs are presumably adapted to this media condition, the effect of high osmolality on MSCs is controversial: some studies suggest that it hampers matrix biosynthesis and cell proliferation (*3*), while others indicate that higher osmolarity actually improves matrix production (*22*). Furthermore, GAG content is lost in degeneration, so osmolality may actually decrease in degenerative discs. Further studies are needed to quantify these changes and their effect on NPCs and MSCs.

Finally, hypoxia is another key feature of the disc microenvironment, and may drop to <5% O_2 in degeneration (*4*). NPCs are adapted to the hypoxic microenvironment, as evidenced by constitutive expression of HIF-1α (*23*). Hypoxia did not appear to affect proliferation, senescence, cell death, or collagen I and II production in NPCs (*13*), and may improve chondrogenesis, uniform matrix deposition, and NPC phenotype maintenance (*24–26*). Although Naqvi and Buckley found that MSCs were more sensitive to combined hypoxia and low glucose conditions than NPCs (*11*), other studies indicate that hypoxia may also have benefits for MSCs, possibly because they are also adapted for a hypoxic environment – bone marrow oxygen concentrations typically range from 4-7% (*27*, *28*). Hypoxia has been extensively shown to enhance chondrogenesis in MSCs (*28–34*), even in an inflammatory environment (*35*). Hypoxia may also inhibit cell senescence and improve proliferation, possibly by suppressing reactive oxygen species (ROS) generation or by stabilization of HIF-1α (*36–40*). However, under very low O_2 tension (1%), hypoxia may still have negative effects (*41*). Because hypoxia pathways have crosstalk with low glucose and cell density responses (*14*, *17*), studying hypoxia in concert with other disc microenvironmental conditions provides a more realistic simulation to predict cell behavior.

In this study, we used a diffusion chamber to simulate challenges present in the disc microenvironment, and to evaluate the effect of two design variables on cell viability in a diffusion-limited system. First, we evaluated the effect of cell type, since MSCs and NPCs may have different response to the disc microenvironment. In particular, MSC and NPC coculture may improve chondrogenesis, increase cell proliferation and reduce senescence, and increase resilience to a degenerative microenvironment (*42–48*),. We hypothesized that coculture of MSCs and NPCs could affect overall cell viability in a diffusion-limited system.

Second, we evaluated the effects of MSC preconditioning on cell viability. Preconditioning-induced protection of MSCs has been studied for several decades and explored in many tissues (*49, 50*). Preconditioning by isolation and/or expansion in hypoxic conditions appears to increase later proliferation and differentiation ability of MSCs, decrease senescence, increase chondrogenesis, and improve mechanical properties of cultured tissue (*39, 50–52*). In many cases, these benefits persisted even when later culture occurred in normoxia, and preconditioning oxygen conditions appeared to have more influence than culture oxygen conditions on chondrogenic gene expression and GAG content (*51, 53, 54*). We hypothesized that preconditioning MSCs by expansion in hypoxia could also improve later cell viability in a diffusion chamber that was cultured in normoxia, but had hypoxic conditions in the center of the chamber due to diffusion limitations.

3.2 Methods

Cell expansion: Bovine NPCs (passage 4, harvested as previously described (*55*) from caudal discs from one individual, obtained from a local slaughterhouse) were cultured in standard disc media (low-glucose DMEM (Invitrogen) with 5% FBS (Hyclone), 1% antibiotic/antimycotic (UCSF Cell Culture Facility), 1% non-essential amino acids (UCSF CCF), and 1.5% osmolarity

salt solution containing 5M NaCl and 0.4M KCl (made in the lab)). Human MSCs from one donor (female, age 20) were purchased from RoosterBio, Inc. (Fredrick, MD) and expanded in hBM-MSC High Performance Media (RoosterBio, Inc.) to population doubling level (PDL) 19, which was calculated with an hMSC age tracker also provided by RoosterBio, Inc. MSCs were either expanded in normoxia or hypoxia (5% O_2, 5% CO_2). 24 hours prior to forming diffusion chambers, MSCs were switched to a 50/50 mix of RB and standard disc media to acclimate them to media conditions. We did not observe any changes in cell appearance or viability after the media change.

Cell type groups: We compared 5 different groups: NPCs-only (NPC), MSCs-only (MSC), MSCs-only with hypoxic preconditioning (MSChyp), NPCs and MSCs cocultured in a 1:1 ratio (NPC-MSC), and NPCs and MSCs cocultured in a 1:1 ratio, using MSCs that were expanded in hypoxia (NPC-MSChyp). Some chambers were damaged during manufacturing and harvesting, so the number of replicates for each cell type group ranged from 6 to 10. A power analysis determined that 6 replicates were sufficient for 80% power (JMP, SAS).

Diffusion chamber materials: As shown in Figure 3.1, we assembled diffusion chambers using two Gold Seal glass slides (75 mm x 25 mm) separated by two spacers (no 1.5 Fisherbrand coverslips, which have a thickness of 170 μm). The coverslips were adhered to the bottom slide using CoverSafe™ mounting media and baked at 60 deg C for at least 2 hours, until dry. They were spaced to create for a chamber of 15 mm width. The width was chosen for compatibility with other experiments using this chamber, which involve sections of cartilage endplate that are generally ~15 mm long. The chamber is similar in design to one used in previous diffusion-limited assays (*5*, *57*).

Diffusion chamber formation: MSCs and NPCs were trypsinized with TrypLE Select (Thermo Fisher Scientific, Waltham, MA), counted, and resuspended in standard disc media. Cell solutions were mixed with autoclaved low-temperature gelling agarose type VII-A (Sigma-Aldrich, St. Louis, MO) to a final concentration of 2, 4, or 8 million cells/ml and loaded onto the bottom chamber slide. Once the top slide was placed, the agarose formed a gel between the glass in less than one minute, and chamber areas not containing cells were sealed with parafilm to hold the chamber together. Chambers were cultured in 100 x 15 mm petri dishes in 25 ml of standard disc media for 72 hours. We used standard disc media to represent disc environmental conditions because it has glucose and osmolality levels similar to those found in discs (*3*, *22*).

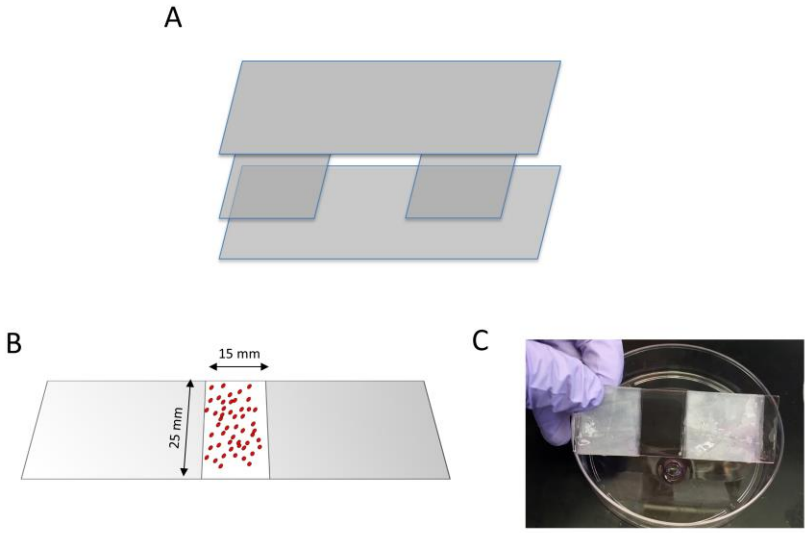

Figure 3.1 Diffusion chamber manufacturing. The diffusion chamber is made with 2 glass slides separated by No. 1.5 coverslips (A), with a sandwiched layer of cells in 1% agarose (B). The slides are cultured in a 100 x 15 mm petri dish (C).

Viable distance measurement: The diffusion chambers were separated by removing the top slide, and the gel was gently washed in PBS. A live/dead cytotoxicity/viability kit (Thermo Fisher Scientific, Waltham, MA), was mixed according to the manufacturer's instructions, and the gel was covered with solution (approximately 200 µL) and incubated at 37°C for 30 minutes.

Afterwards, the gels were imaged both a lower-magnification, with a Leica MZ FLIII microscope, and at higher-magnification with a Leica DMi8 microscope. Using the lower-magnification images, the top & bottom viable distance was measured for each chamber using ImageJ. Areas with large bubbles or ripped gel sections were excluded. In some cases where background fluorescence made the viable distance threshold difficult to detect, the higher-magnification image was also measured and confirmed to be within 10% of the first measurement. We also compared viable distance measurements between two raters to ensure inter-rater reliability.

Cell density estimate: After imaging the gels, we determined that original cell seeding densities resulted in a wide range of actual cell density in the gels, most likely because the counting the cells by hemocytometer was inexact. Therefore, higher magnification images were used to get a cell count estimate, by choosing a representative frame of live cells (3-5 frames from the chamber edge), and counting the number of cells present in ImageJ. Cell count were divided by the frame dimension (1.79 mm x 1.34 mm) and approximate gel thickness (170 μm) to calculate an estimated cell density. This number was used for data analysis rather than the original cell seeding density.

Statistics: Viable distance results for different cell type groups were analyzed with a linear fit model in JMP (SAS). Live cell estimates for different cell type groups were also compared using a one-way ANOVA with a Tukey multiple hypothesis correction (Prism, Graphpad). p values < 0.05 were considered significant.

3.3 Results

The diffusion chamber images had a clear threshold between live and dead cells, which allowed us to measure the viable distance (Figure 3.2A). Viable distance decreased with original

cell seeding density, and the cell counts increased (Figure 3.2B). We used the cell counts from higher-magnification images to calculate an estimate of cell density specific to each replicate.

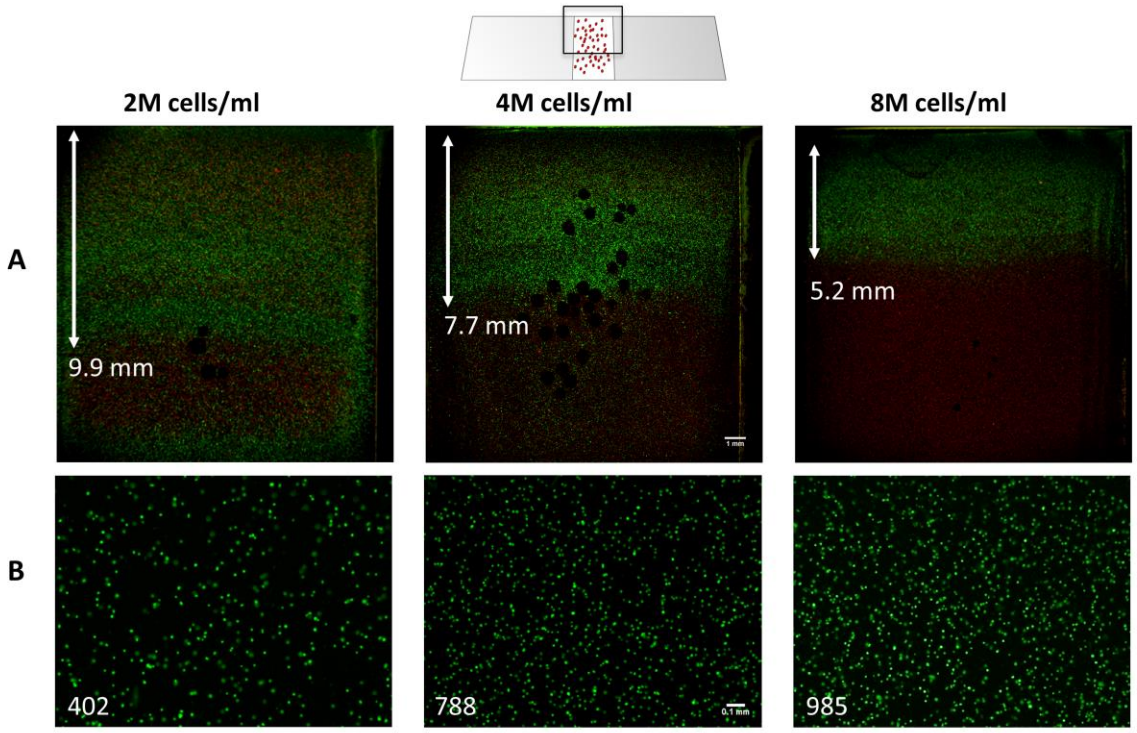

Figure 3.2 Representative viable distance images. Live/dead stains of chambers with various seeding densities (A) indicate decreasing viable distance with higher cell density, as well as a visible threshold for cell viability (scale bar 1 mm). Cell counts of higher-magnification cell images (B) were used as a more accurate measure of cell density rather than seeding density (scale bar 0.1 mm).

We used a multifactorial least squares model (JMP) to fit viable distance with cell type, the log of the estimated cell density, and the cross of cell type and estimated cell density, which resulted in a model with $R^2 = 0.91$ (Figure 3.3). The log of the cell density was used based on previous proposed models of cell metabolism (Stairmand et al. 1991, Horner and Urban 2001). As expected, viable distance was significantly correlated with cell density ($p < 0.0001$), but the slope of this relationship was not dependent on cell type ($p = 0.28$). Cell type also accounted for 28% of the observed variance in our data, and varying cell type resulted in a trend of shifting the

intercept of the trendline ($p = 0.069$) that did not reach significance. For a given cell density, NPCs appear to have the shortest viable distance, while MSCs with hypoxia preconditioning have the highest.

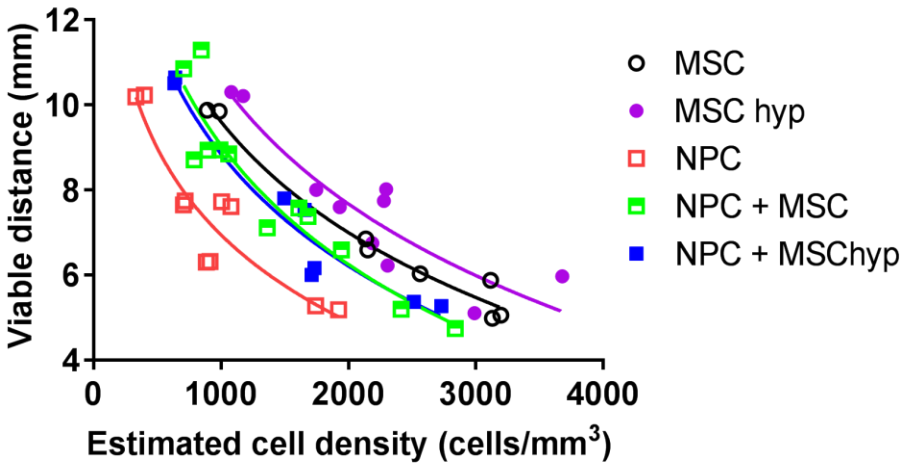

Figure 3.3 Viable distance model fit with estimated cell density and cell types. Viable distance was fitted with the log of the density and cell types using a multifactorial least squares model (JMP).

Using the viable distance and estimated cell density, we calculated an estimated live cell number for each sample (live cell number = viable distance * chamber width * chamber thickness * estimated cell density). This allowed us to compare different cell type groups independent of cell density, as shown in Figure 3.4. A one-way ANOVA determined that cell type significantly affects estimated live cell numbers ($p < 0.0001$). Estimated live cell numbers for the NPC group were significantly lower than those for all other groups, which correlates with observations from the curve fit in Figure 3.3. Estimated live cell numbers for the coculture groups were also lower than cell numbers in the MSC and MSChyp groups, although not all combinations reached significance (Figure 3.4). Estimated live cell numbers for the MSC and

MSChyp groups were not significantly different, nor were the numbers for the NPC + MSC and NPC + MSChyp groups ($p > 0.1$).

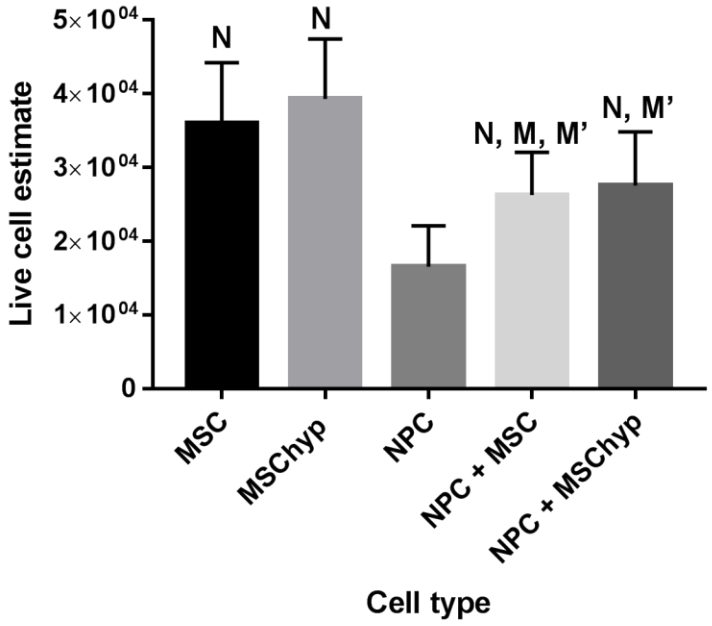

Figure 3.4 Live cell estimate of different cell type groups. Error bars represent standard deviation. Groups were analyzed by a one-way ANOVA with the result $p<0.0001$, and by multiple comparisons with a Tukey correction ($p<0.05$), as shown on the graph. N = significantly different from the NPC-only group, M = significantly different from the MSC-only group, and M' = significantly different from the MSC-only group. (The NPC group is significantly different from all other groups).

Finally, we compared viability among single-cell-type and coculture groups. Performance of the coculture groups represented an average of MSC-only and NPC-only groups, showing no synergy or increase in viability due to coculture (Figure 3.5). Hypoxic preconditioning also did not appear to modulate the effects of coculture.

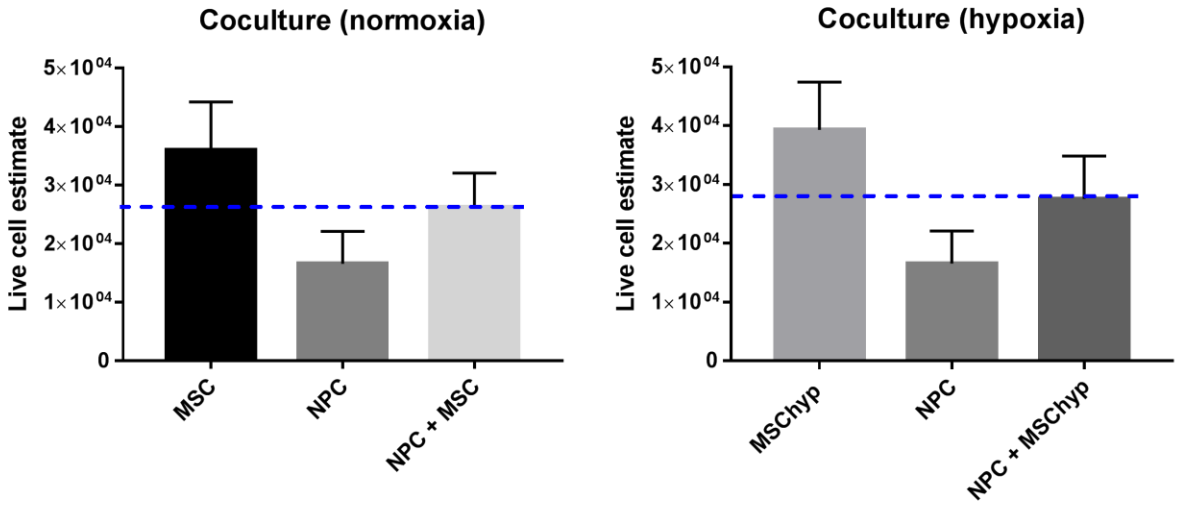

Figure 3.5 Live cell estimate of coculture comparison groups, with and without hypoxia preconditioning. Error bars represent standard deviation. The dotted line represents the mean of MSC-only and NPC-only groups.

3.4 Discussion

In this study, we used a diffusion chamber system to simulate nutrition limits that would occur in the disc microenvironment. As observed in previous studies (*5*), cell death was highest in the center of the chambers, which were the farthest away from media and oxygen. We initially expected that MSCs might have lower viability in diffusion-limited conditions because they lack adaptations to the disc microenvironment and have been shown to have a higher glucose consumption rate than NPCs in IVD-like conditions (*11*). However, in our study, MSCs had a higher viable distance and significantly higher estimated live cell number than NPCs. This may be due to some metabolic changes in MSCs induced by hypoxia, such as downregulation of senescence or changes in oxygen consumption (*37*, *38*).

Since MSCs had a high viability compared with other cell types, they may be a good candidate for cell therapy injections into the NP. However, cell density is an important variable to consider. At original seeding densities of 8 x 10^6 cells/ml, the average viable distance over all

groups was 5.2 mm, meaning that over 50% of cells in the chamber were already dead after 72 hours of culture. Higher cell seeding densities of 2 x 10^7 or 4 x 10^7 cells/ml have been used for tissue engineering constructs *in vitro* (*58*, *59*), but such high densities could negatively impact cell survival in a disc environment. In an *in vivo* study, Serigano *et al.* found that transplanting 10^6 MSCs per disc resulted in less apoptosis and greater cell viability than both 10^5 and 10^7 cells per disc (*60*). A recent clinical trial also found that a lower-density injection of 3 x 10^6 cells/ml resulted in more patient improvement than injections of 9 x 10^6 cells/ml (clinicaltrials.gov identifier NCT01290367) (*61*). Therefore, a more extensive understanding of cell viability in the disc microenvironment can have important clinical implications.

In this study, we originally hypothesized that hypoxic preconditioning would prime MSCs for survival in a diffusion-limited environment. However, we did not observe a significant improvement in viable distance with hypoxic preconditioning for either MSC-only or coculture groups. Other groups observed improvements in proliferation, chondrogenesis, and mechanical properties in long-term tissue culture, so perhaps the effects of hypoxic preconditioning would be more apparent at later timepoints (*39*, *51*). Future experiments could also include NPC groups expanded in hypoxia: some studies using articular chondrocytes showed improved chondrogenesis with preconditioning (*62*), although others found no significant benefit (*63*).

We also did not observe any synergistic benefits of coculture on cell viability, which was another objective of this study. This suggests that MSCs and NPCs are not exchanging survival signals. However, coculture may have more subtle effects on cell growth, telomerase activity, or the response to inflammation (*64*, *65*). In general, coculture studies may also have variable results due differences in experimental conditions, such as scaffold materials, overall cell density, ratios of cocultured cell types, and media composition (*60*, *66*, *67*). Not many studies

have tested MSC-NPC coculture in combination with hypoxia or low glucose, but Stoyanov *et al.* found that hypoxia and growth factors had a more significant effect on cell chondrogenesis than coculture (*29*). Another study with MSCs and articular chondrocytes found that hypoxia decreased DNA content for all groups regardless of coculture, but coculture may also inhibit hypoxia-induced hypertrophy of MSCs (*68*). More research is needed to observe long-term effects of coculture in a diffusion-limited environment.

One of the limitations of our study is the lack of the long-term timepoints mentioned above. We used a short culture period (72 hours) based on viable distance equilibrium data from past studies (*5*), concerns about the long-term biocompatibility of the diffusion chamber materials, and concerns about how bulk media changes would affect the diffusion gradient. However, longer-term culture data could provide more information about synthetic ability of the cells, and highlight adaptations they might develop when exposed to longer periods of nutrient deprivation as well as any negative effects of cell debris or waste products accumulating in the center of the chamber. Hypoxia effects have been shown to be time-dependent, so a range of timepoints is helpful to understand how cells might respond both immediately after and several months following a cell therapy treatment (*24*, *68*). A bioreactor system could provide more consistent environmental conditions during media replacement (*68*, *69*).

Another limitation of our study is only using MSCs and NPCs from one donor for each cell type. Horner and Urban found that NPCs from different bovine donors had a higher standard deviation in viability measurements than replicates from a single donor (*5*). They hypothesized that individual animals may have metabolic differences, leading to slightly different cell nutrition requirements. The metabolic differences might be influenced by age (*70*). In a pilot study, we

also observed some differences between individual NPC donors, although coculture with MSCs may help to mitigate these differences (Appendix B).

Individual differences among MSC donors may also affect viability. Previous studies have found that donor age slightly affected MSC proliferation, but not responses to degenerative microenvironment conditions (*3*, *12*, *20*). Other studies have shown positive responses to hypoxia for multiple MSC, NPC, and AF cell lines (*25*, *54*, *71*). One possible donor difference is that while trends in responses may be similar, magnitude of the effect can vary (*51*). Even within single donors, heterogeneous subpopulations may have differences in cell response and matrix production under stress (*14*). Therefore, further research with more biological replicates is needed to determine the extent of variation among individual donors, especially in a degenerative microenvironment.

To improve our simulation of the degenerative disc microenvironment, it would be useful to monitor glucose, oxygen, pH, and osmolality levels in the center of the diffusion chamber in real time. These measurements could be compared to those made in human discs (*72*). In addition, we could impose more external stresses, for example by culturing the chambers in hypoxia or artificially lowering media pH, to create additional cellular stress and map a gradient of cell responses to increasingly harsh conditions. Inflammatory cytokines could also be added to the system to more accurately simulate degeneration. Furthermore, many other culture variables, such as carrier properties and the mechanical loading environment, also affect cell viability (*15*, *73*). The diffusion chamber can be formed with different biomaterials, allowing for a more realistic screening assay.

Finally, outcome measures other than cell viability are also important. As previously mentioned, longer time points will allow for measurement of chondrogenesis and matrix

synthesis. Naqvi and Buckley found that cells cultured in very low glucose (1 mM) still appeared viable but deposited very little matrix, so viability alone is not a sufficient indicator of regenerative potential (*11*). A senescence assay would also provide more nuanced information about cell phenotypes under diffusion-limited conditions.

Overall, this study investigated effects of cell type and hypoxic preconditioning on cell viability in a diffusion-limited environment. We found some differences in cell types, but found that hypoxic preconditioning and coculture did not significantly influence viability in a disc microenvironment. Improved understanding of factors influencing viability could optimize cell survival after injection into a degenerative disc. In the future, our diffusion chamber system could also be a useful early-stage test for new therapies and technologies, since it provides an *in vitro* simulation of disc microenvironment constraints and diffusion gradients.

3.5 References

1. Y. Moriguchi *et al.*, Biological Treatment Approaches for Degenerative Disk Disease: A Literature Review of In Vivo Animal and Clinical Data. *Glob. Spine J.* **6**, 497–518 (2016).
2. D. Drazin, J. Rosner, P. Avalos, F. Acosta, Stem Cell Therapy for Degenerative Disc Disease. *Adv. Orthop.* **2012**, 1–8 (2012).
3. K. Wuertz, K. E. Godburn, C. Neidlinger-Wilke, J. Urban, J. C. Iatridis, Behavior of mesenchymal stem cellsin the chemical microenvironment of the intervertebral disc. *Spine (Phila. Pa. 1976).* **33**, 1843–1849 (2008).
4. S. M. Naqvi, C. T. Buckley, Bone Marrow Stem Cells in Response to Intervertebral Disc-Like Matrix Acidity and Oxygen Concentration. *Spine (Phila. Pa. 1976).* **41**, 743–750 (2016).
5. H. a Horner, J. P. Urban, 2001 Volvo Award Winner in Basic Science Studies: Effect of

nutrient supply on the viability of cells from the nucleus pulposus of the intervertebral disc. *Spine (Phila. Pa. 1976).* **26**, 2543–9 (2001).

6. H. Li *et al.*, Influence of hypoxia in the intervertebral disc on the biological behaviors of rat adipose- and nucleus pulposus-derived mesenchymal stem cells. *Cells. Tissues. Organs*. **198**, 266–77 (2013).
7. J. A. Buckwalter, Aging and degeneration of the human intervertebral disc. *Spine (Phila. Pa. 1976).* **20** (1995), pp. 1307–14.
8. P. P. A. Vergroesen *et al.*, Mechanics and biology in intervertebral disc degeneration: A vicious circle. *Osteoarthr. Cartil.* **23**, 1057–1070 (2015).
9. M. V Risbud *et al.*, Nucleus pulposus cells express HIF-1 alpha under normoxic culture conditions: a metabolic adaptation to the intervertebral disc microenvironment. *J. Cell. Biochem.* **98**, 152–9 (2006).
10. J. Zeckser, M. Wolff, J. Tucker, J. Goodwin, Multipotent Mesenchymal Stem Cell Treatment for Discogenic Low Back Pain and Disc Degeneration. *Stem Cells Int.* **2016**, 1–13 (2016).
11. S. M. Naqvi, C. T. Buckley, Extracellular matrix production by nucleus pulposus and bone marrow stem cells in response to altered oxygen and glucose microenvironments. *J. Anat.* **227**, 757–766 (2015).
12. C. Liang *et al.*, Responses of human adipose-derived mesenchymal stem cells to chemical microenvironment of the intervertebral disc. *J. Transl. Med.* **10**, 49 (2012).
13. W. E. B. Johnson, S. Stephan, S. Roberts, The influence of serum, glucose and oxygen on intervertebral disc cell growth in vitro: implications for degenerative disc disease. *Arthritis Res. Ther.* **10**, R46 (2008).

14. M. J. Farrell, J. I. Shin, L. J. Smith, R. L. Mauck, Functional consequences of glucose and oxygen deprivation on engineered mesenchymal stem cell-based cartilage constructs. *Osteoarthr. Cartil.* **23**, 134–142 (2015).

15. B. Deorosan, E. A. Nauman, The Role of Glucose, Serum, and Three-Dimensional Cell Culture on the Metabolism of Bone Marrow-Derived Mesenchymal Stem Cells. *Stem Cells Int.* **2011**, 1–12 (2011).

16. S. R. S. Bibby, J. P. G. Urban, Effect of nutrient deprivation on the viability of intervertebral disc cells. *Eur. Spine J.* **13**, 695–701 (2004).

17. S. Stephan, W. Johnson, S. Roberts, The influence of nutrient supply and cell density on the growth and survival of intervertebral disc cells in 3D culture. *Eur. Cells Mater.* **22**, 97–108 (2011).

18. H. T. J. Gilbert, N. Hodson, P. Baird, S. M. Richardson, J. A. Hoyland, Acidic pH promotes intervertebral disc degeneration: Acid-sensing ion channel -3 as a potential therapeutic target. *Sci. Rep.* **6**, 37360 (2016).

19. B. Han *et al.*, Nucleus pulposus mesenchymal stem cells in acidic conditions mimicking degenerative intervertebral discs give better performance than adipose tissue-derived mesenchymal stem cells. *Cells. Tissues. Organs*. **199**, 342–52 (2014).

20. K. Wuertz, K. Godburn, J. C. Iatridis, MSC response to pH levels found in degenerating intervertebral discs. *Biochem. Biophys. Res. Commun.* **379**, 824–9 (2009).

21. K. Ichimura, H. Tsuji, H. Matsui, N. Makiyama, Cell culture of the intervertebral disc of rats: factors influencing culture, proteoglycan, collagen, and deoxyribonucleic acid synthesis. *J. Spinal Disord.* **4**, 428–36 (1991).

22. G. D. O'Connell, I. B. Newman, M. A. Carapezza, Effect of Long-Term Osmotic Loading

Culture on Matrix Synthesis from Intervertebral Disc Cells. *Biores. Open Access*. **3**, 242–249 (2014).

23. M. V Risbud *et al.*, Defining the phenotype of young healthy nucleus pulposus cells: recommendations of the Spine Research Interest Group at the 2014 annual ORS meeting. *J. Orthop. Res.* **33**, 283–93 (2015).

24. D. J. Gorth *et al.*, Hypoxic regulation of functional extracellular matrix elaboration by nucleus pulposus cells in long-term agarose culture. *J. Orthop. Res.* **33**, 747–754 (2015).

25. G. Feng *et al.*, Hypoxia differentially regulates human nucleus pulposus and annulus fibrosus cell extracellular matrix production in 3D scaffolds. *Osteoarthritis Cartilage*. **21**, 582–8 (2013).

26. G. Feng *et al.*, Hypoxia promotes nucleus pulposus phenotype in 3D scaffolds in vitro and in vivo. *J. Neurosurg. Spine*. **21**, 303–309 (2014).

27. H. Kofoed, E. Sjøntoft, S. O. Siemssen, H. P. Olesen, Bone marrow circulation after osteotomy: Blood flow, pO 2 , pCO 2 , and pressure studied in dogs. *Acta Orthop. Scand.* **56**, 400–403 (1985).

28. L. Baumgartner, S. Arnhold, K. Brixius, K. Addicks, W. Bloch, Human mesenchymal stem cells: Influence of oxygen pressure on proliferation and chondrogenic differentiation in fibrin glue in vitro. *J. Biomed. Mater. Res. A.* **93**, 930–40 (2010).

29. J. V Stoyanov *et al.*, Role of hypoxia and growth and differentiation factor-5 on differentiation of human mesenchymal stem cells towards intervertebral nucleus pulposus-like cells. *Eur. Cells Mater.* **21**, 533–47 (2011).

30. M. V Risbud *et al.*, Differentiation of mesenchymal stem cells towards a nucleus pulposus-like phenotype in vitro: implications for cell-based transplantation therapy. *Spine*

(Phila. Pa. 1976). **29**, 2627–32 (2004).

31. B. D. Markway *et al.*, Enhanced chondrogenic differentiation of human bone marrow-derived mesenchymal stem cells in low oxygen environment micropellet cultures. *Cell Transplant.* **19**, 29–42 (2010).

32. B. Cao, Z. Li, R. Peng, J. Ding, Effects of cell–cell contact and oxygen tension on chondrogenic differentiation of stem cells. *Biomaterials*. **64**, 21–32 (2015).

33. H.-H. Lee *et al.*, Hypoxia Enhances Chondrogenesis and Prevents Terminal Differentiation through PI3K/Akt/FoxO Dependent Anti-Apoptotic Effect. *Sci. Rep.* **3**, 2683 (2013).

34. M. Kanichai, D. Ferguson, P. J. Prendergast, V. A. Campbell, Hypoxia promotes chondrogenesis in rat mesenchymal stem cells: A role for AKT and hypoxia-inducible factor (HIF)-1α. *J. Cell. Physiol.* **216**, 708–715 (2008).

35. T. Felka, R. Schäfer, B. Schewe, K. Benz, W. K. Aicher, Hypoxia reduces the inhibitory effect of IL-1β on chondrogenic differentiation of FCS-free expanded MSC. *Osteoarthr. Cartil.* **17**, 1368–1376 (2009).

36. N. Haque, M. T. Rahman, N. H. Abu Kasim, A. M. Alabsi, Hypoxic Culture Conditions as a Solution for Mesenchymal Stem Cell Based Regenerative Therapy. *Sci. World J.* **2013**, 1–12 (2013).

37. G. Pattappa *et al.*, Continuous and uninterrupted oxygen tension influences the colony formation and oxidative metabolism of human mesenchymal stem cells. *Tissue Eng. Part C. Methods*. **19**, 68–79 (2013).

38. C.-C. Tsai *et al.*, Hypoxia inhibits senescence and maintains mesenchymal stem cell properties through down-regulation of E2A-p21 by HIF-TWIST. *Blood*. **117**, 459–69

(2011).

39. E. J. Sheehy, C. T. Buckley, D. J. Kelly, Oxygen tension regulates the osteogenic, chondrogenic and endochondral phenotype of bone marrow derived mesenchymal stem cells. *Biochem. Biophys. Res. Commun.* **417**, 305–10 (2012).

40. R. Das, H. Jahr, G. J. V. M. van Osch, E. Farrell, The Role of Hypoxia in Bone Marrow–Derived Mesenchymal Stem Cells: Considerations for Regenerative Medicine Approaches. *Tissue Eng. Part B Rev.* **16**, 159–168 (2010).

41. C. Holzwarth *et al.*, Low physiologic oxygen tensions reduce proliferation and differentiation of human multipotent mesenchymal stromal cells. *BMC Cell Biol.* **11**, 11 (2010).

42. K. Tsuchiya, G. Chen, T. Ushida, T. Matsuno, T. Tateishi, The effect of coculture of chondrocytes with mesenchymal stem cells on their cartilaginous phenotype in vitro. *Mater. Sci. Eng. C.* **24**, 391–396 (2004).

43. L. Wu *et al.*, Trophic effects of mesenchymal stem cells increase chondrocyte proliferation and matrix formation. *Tissue Eng. Part A.* **17**, 1425–36 (2011).

44. N. Watanabe *et al.*, Suppression of differentiation and proliferation of early chondrogenic cells by Notch. *J. Bone Miner. Metab.* **21**, 344–52 (2003).

45. A. A. Allon, K. Butcher, R. A. Schneider, J. C. Lotz, Structured coculture of mesenchymal stem cells and disc cells enhances differentiation and proliferation. *Cells Tissues Organs.* **196**, 99–106 (2012).

46. C. Manferdini *et al.*, Adipose-derived mesenchymal stem cells exert antiinflammatory effects on chondrocytes and synoviocytes from osteoarthritis patients through prostaglandin E2. *Arthritis Rheum.* **65**, 1271–81 (2013).

47. S. Yang, C.-C. Wu, T. T.-F. Shih, Y.-H. Sun, F.-H. Lin, In vitro study on interaction between human nucleus pulposus cells and mesenchymal stem cells through paracrine stimulation. *Spine (Phila. Pa. 1976).* **33**, 1951–7 (2008).

48. M. Zscharnack, C. Poesel, J. Galle, A. Bader, Low oxygen expansion improves subsequent chondrogenesis of ovine bone-marrow-derived mesenchymal stem cells in collagen type I hydrogel. *Cells Tissues Organs*. **190**, 81–93 (2009).

49. C. E. Murry, R. B. Jennings, K. A. Reimer, Preconditioning with ischemia: a delay of lethal cell injury in ischemic myocardium. *Circulation*. **74**, 1124–36 (1986).

50. M. Pei, Environmental preconditioning rejuvenates adult stem cells' proliferation and chondrogenic potential. *Biomaterials*. **117**, 10–23 (2017).

51. K. D. Hudson, L. J. Bonassar, *Tissue Eng. Part A*, in press, doi:10.1089/ten.TEA.2016.0270.

52. J. Müller, K. Benz, M. Ahlers, C. Gaissmaier, J. Mollenhauer, Hypoxic conditions during expansion culture prime human mesenchymal stromal precursor cells for chondrogenic differentiation in three-dimensional cultures. *Cell Transplant.* **20**, 1589–602 (2011).

53. Y. Xu *et al.*, In vitro expansion of adipose-derived adult stromal cells in hypoxia enhances early chondrogenesis. *Tissue Eng.* **13**, 2981–93 (2007).

54. A. B. Adesida, A. Mulet-Sierra, N. M. Jomha, Hypoxia mediated isolation and expansion enhances the chondrogenic capacity of bone marrow mesenchymal stromal cells. *Stem Cell Res. Ther.* **3**, 9 (2012).

55. A. Allon, R. Schneider, J. Lotz, Co-culture of adult mesenchymal stem cells and nucleus pulposus cells in bilaminar pellets for intervertebral disc regeneration. *SAS J.* **3**, 41–49 (2009).

56. S. K. Greenwood *et al.*, Population doubling: a simple and more accurate estimation of cell growth suppression in the in vitro assay for chromosomal aberrations that reduces irrelevant positive results. *Environ. Mol. Mutagen.* **43**, 36–44 (2004).

57. L. Hlatky, E. L. Alpen, Two-dimensional diffusion limited system for cell growth. *Cell Tissue Kinet.* **18**, 597–611 (1985).

58. R. L. Mauck, X. Yuan, R. S. Tuan, Chondrogenic differentiation and functional maturation of bovine mesenchymal stem cells in long-term agarose culture. *Osteoarthritis Cartilage*. **14**, 179–89 (2006).

59. L. J. Smith *et al.*, Nucleus pulposus cells synthesize a functional extracellular matrix and respond to inflammatory cytokine challenge following long-term agarose culture. *Eur. Cell. Mater.* **22**, 291–301 (2011).

60. K. Serigano *et al.*, Effect of cell number on mesenchymal stem cell transplantation in a canine disc degeneration model. *J. Orthop. Res.* **28**, 1267–75 (2010).

61. Mesoblast, Trial Results: MPC-06-ID Phase 2 Chronic Low Back Pain Due to Disc Degeneration Clinical Trial (2015), (available at http://www.mesoblast.com/clinical-trial-results/mpc-06-id-phase-2).

62. R. J. Egli, J. D. Bastian, R. Ganz, W. Hofstetter, M. Leunig, Hypoxic expansion promotes the chondrogenic potential of articular chondrocytes. *J. Orthop. Res.* **26**, 977–85 (2008).

63. S. Ströbel *et al.*, Anabolic and catabolic responses of human articular chondrocytes to varying oxygen percentages. *Arthritis Res. Ther.* **12**, R34 (2010).

64. A. Ouyang *et al.*, Effects of cell type and configuration on anabolic and catabolic activity in 3D co-culture of mesenchymal stem cells and nucleus pulposus cells. *J. Orthop. Res.* **35**, 61–73 (2017).

65. C.-C. Niu, L.-J. Yuan, S.-S. Lin, L.-H. Chen, W.-J. Chen, Mesenchymal stem cell and nucleus pulposus cell coculture modulates cell profile. *Clin. Orthop. Relat. Res.* **467**, 3263–72 (2009).

66. P. Bernstein *et al.*, Sox9 expression of alginate-encapsulated chondrocytes is stimulated by low cell density. *J. Biomed. Mater. Res. A.* **91**, 910–8 (2009).

67. Y.-H. Yang, A. J. Lee, G. a Barabino, Coculture-driven mesenchymal stem cell-differentiated articular chondrocyte-like cells support neocartilage development. *Stem Cells Transl. Med.* **1**, 843–54 (2012).

68. V. V. Meretoja, R. L. Dahlin, S. Wright, F. K. Kasper, A. G. Mikos, The effect of hypoxia on the chondrogenic differentiation of co-cultured articular chondrocytes and mesenchymal stem cells in scaffolds. *Biomaterials*. **34**, 4266–4273 (2013).

69. A. A. Allon, K. Butcher, R. A. Schneider, J. C. Lotz, Structured bilaminar coculture outperforms stem cells and disc cells in a simulated degenerate disc environment. *Spine (Phila. Pa. 1976).* **37**, 813–8 (2012).

70. R. B. Lee, J. P. Urban, Evidence for a negative Pasteur effect in articular cartilage. *Biochem. J.* **321**, 95–102 (1997).

71. F. Mwale *et al.*, Effect of oxygen levels on proteoglycan synthesis by intervertebral disc cells. *Spine (Phila. Pa. 1976).* **36**, E131-8 (2011).

72. E. M. Bartels, J. C. Fairbank, C. P. Winlove, J. P. Urban, Oxygen and lactate concentrations measured in vivo in the intervertebral discs of patients with scoliosis and back pain. *Spine (Phila. Pa. 1976).* **23**, 1–7; discussion 8 (1998).

73. J. C. Iatridis, J. J. MacLean, P. J. Roughley, M. Alini, Effects of mechanical loading on intervertebral disc metabolism in vivo. *J. Bone Jt. Surg.* **88 Suppl 2**, 41–6 (2006).

Chapter 4: Conclusions and Future Directions

4.1 Research Summary

The research performed as part of this dissertation investigated effects of various design factors on performance of intervertebral disc tissue engineering constructs, especially in the context of a degenerative disc microenvironment. First, we studied the effect of cell type and configuration on MSCs and NPCs in a hypoxic and inflammatory microenvironment. We compared MSC-only, NPC-only, and 50:50 coculture groups in individual cell and micropellet configurations. Individual cell configurations limited cell communication to paracrine signaling, while micropellet configurations allowed for direct cell-cell contact, as well as shorter diffusion distances for soluble factors. We evaluated anabolic and catabolic performance in both basal media conditions and simulated degenerative media conditions with hypoxia and inflammatory cytokines.

Cell type affected both anabolic and catabolic outcomes. Gene expression of Agg and Col2A1, glycosaminoglycan (GAG) content, and aggrecan immunohistochemistry (IHC), were significantly higher in NPC-only and coculture groups than in MSC-only groups, with NPC-only groups exhibiting the highest anabolic gene expression levels. However, NPC-only constructs also responded to inflammation and hypoxia with significant upregulation of catabolic genes (MMP-1, MMP-9, MMP-13, and ADAMTS-5). MSC-only groups were unaffected by degenerative media conditions, and coculture with MSCs modulated catabolic induction of the NPCs, possibly due to trophic and immunomodulatory roles of MSCs.

Configuration was also important in this system, especially in catabolic performance. Culturing cells in a micropellet configuration dramatically reduced catabolic induction in both coculture and NPC-only groups. Furthermore, coculture micropellets, which take advantage of

both cell type and configuration effects, had the most immunomodulatory response, with a significant decrease in MMP-13 and ADAMTS-5 expression in hypoxic and inflammatory media conditions. Coculture micropellets were also found to self-organize into bilaminar formations with an MSC core and NPC outer layer. The bilayered structure is interesting because it may have implications for cell communication that mimics developmental processes.

Studying cell type and configuration in a hypoxic and inflammatory setting highlighted possible immunomodulatory effects of MSCs. Although NPCs had the best anabolic performance, MSCs were beneficial to reduce the induction of catabolic genes (which could ultimately exacerbate degeneration), suggesting that coculture therapies may be beneficial if they include both synthetic and immunomodulatory cell types. Since direct cell-cell contact also had immunomodulatory benefits, this indicates that cell therapy treatments should optimize cell contact, and also motivates further inquiry into the mechanisms of contact-mediated signaling in this setting.

In the second part of this dissertation, we continued investigating cell type and cocutlure in a different system. Using a diffusion chamber system that simulates nutrient constraints present in the disc microenvironment, we compared MSC-only and NPC-only groups with a 50:50 culture, and also tested groups with hypoxia-preconditioned MSCs. We found that cell type influenced viability, and NPCs had significantly lower viability than MSC-only or coculture groups, suggesting that MSCs or cocultured cells could improve cell survival in the disc. However, coculture did not provide any synergistic benefits for viability. We also did not see any significant changes in viability from preconditioning MSCs in hypoxia. However, studying this system with longer timepoints or different outcome measures such as chondrogenesis may reveal additional effects of coculture and hypoxic preconditioning.

Overall, our research highlights the importance of evaluating tissue engineering constructs in a more realistic setting, since limitations of the disc microenvironment can severely impact cell viability and performance. Ultimately, a clearer understanding of how different design decisions impact cell performance can lead to improvements in treatments for degenerative disc disease.

4.2 Future Directions

4.2.1 Mechanisms of cell-cell communication in coculture systems

In Chapter 2 of this dissertation, we concluded that both cell type and configuration modulated response to inflammation in IVD tissue engineering constructs. However, further research is needed to more fully answer the main questions about mechanisms of cell-cell communication in coculture posed in Section 1.4.3.

4.2.1.1 Role of soluble factors and direct cell-cell contact in MSC:NPC coculture

In our study, both coculture individual-cell groups and coculture micropellet groups displayed immunomodulatory activity and matrix deposition, but the coculture micropellet group had more dramatic downregulation of catabolic genes. This suggests that both soluble factors and direct cell-cell contact contributed to the results. One interesting next step would be to identify some of these specific factors and contact-associated signaling mechanisms.

Soluble factors that could affect cell performance in coculture include growth factors (including inducers of chondrogenesis), cytokines, and immunomodulatory molecules. Previous studies have identified many possible candidates, including TGF-β1, which may be secreted by NPCs to promote chondrogenesis in cocultured MSCs (*1–3*). MSCs may also secrete TGF-β1 and 3 to promote matrix synthesis in other cell types (*4–6*). Another chondrogenic mediator, BMP-2, has also been shown to increase in coculture (*2–4*). Growth factors such as IGF-1, EGF, PDGF, FGF-2, FGF-4, and FGF-6 may also be secreted by either cell type to promote

proliferation and matrix synthesis, and PTHrP (parathyroid hormone-related protein) may be secreted to prevent hypertrophy (*1–9*). Wu *et al.* hypothesized that MSCs may secrete FGF-1 in coculture to increase chondrocyte proliferation (*10*). Some soluble factors, such as IL-6, IL-10, PGE2, TIMPs, and nitric oxide (NO), may also have an immunomodulatory effect (*6*, *11–13*). Since there are many possible soluble factor candidates, a microarray or mass spectrometry screening technique may be useful to identify the ones that show the most dramatic change with coculture. The presence of promising factors can then be verified by qPCR and protein assays, and their role in chondrogenesis, proliferation, or response to inflammation can be determined using knockdown experiments. In preliminary experiments, we tested gene expression levels of FGF-1 as well as media levels of PGE2 and NO, but did not find significant differences between groups. This may have been due to time-dependent changes in expression levels, as well as insufficient sensitivity of the assays used.

Direct-contact-mediated signaling may also contribute to cell phenotype in coculture. Formation of gap junctions (*14*) may affect calcium transport between cells, and can be visualized by staining for associated proteins such as connexin 43 (Cx-43) and calcium-sensitive dyes (*15*, *16*). Real-time visualization of gap junction activity may also provide important information about time scale of signaling. Exchange of membrane components may also occur between cells in coculture, and can be visualized with membrane dyes (*17*). We used similar membrane dyes in our study and did not observe exchange of dye between neighboring cells in fluorescent microscopy, but our imaging resolution may have been insufficient to see small amounts of dye exchange. Other contact-associated genes that are important during mesenchymal condensation in development include N-cadherin, N-CAM, and Cx-43 (*14*, *18*). We tested N-cadherin and N-CAM gene expression, but did not find significant differences

between cell type or configuration groups. We also tested the effect of N-cadherin blocking antibodies on large NPC pellet formation, but did not see major changes in pellets or subsequent chondrogenesis. A high antibody concentration is required to disrupt pellet formation (*19*), so perhaps the antibody dose we used was too low to affect contact-mediated signaling, or delivered at the wrong time during pellet condensation. Blocking N-cadherin may be more effective for MSCs than for NPCs.

In addition, some of our preliminary experiments suggested that hypoxia and cell-cell contact together regulate synthetic and catabolic activity of NPCs in an inflammatory microenvironment. We found that interactions between configuration, oxygen tension, and inflammatory media are significantly associated with anabolic and catabolic gene expression in NPCs (Appendix C), and that hypoxia appeared to reduce induction of catabolic genes, but did not prevent loss of overall DNA or GAG content. Further research is needed to determine the long-term effects of these culture conditions, as well as to identify mechanisms that affect gene and protein expression, and possible crosstalk between hypoxia and direct-contact-induced pathways, including the notch signaling pathway in development (*20*, *21*).

Finally, cell clusters with a similar histological appearance to micropellets have been observed in degenerated and herniated discs, as well as osteoarthritic cartilage. These clusters have increased expression of MMPs, inflammatory proteins, senescence markers, and stress response markers, which contradicts the immunomodulatory response that we observed in micropellets in Chapter 2 (*22–24*). Formation of cell clusters may be a protective response to degenerative microenvironments, but more research is needed to determine the role of contact-mediated signaling in these clusters, and how these clusters contribute to matrix synthesis and catabolism *in vivo*.

4.2.1.2 MSC Roles in Coculture: Differentiation versus Trophic Effects

Another question arising from coculture studies is whether MSCs differentiate into a chondrogenic phenotype and synthesize matrix, or instead influence NPCs and chondrocytes to synthesize more matrix through secretion of trophic factors. Evidence increasingly suggests that MSCs may play an immunomodulatory role (*25*). Identifying key soluble factors secreted by MSCs, as mentioned in the previous section, could provide evidence of their trophic and immunomodulatory effects. On the other hand, identifying aggrecan and collagen II expression that is directly attributable to MSCs could indicate that they are differentiating in coculture. Cell types can be easily separated in an indirect coculture system, but separating them after direct coculture is more difficult. Some groups have used FACS to sort by surface markers or previously-engineered cell labels (*26*, *27*), while others have used xenogenic coculture models. After culture, species-specific primers or antibodies can be used to distinguish between cell types (*4*, *11*, *15*, *28*, *29*). Cell types from donors of different genders can be used to distinguish cell types at a later time point. For example, chromosomal staining with FISH can be used to localize male-donor-isolated chondrocytes and female-donor-isolated MSCs in direct coculture (*30*). To determine whether they have a significant impact in coculture, trophic factors could be selectively knocked down in MSCs (for example, using siRNA or a CRISPR-Cas knockdown during the MSC expansion phase).

Another observation that motivates MSC trophic factor investigation is the disappearance of MSCs in cocultures and *in vivo* systems. Previous studies have tracked species-specific genomic DNA and mRNA to measure cell-type ratios in xenogenic coculture, and generally found an increase in the NPC or AC to MSC ratio, suggesting either MSC cell death or increased proliferation of the NPCs and ACs (*4*, *6*, *11*, *15*, *31*, *32*). To differentiate between the two

possibilities, cell tracking over multiple timepoints could identify dying and proliferating cells. In addition, imaging and FACS methods that combine cell labels (via surface markers or membrane dyes) with apoptosis and proliferation markers can more accurately identify the fate of each cell type. We measured species-specific GAPDH mRNA for human MSC and bovine NPC cocultures over 21 days and found that MSCs almost completely disappeared by the end of the culture period (Appendix D). However, imaging results with live/dead, TUNEL, and Brdu staining were not conclusive (Appendix D), so more trials and assay optimization are needed to answer the question of MSC cell fate. This technique can also be used to compare rates of cell death in MSCs and NPCs in a cocultured diffusion chamber system.

4.2.2 Self-organization in coculture systems

We observed self-organization of coculture micropellets within 24 hours, where cultures formed a bilayered structure with an MSC core and NPC outer shell, most likely due to differences in intercellular cohesivity. This self-organization has been observed in other studies also (*11*, *33*), and may be beneficial because it is similar to mesenchymal condensation organization during development (*17*, *34*). To further investigate how the organization affects anabolic and catabolic performance of the cocultured cells, chemically programmed assembly with oligonucleotides could be used to "force" an opposite organization (*35*). Imposing an opposite organization with an NPC core and MSC outer layer on a larger scale using centrifugation resulted in decreased cell proliferation and some differences in matrix deposition patterns (*28*). Finally, different carrier properties may also influence self-organization patterns, so it would be interesting to test micropellet formation in microwells made of materials other than agarose. One caveat is that micropellets do not form if the surrounding material is too stiff or adhesive, because cells prefer to attach to the substrate instead of each other (Appendix A).

4.2.3. Mechanisms of hypoxia response

Hypoxia-inducible factors such as HIF-1α are known to modulate cellular response to hypoxia, but may have many different downstream effects in different cell types. Using a diffusion-limited system, HIF-1α activity could be assayed in more detail in MSCs and NPCs, as well as cocultured groups with both cell types. Efforts to extract mRNA from agarose chambers to analyze gene expression of HIF-1α and other genes are described in Appendix E. Previous studies have shown that NPCs constitutively express HIF-1α, but its domain activation may change in hypoxia, so protein and functional assays are needed in addition to gene expression measurements (*36–38*). NPCs may also maintain HIF-subunit degradation through a different pathway than other cell types, which may be less sensitive to oxygen tension (*39*). Studying the downstream effects of HIF-1α could also elucidate mechanisms through which hypoxia modulates chondrogenesis and senescence in MSCs and NPCs (*40–42*). Furthermore, hypoxia also affects glucose transporters GLUT1 and GLUT3, suggesting crosstalk between hypoxic and low-glucose response pathways that could affect cell responses in a degenerative microenvironment (*43*).

4.2.4 Effect of individual differences on cell viability

As mentioned in Chapter 3, further research is needed to determine the effect of individual differences on MSC and NPC viability in a diffusion-limited environment. Although we did not have enough replicates for sufficient statistical power, our preliminary experiments suggest that NPCs from different individuals had different baseline viable distances. However, when cocultured with MSCs, these differences were smaller (Appendix B). This suggests that coculture with allogenic MSCs could help standardize treatment outcomes for different patients.

More samples are needed to confirm this benefit, as well as more investigation into the important of MSC individual donors.

4.3 References

1. Y. Yamamoto *et al.*, Upregulation of the viability of nucleus pulposus cells by bone marrow-derived stromal cells: significance of direct cell-to-cell contact in coculture system. *Spine (Phila. Pa. 1976).* **29**, 1508–1514 (2004).
2. X. Liu *et al.*, In vivo ectopic chondrogenesis of BMSCs directed by mature chondrocytes. *Biomaterials*. **31**, 9406–14 (2010).
3. Y.-H. Yang, A. J. Lee, G. a Barabino, Coculture-driven mesenchymal stem cell-differentiated articular chondrocyte-like cells support neocartilage development. *Stem Cells Transl. Med.* **1**, 843–54 (2012).
4. V. V Meretoja, R. L. Dahlin, F. K. Kasper, A. G. Mikos, Enhanced chondrogenesis in co-cultures with articular chondrocytes and mesenchymal stem cells. *Biomaterials*. **33**, 6362–9 (2012).
5. I. Sekiya, J. T. Vuoristo, B. L. Larson, D. J. Prockop, In vitro cartilage formation by human adult stem cells from bone marrow stroma defines the sequence of cellular and molecular events during chondrogenesis. *Proc. Natl. Acad. Sci. U. S. A.* **99**, 4397–402 (2002).
6. C. Acharya *et al.*, Enhanced chondrocyte proliferation and mesenchymal stromal cells chondrogenesis in coculture pellets mediate improved cartilage formation. *J. Cell. Physiol.* **227**, 88–97 (2012).
7. S.-H. Yang, C.-C. Wu, T. T.-F. Shih, P.-Q. Chen, F.-H. Lin, Three-dimensional culture of human nucleus pulposus cells in fibrin clot: comparisons on cellular proliferation and

matrix synthesis with cells in alginate. *Artif. Organs*. **32**, 70–3 (2008).

8. J. Fischer, A. Dickhut, M. Rickert, W. Richter, Human articular chondrocytes secrete parathyroid hormone-related protein and inhibit hypertrophy of mesenchymal stem cells in coculture during chondrogenesis. *Arthritis Rheum.* **62**, 2696–706 (2010).
9. S. Weiss, T. Hennig, R. Bock, E. Steck, W. Richter, Impact of growth factors and PTHrP on early and late chondrogenic differentiation of human mesenchymal stem cells. *J. Cell. Physiol.* **223**, 84–93 (2010).
10. L. Wu, J. Leijten, C. a van Blitterswijk, M. Karperien, Fibroblast growth factor-1 is a mesenchymal stromal cell-secreted factor stimulating proliferation of osteoarthritic chondrocytes in co-culture. *Stem Cells Dev.* **22**, 2356–67 (2013).
11. L. Wu *et al.*, Trophic effects of mesenchymal stem cells increase chondrocyte proliferation and matrix formation. *Tissue Eng. Part A.* **17**, 1425–36 (2011).
12. L. Bian, D. Y. Zhai, R. L. Mauck, J. A. Burdick, Coculture of human mesenchymal stem cells and articular chondrocytes reduces hypertrophy and enhances functional properties of engineered cartilage. *Tissue Eng. Part A.* **17**, 1137–45 (2011).
13. C. Manferdini *et al.*, Adipose-derived mesenchymal stem cells exert antiinflammatory effects on chondrocytes and synoviocytes from osteoarthritis patients through prostaglandin E2. *Arthritis Rheum.* **65**, 1271–81 (2013).
14. W. Zhang, C. Green, N. S. Stott, Bone morphogenetic protein-2 modulation of chondrogenic differentiation in vitro involves gap junction-mediated intercellular communication. *J. Cell. Physiol.* **193**, 233–43 (2002).
15. T. S. de Windt *et al.*, Direct Cell–Cell Contact with Chondrocytes Is a Key Mechanism in Multipotent Mesenchymal Stromal Cell-Mediated Chondrogenesis. *Tissue Eng. Part A.*

21, 2536–2547 (2015).

16. P.-H. G. Chao, A. C. West, C. T. Hung, Chondrocyte intracellular calcium, cytoskeletal organization, and gene expression responses to dynamic osmotic loading. *Am. J. Physiol. Cell Physiol.* **291**, C718-25 (2006).

17. S. Strassburg, N. W. Hodson, P. I. Hill, S. M. Richardson, J. a Hoyland, Bi-directional exchange of membrane components occurs during co-culture of mesenchymal stem cells and nucleus pulposus cells. *PLoS One*. **7**, e33739 (2012).

18. L. Quintana, N. I. zur Nieden, C. E. Semino, Morphogenetic and regulatory mechanisms during developmental chondrogenesis: new paradigms for cartilage tissue engineering. *Tissue Eng. Part B. Rev.* **15**, 29–41 (2009).

19. R. Tuli *et al.*, Transforming growth factor-beta-mediated chondrogenesis of human mesenchymal progenitor cells involves N-cadherin and mitogen-activated protein kinase and Wnt signaling cross-talk. *J. Biol. Chem.* **278**, 41227–36 (2003).

20. M. Pei *et al.*, Modulation of In Vitro Microenvironment Facilitates Synovium-Derived Stem Cell-Based Nucleus Pulposus Tissue Regeneration. *Spine (Phila. Pa. 1976).* **37**, 1538–1547 (2012).

21. A. Hiyama *et al.*, Hypoxia activates the notch signaling pathway in cells of the intervertebral disc: implications in degenerative disc disease. *Arthritis Rheum.* **63**, 1355–64 (2011).

22. S. Roberts, H. Evans, Histology and Pathology of the human intervertebral disc. *J. Bone Jt. Surg.*, 2000 (2006).

23. M. K. Lotz *et al.*, Cartilage cell clusters. *Arthritis Rheum.* **62**, 2206–2218 (2010).

24. C. a. Sharp, S. Roberts, H. Evans, S. J. Brown, Disc cell clusters in pathological human

intervertebral discs are associated with increased stress protein immunostaining. *Eur. Spine J.* **18**, 1587–1594 (2009).

25. N. G. Singer, A. I. Caplan, Mesenchymal stem cells: mechanisms of inflammation. *Annu. Rev. Pathol.* **6**, 457–478 (2011).

26. S. M. Richardson *et al.*, Intervertebral disc cell-mediated mesenchymal stem cell differentiation. *Stem Cells*. **24**, 707–16 (2006).

27. G. Vadalà *et al.*, Coculture of bone marrow mesenchymal stem cells and nucleus pulposus cells modulate gene expression profile without cell fusion. *Spine (Phila. Pa. 1976).* **33**, 870–6 (2008).

28. A. A. Allon, K. Butcher, R. A. Schneider, J. C. Lotz, Structured coculture of mesenchymal stem cells and disc cells enhances differentiation and proliferation. *Cells Tissues Organs*. **196**, 99–106 (2012).

29. X. Mo *et al.*, Variations in the ratios of co-cultured mesenchymal stem cells and chondrocytes regulate the expression of cartilaginous and osseous phenotype in alginate constructs. *Bone*. **45**, 42–51 (2009).

30. M. E. Cooke *et al.*, Structured three-dimensional co-culture of mesenchymal stem cells with chondrocytes promotes chondrogenic differentiation without hypertrophy. *Osteoarthritis Cartilage*. **19**, 1210–8 (2011).

31. J. H. Jeong *et al.*, Human mesenchymal stem cells implantation into the degenerated coccygeal disc of the rat. *Cytotechnology*. **59**, 55–64 (2009).

32. F. L. Acosta *et al.*, Porcine Intervertebral Disc Repair Using Allogeneic Juvenile Articular Chondrocytes or Mesenchymal Stem Cells. *Tissue Eng. Part A*. **17**, 3045–3055 (2011).

33. A. Allon, R. Schneider, J. Lotz, Co-culture of adult mesenchymal stem cells and nucleus

pulposus cells in bilaminar pellets for intervertebral disc regeneration. *SAS J.* **3**, 41–49 (2009).

34. L. J. Smith, N. L. Nerurkar, K.-S. Choi, B. D. Harfe, D. M. Elliott, Degeneration and regeneration of the intervertebral disc: lessons from development. *Dis. Model. Mech.* **4**, 31–41 (2011).

35. M. E. Todhunter *et al.*, Programmed synthesis of three-dimensional tissues. *Nat. Methods*. **12**, 975–981 (2015).

36. A. Agrawal *et al.*, Normoxic stabilization of HIF-1alpha drives glycolytic metabolism and regulates aggrecan gene expression in nucleus pulposus cells of the rat intervertebral disk. *Am. J. Physiol. Cell Physiol.* **293**, C621-31 (2007).

37. M. V Risbud *et al.*, Defining the phenotype of young healthy nucleus pulposus cells: recommendations of the Spine Research Interest Group at the 2014 annual ORS meeting. *J. Orthop. Res.* **33**, 283–93 (2015).

38. G. Feng *et al.*, Hypoxia differentially regulates human nucleus pulposus and annulus fibrosus cell extracellular matrix production in 3D scaffolds. *Osteoarthritis Cartilage*. **21**, 582–8 (2013).

39. H. Li, C. Z. Liang, Q. X. Chen, Regulatory role of hypoxia inducible factor in the biological behavior of nucleus pulposus cells. *Yonsei Med. J.* **54**, 807–812 (2013).

40. H.-H. Lee *et al.*, Hypoxia Enhances Chondrogenesis and Prevents Terminal Differentiation through PI3K/Akt/FoxO Dependent Anti-Apoptotic Effect. *Sci. Rep.* **3**, 2683 (2013).

41. M. Pei, Environmental preconditioning rejuvenates adult stem cells' proliferation and chondrogenic potential. *Biomaterials*. **117**, 10–23 (2017).

42. C.-C. Tsai *et al.*, Hypoxia inhibits senescence and maintains mesenchymal stem cell properties through down-regulation of E2A-p21 by HIF-TWIST. *Blood*. **117**, 459–69 (2011).

43. A. Mobasheri *et al.*, *Adv. Anat. Embryol. Cell Biol.*, in press.

Appendix A: Micropellet formation parameters

This data was submitted in 2013 as a progress report for NIH grant R21 AR063357-02.

A.1 Introduction

Seeding of cocultured cells in agarose microwells is a promising method to generate large batches of uniform, self-organizing micropellets (*1*). In these experiments, we investigated the effect of microwell diameter on pellet formation, as well as the effect of microwell material. The microwells are normally made of agarose, but experiments from our lab suggested that fibrin is a useful carrier for cells in disc tissue engineering applications (*2*).

A.2 Methods and Results

As described in Chapter 2 and (*1*), we used microfabrication techniques to create silicon wafers with microwells of various diameters and spacings. The silicon master plates were used to create PDMS "stamps" with cylindrical posts, and these stamps were used to create microwells in other materials, namely agarose and fibrin. Microwells were loaded with a 50:50 coculture of human mesenchymal stem cells (MSCs) and bovine nucleus pulposus cells (NPCs), which were cultured, labeled with membrane dyes, and loaded as described in Chapter 2.

Well spacing:

The distance between microwells was 4x the well diameter, as measured between the centers of each well. However, for 200 μm-diameter wells, we also tested a smaller spacing of 3x the well diameter, which would allow for future paracrine signaling measurements. The well spacing did not appear to affect self-organization or micropellet formation.

Well diameter:

We tested agarose microwells with diameters of 50, 100, and 200 μm to determine how well diameter would affect self-organization of cocultured micropellets. Immediately after cell

loading (Figure A.1), all the wells appeared to be filled with a mixture of MSCs (green dye) and NPCs (red dye). However, the smallest diameter wells (50 µm) showed heterogeneity in cell-type ratio. In other words, while some small wells received ~50% hMC and 50% bNPC, others exhibited 100% hMSC or 100% bNPCs.

After a 48-hour incubation (Figure A.2), all micropellet sizes were observed to self-organize with an hMSC core surrounded by a bNPC outer layer. While the 50 and 100-µm micropellets appeared organized after 24 hours in culture, the 200-µm micropellets took at least 48 hours to exhibit organizational patterns. We also observed that 200 µm-diameter wells promoted the formation of multiple hMSCs cores within the same cell aggregate that coalesced only at later timepoints (> 48hrs). Another important observation was the effect of the well-diameter to well-depth ratio. Since the well depth was kept constant (approximately 100 µm), the 200-µm diameter wells were wide and shallow, making it easy for cells to escape during the wash steps. This contributed to increased heterogeneity in final cluster size (not observed for medium and small sized wells). This effect could be potentially minimized by keeping a constant depth to diameter ratio but would require us to revise the photolithographic steps.

The medium well diameter, 100 µm, had advantages over the other well diameters in even cell seeding ratios, cell retention, and single-core organization. Therefore, we used this size of microwell for later experiments.

Microwell materials:

We formed microwells with low gelling agarose type VII-A (Sigma-Aldrich) and TISEEL fibrin sealant (Baxter). As shown in Figure A.3, cells in fibrin wells did not self-organize. Many migrated out of the wells, and those remaining in the wells did not have much cell-cell contact,

most likely because unlike agarose, fibrin provides an attractive surface for attachment and migration.

When forming agarose microwells, we also tested several different agarose concentrations. Low agarose concentrations tended to experience microwell deformation during PDMS unmolding steps, but higher concentrations created a stiff surface that promoted cell attachment and spreading instead of micropellet condensation. We found that 3.5% was an optimal concentration, and that agarose was more uniform when dissolved in an autoclaving step instead of in the microwave.

A.3 References

1. A. E. Cerchiari *et al.*, A strategy for tissue self-organization that is robust to cellular heterogeneity and plasticity. *Proc. Natl. Acad. Sci.* **112**, 2287–2292 (2015).
2. Z. Buser *et al.*, Biological and biomechanical effects of fibrin injection into porcine intervertebral discs. *Spine (Phila. Pa. 1976).* **36**, E1201-9 (2011).

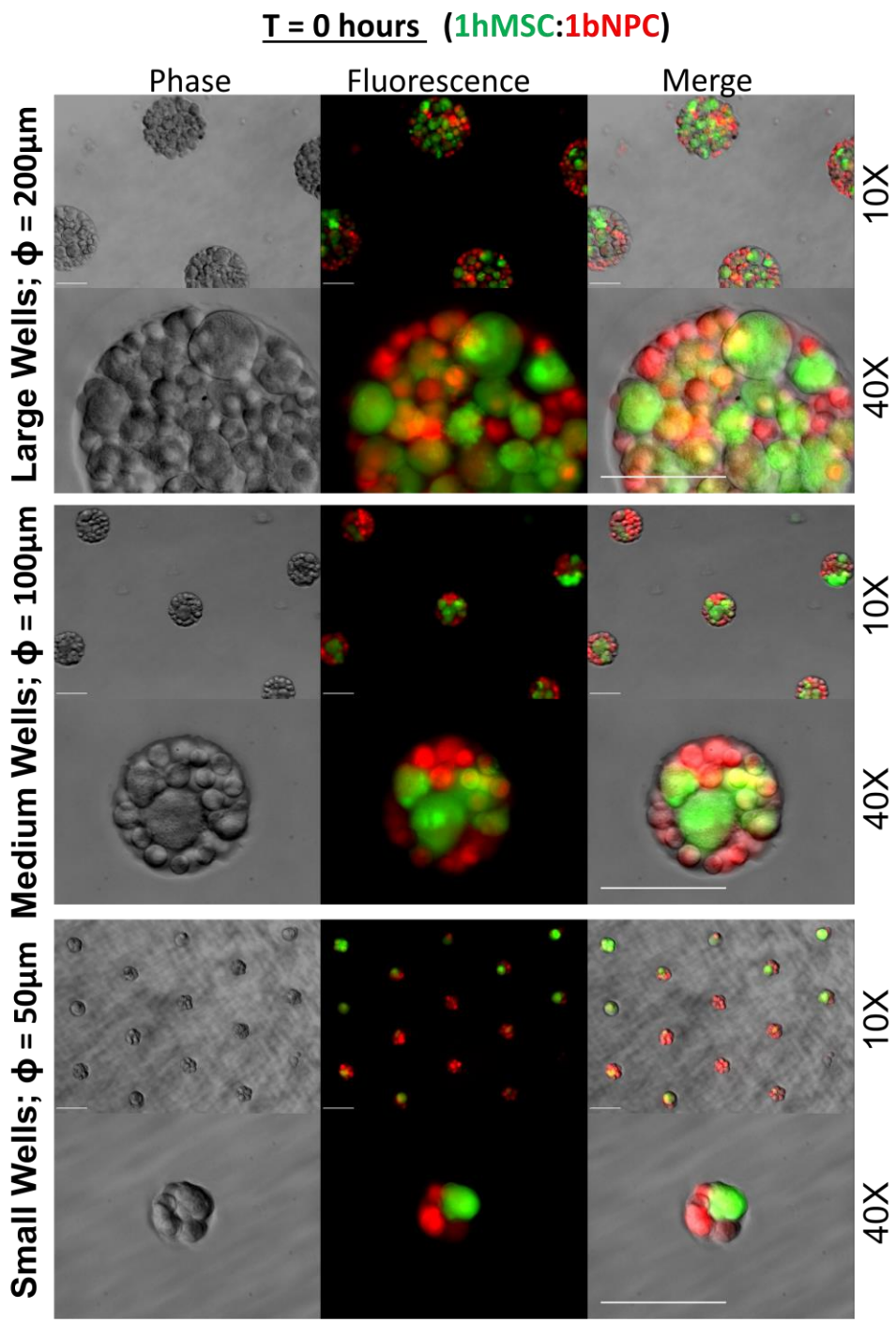

Figure A.1 Agarose microwells of various diameters immediately following cell loading. Scale bars represent 100 µm.

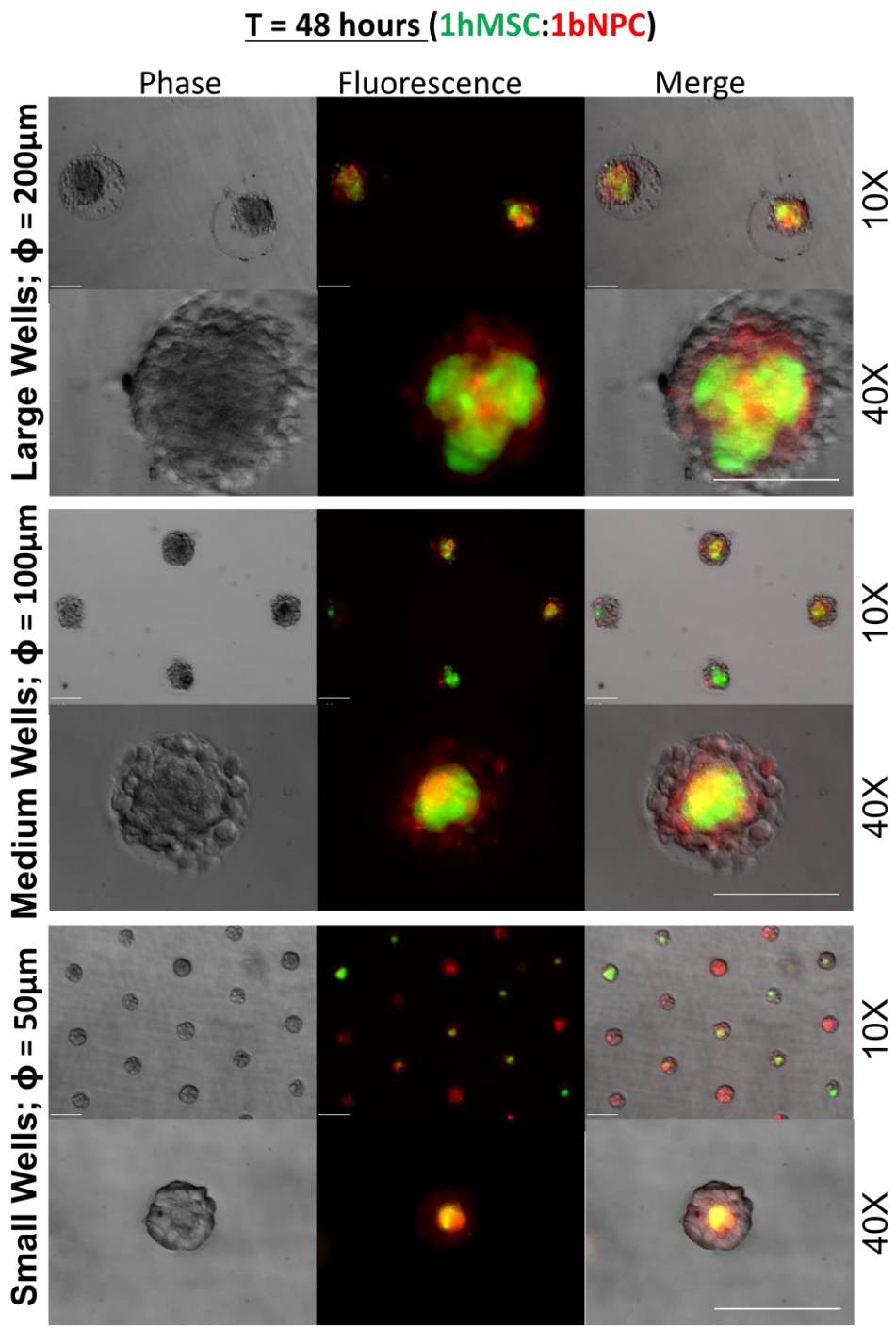

Figure A.2 Agarose microwells of various diameters 48 hours following cell loading. Scale bars represent 100 µm.

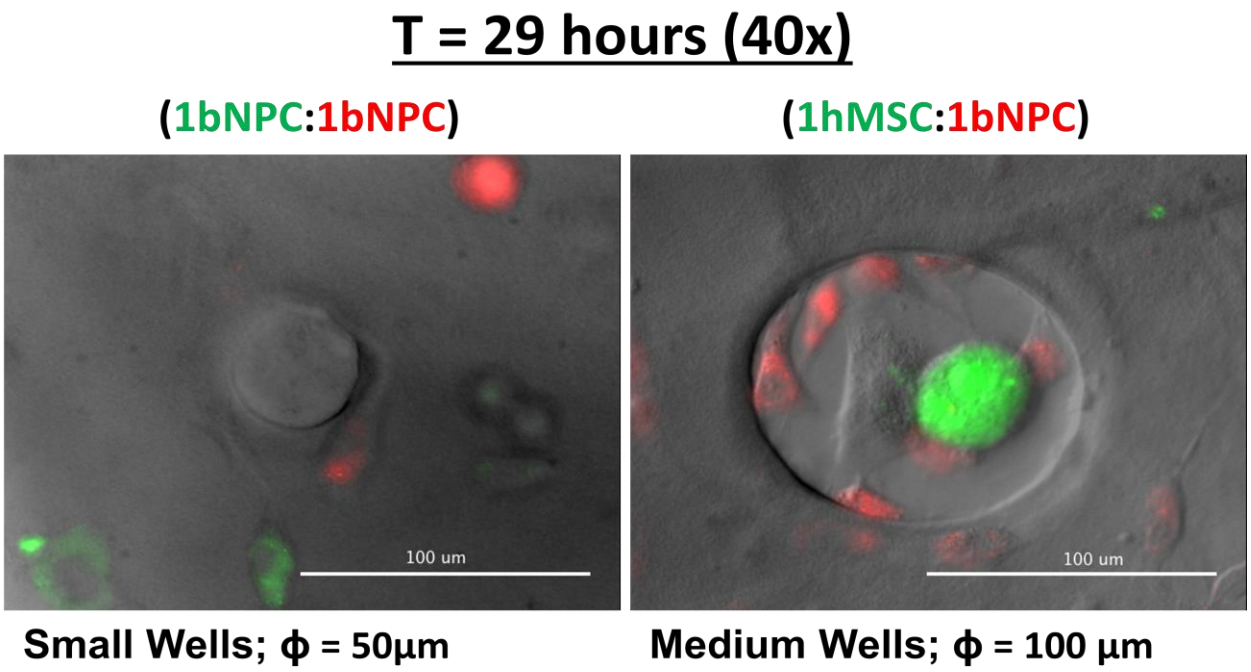

Figure A.3 Fibrin microwells 29 hours after cell loading.

Appendix B: Effects of NPC donor variation on cell viability in a diffusion-limited system

B.1 Introduction

In Chapter 3, we investigated the effects of cell type and coculture on viable distance in a diffusion-limited system using NPCs from one donor. Since NPCs from different individuals may vary in metabolism and cell viability (*1*), we also performed a pilot study testing NPCs from different donors and comparing their viability in both NPC-only diffusion chambers and coculture diffusion chambers with MSCs.

B.2 Methods

Diffusion chambers were prepared as described in Chapter 3, and NPCs were isolated from bovine caudal discs as previously described (*2*). We isolated NPCs from three individuals, labeled Tail 1, Tail 2, and Tail A. Tail 2 was used for the larger study described in Chapter 3, and therefore had the most replicates, while the other tails had fewer (Table B.2). After 72 hours of diffusion chamber culture, viable distance and live cell estimates were measured and calculated as described in Chapter 3. We performed a one-way ANOVA test on the live cell estimate groups, but the replicate numbers were too low to achieve sufficient power (a power analysis determined that 6 replicates are needed for 80% power).

Tail Number	Individual Cell Groups	Coculture Groups
Tail 1	4	2
Tail 2	10	12
Tail A	4	2

Table B.2 Number of replicates available for diffusion chambers from different bovine individual donors.

B.3 Results and Discussion

Plots of viable distance and live cell estimates from the three different NPC lines are shown in Figure B.1. In NPC-only groups (left column), individual donors had distinctly different viable distances. However, these differences were less obvious in coculture groups (right column),

suggesting that coculture with MSCs may mitigate the variability. This would suggest that coculture with MSCs is a useful clinical strategy to standardize treatments for individual patients. However, more replicates are needed to confirm this conclusion.

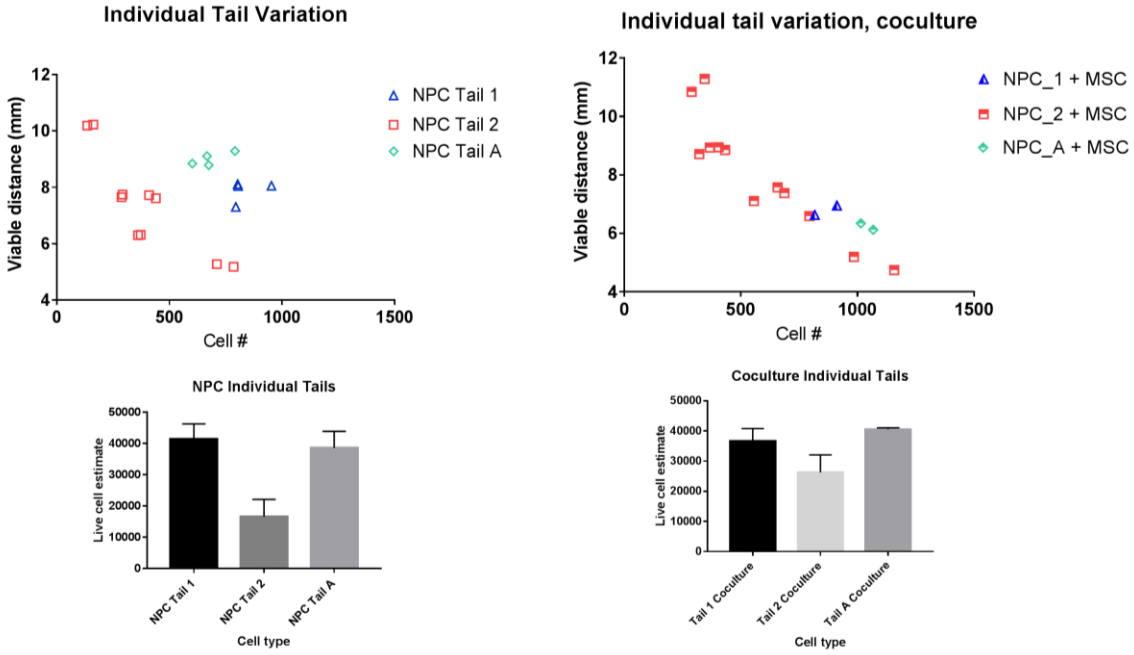

Figure B.1 Viable distance and live cell number variation in NPCs from three different donors.

B.4 References

1. H. a Horner, J. P. Urban, 2001 Volvo Award Winner in Basic Science Studies: Effect of nutrient supply on the viability of cells from the nucleus pulposus of the intervertebral disc. *Spine (Phila. Pa. 1976).* **26**, 2543–9 (2001).
2. A. Allon, R. Schneider, J. Lotz, Co-culture of adult mesenchymal stem cells and nucleus pulposus cells in bilaminar pellets for intervertebral disc regeneration. *SAS J.* **3**, 41–49 (2009).

Appendix C: Effects of hypoxia, configuration, and inflammatory media on NPC synthetic and catabolic activity

This work was an abstract and poster presentation at the 2016 ORS Annual Meeting, with the following citation: Ouyang, A., Cerchiari, A., Liebenberg, E., Gartner, Z.J., Alliston, T., Lotz, J.C. "Oxygen Tension, 3D Configuration, and Inflammatory Media Regulate NPC Synthetic and Catabolic Activity." Poster presentation, ORS Annual Meeting, 2016 March 5-8; Orlando, FL.

C.1 Introduction

In Chapters 2 and 3, we found that the hypoxic and inflammatory environment of degenerative IVDs is challenging for cell survival and biosynthesis. However, is unclear how hypoxia and inflammation interact within the disc: while inflammation generally reduces regeneration capacity, hypoxia may also promote matrix production, and may also improve cell performance in an inflammatory environment (*1–3*). Another variable that influences regeneration capacity is spatial arrangement of the cells. 3D configuration strongly influences exposure to extracellular cues and direct cell-cell contact, which can in turn influence chondrogenic capacity. Furthermore, 3D clustering of NPCs or other chondrogenic cells may be related to inflammatory and hypoxic conditions, and the size of cell aggregates may affect chondrogenesis (*4–6*). In this study, we investigated how configuration, media, and O_2 tension interact to regulate synthetic and catabolic activity of nucleus pulposus cells (NPCs).

C.2 Methods

We varied configuration, O_2 tension, and media in passage 4 bovine NPCs (n=3 for each condition). O_2 tension was varied between normoxia (20% O_2) and hypoxia (2% O_2). Media treatment was either basal (low-glucose DMEM, 5% FBS, 1% antibiotic/antimyotic, 1% NEAA, and 1.5% osmolarity salt), or inflammatory (basal media with the addition of 10 ng/ml IL-1β and

TNF-α). Cells were cultured for 21 days in 3 configurations: individual cells, micropellets, and large pellets (Figure C.1). Individual cells were encapsulated in 1.2% alginate beads (2M cells/ml). Micropellets of 100-μm-diameter, formed in agarose wells as described in Chapter 2, were also encapsulated in alginate. Finally large pellets were formed by centrifuging 500,000 NPCs. We measured gene expression with qRT-PCR and calculated fold changes using the ΔΔCt method (normalized to GAPDH). We used a least-squares regression model with a one-way ANOVA to identify significant associations among the variables (JMP, SAS).

We also measured GAG and DNA concentrations of samples digested in papain using DMMB (Sigma) and Picogreen (Life Technologies) assays. Differences in concentrations were analyzed with multiple t-tests. P values < 0.05 were considered significant after multiple hypothesis corrections.

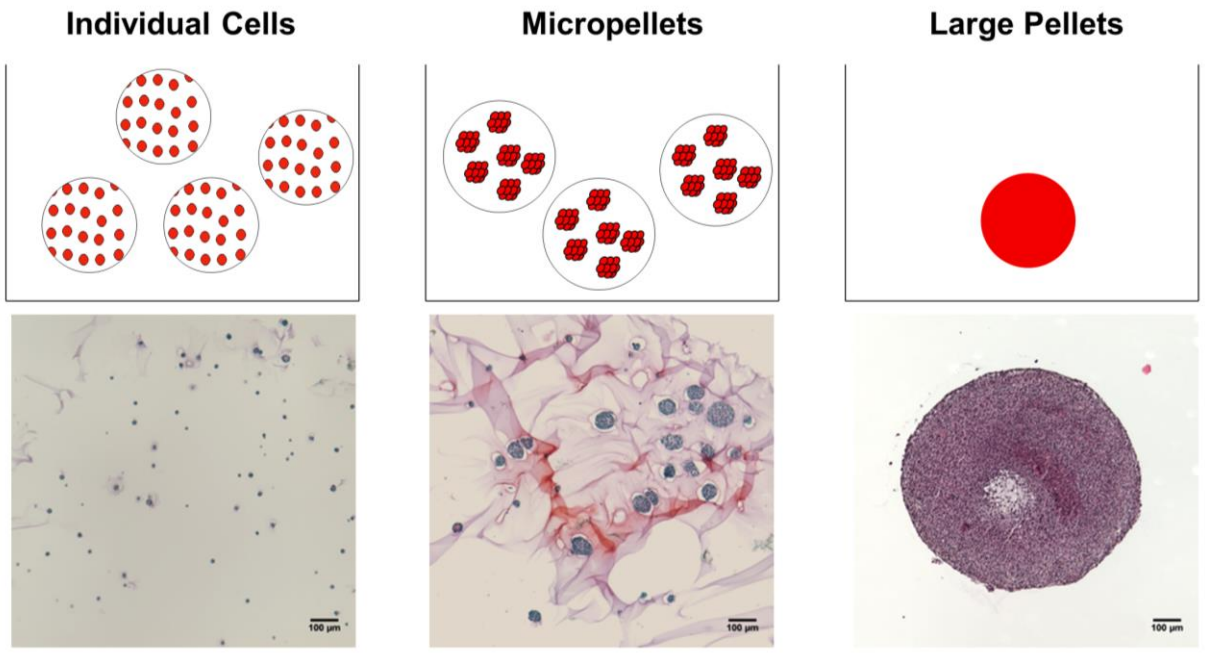

Figure C.1 Diagrams and histology images of configurations of individual cells, micropellets, and large pellets. The scale bars for the histology images are 100 μm.

C.3 Results

Gene expression:

We measured the gene expression of synthetic and catabolic genes (Figure C.2) and used a least-squares regression model to identify significant associations between the genes and our variables of interest (media conditions, O_2 tension, and configuration) (Table C.1). O_2 tension was not independently associated with aggrecan or Col2a1 expression. However, the interaction of configuration and oxygen was associated with aggrecan. In addition, configuration, as well as the interaction between configuration and media, was weakly associated with Col2a1 expression changes, while media was strongly associated. Media and configuration were both strongly associated with variation in IL-6 and MMP-13 expression. As expected, inflammatory media upregulated catabolic genes, while the configuration association was related to a much stronger inflammation-induced upregulation in large pellets. Both IL-6 and MMP-13 expression were also associated with a triple media, configuration, and oxygen interaction.

Glycosaminoglycan and DNA content:

GAG content was below the assay threshold for all groups in alginate beads, but was measureable in pellets (Figure C.3). When normalized to starting cell numbers, all groups exhibited similar GAG content, except the hypoxic inflammatory group, which displayed a significant decrease in GAG content compared with the hypoxic and basal condition. In large pellets, DNA content was also significantly lower in the hypoxic inflammatory group (Figure C.3). In individual cell and micropellet configurations, however, DNA content showed a trend of increasing in inflammatory media, with a significant increase in the hypoxic and inflammatory group.

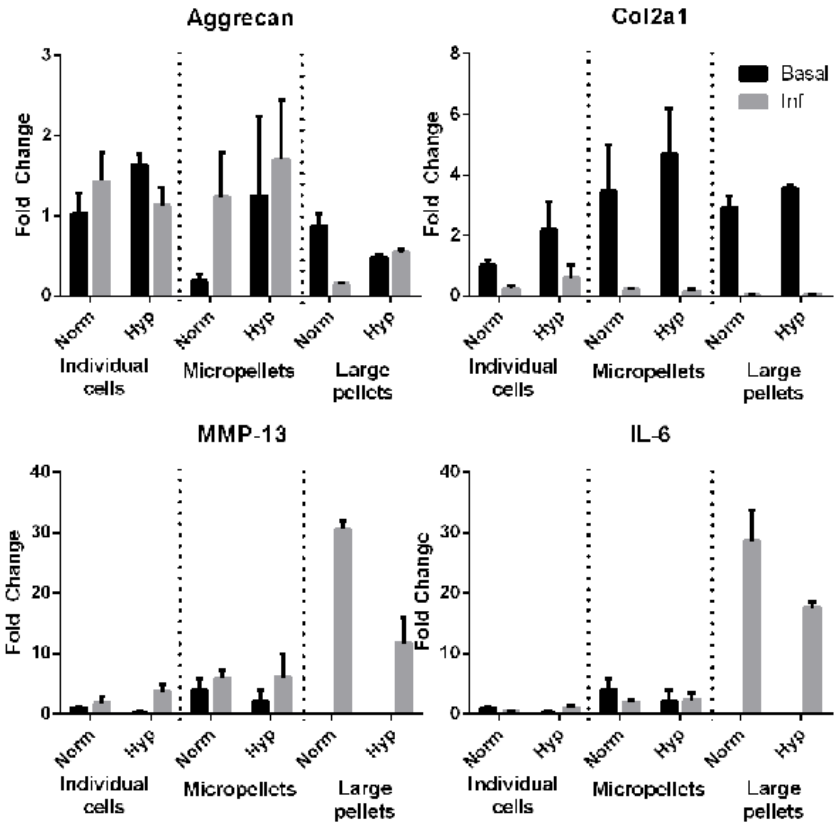

Figure C.2 Gene expression of chondrogenic and catabolic markers in NPC constructs after 21 days. Error bars show standard deviation (n=3).

Gene	R^2 variance	Contribution of association						
		Media	O_2	Config.	Media x Config.	Media x O_2	Config. x O_2	Media x Config. x O_2
Agg	19%	-	-	-	-	-	19%	-
Col2a1	84%	65%	-	18%	12%	-	-	-
MMP-13	72%	27%	3%	24%	-	-	-	17%
IL-6	61%	19%	3%	30%	-	-	-	9%

Table C.1 Significant associations with synthetic and catabolic gene expression levels ($p < 0.05$)

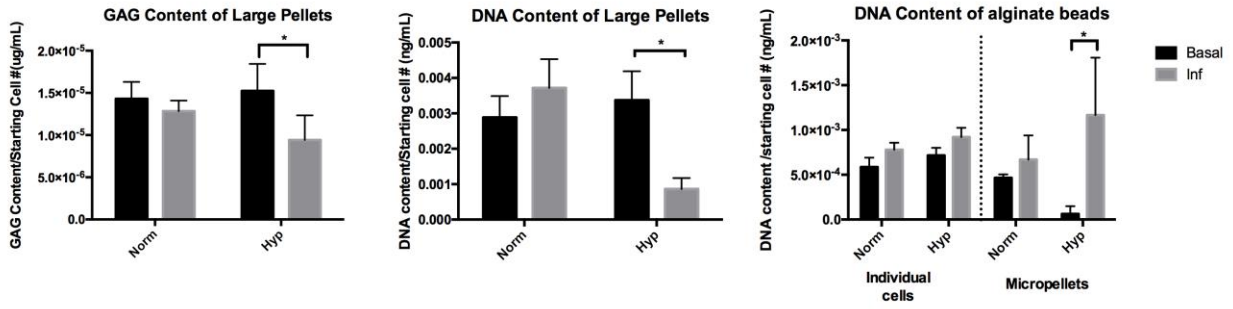

Figure C.3 GAG and DNA content of large pellets and individual cell and micropellet configurations. Error bars show standard deviation (n=3). Differences in basal and inflammatory concentrations were analyzed with multiple t-tests. $p < 0.05$ was considered significant after multiple hypothesis corrections.

C.4 Discussion

Understanding how inflammation, hypoxia, and cell configuration interact can help evaluate IVD therapies. We detected significant associations between anabolic and catabolic genes and all three variables, suggesting that all regulate synthesis and catabolism. Gene expression of MMP-13 and IL-6 in large pellets was higher in normoxic inflammatory conditions than in hypoxic inflammatory conditions, suggesting that hypoxia induced a protective effect. However, measurements of GAG and DNA content in large pellets had the opposite trend: a combined hypoxic and inflammatory environment negatively impacted both cell numbers and matrix production. The disparity between the two outcome measures might be explained by the fact that GAG and DNA content changes compound slowly over time, while gene expression changes are more transient.

The large pellets had more GAG content than the other two configurations, which is consistent with previous observations (*7*) and may be due to higher total starting cell number and density. In the individual cell and micropellet groups, DNA content exhibited increasing trends in inflammatory media, which is surprising because inflammatory media is usually detrimental to

cell health. This result might be clarified by more information about DNA changes during different time points in the 21-day incubation.

Inflammation, O_2 tension, and configuration all contribute to regulate synthetic and catabolic activity of NPCs, but the mechanisms of their interactions are still unclear. In future experiments, we hope to elucidate their associations to improve IVD tissue engineering designs.

C.5 References

1. H. Li *et al.*, Influence of hypoxia in the intervertebral disc on the biological behaviors of rat adipose- and nucleus pulposus-derived mesenchymal stem cells. *Cells. Tissues. Organs*. **198**, 266–77 (2013).
2. S. Tsuchida *et al.*, HIF-1α-induced HSP70 regulates anabolic responses in articular chondrocytes under hypoxic conditions. *J. Orthop. Res.* (2014), doi:10.1002/jor.22623.
3. T. Felka, R. Schäfer, B. Schewe, K. Benz, W. K. Aicher, Hypoxia reduces the inhibitory effect of IL-1β on chondrogenic differentiation of FCS-free expanded MSC. *Osteoarthr. Cartil.* **17**, 1368–1376 (2009).
4. D. R. Albrecht, G. H. Underhill, T. B. Wassermann, R. L. Sah, S. N. Bhatia, Probing the role of multicellular organization in three-dimensional microenvironments. *Nat. Methods*. **3**, 369–75 (2006).
5. C. a. Sharp, S. Roberts, H. Evans, S. J. Brown, Disc cell clusters in pathological human intervertebral discs are associated with increased stress protein immunostaining. *Eur. Spine J.* **18**, 1587–1594 (2009).
6. B. D. Markway *et al.*, Enhanced chondrogenic differentiation of human bone marrow-derived mesenchymal stem cells in low oxygen environment micropellet cultures. *Cell Transplant.* **19**, 29–42 (2010).

7. P. Bernstein *et al.*, Pellet culture elicits superior chondrogenic redifferentiation than alginate-based systems. *Biotechnol. Prog.* **25**, 1146–52 (2009).

Appendix D: Cell fate tracking in coculture

D.1 Introduction

As outlined in Chapter 1, the role of MSCs in coculture is controversial because they may differentiate and contribute to matrix formation, but may also exert trophic effects and disappear. We attempted to investigate the fate of MSCs in coculture constructs by tracking species-specific mRNA ratios of a xenogenic coculture, and by using membrane labels in conjunction with live/dead assays.

D.2 Methods

Species-specific gene expression and cell type ratios:

We formed human MSC and bovine NPC coculture constructs in 3 different configurations: individual cells in alginate, micropellets, and large pellets. Formation of the first two configurations is described in Chapter 2 with a 50:50 mixture of both cell types, while the large coculture pellets, or bilaminar cell pellets, were formed with 75% MSCs and 25% NPCs according to previous protocols in the lab (*1*). We extracted mRNA from the constructs and performed qPCR as previously described, with one replicate per group (Chapter 2, (*2*)). We harvested samples at the following timepoints: Day -1 for the micropellets (when cells were seeded into microwells, before they self-organized), Day 0 for all groups (when micropellets had already self-organized, and when individual cell and large pellet groups were formed), and Day 14 for all groups (after culture in both basal and inflammatory media, as described in Chapter 2).

To calculate cell type ratios, we performed qPCR using species-specific primer sequences for GAPDH, a stable housekeeping gene (Table D.1). We normalized human and bovine Ct values to universal GAPDH values, then calculated an NPC:MSC ratio based on human and bovine GAPDH fold change.

Gene (mRNA)	Forward primer (5’ to 3’)	Reverse primer (5’ to 3’)
Universal GAPDH	AGCTCACTGGCATGGCCTTC	CGCCTGCTTCACCACCTTCT
Human GAPDH	CGCTCTCTGCTCCTCCTGTT	CCATGGTGTCTGAGCGATGT
Bovine GAPDH	GCCATCACTGCCACCCAGAA	GCGGCAGGTCAGATCCACAA

Table D.1 Species-specific primer sequences, from Wu *et al.* 2011 (*3*)

Membrane dye tracking:

We also used cell membrane labeling to track MSC fate in coculture constructs. We labeled hMSCs with Vybrant DiD far red membrane dye (Thermo Fisher) according to manufacturer protocols, and then used these MSCs to form cocultured micropellets and diffusion chambers as described in Chapters 2 and 3. To visualize cell viability, we used a live/dead cytotoxicity/viability kit (Thermo Fisher) according to manufacturer instructions. We also used an In Situ Cell Proliferation Kit, FLUOS and an In Situ Cell Death Detection Kit, Fluorescein (both from Sigma-Aldrich, St. Louis, MO) to detect more specific proliferation and apoptosis markers in coculture micropellets. Samples were imaged using a Leica TCS SPE confocal microscope. Micropellets were treated and imaged 24 hours after initial cell seeding, and diffusion chambers were imaged after 72 hours of culture.

In live/dead assay-treated diffusion chamber samples, we quantified live and dead MSCs using a Matlab script adapted from others used in the lab (*4*). We first thresholded images, then identified cell centers, counted the number of identified cells, and defined overlapping membrane dye with live or dead dye cells that were within a fixed distance (2.5 pixels).

D.3 Results and Discussion

Cell type ratios:

NPC:MSC ratios calculated based on species-specific GAPDH expression are shown in Figure D.1. In individual cell groups and large pellets (BCPs), cell type ratios at Day 0 were close to the expected cell seeding ratios. However, by Day 14 the NPC:MSC ratio increased

dramatically, and in some cases human GAPDH signal from MSCs was undetectable. This was also true for micropellets, which already had a highly skewed NPC:MSC ratio after only one day of pellet condensation. This suggests that within one day, NPCs are either able to dramatically proliferate, or MSCs experience high amounts of cell death. These skewed ratios are consistent with other observations in the literature, and Wu *et al*. hypothesized that the drastic ratio change is due to MSC secretion of FGF-1, which stimulates chondrocyte proliferation (*3*, *5*, *6*). We did not find high levels of FGF-1 gene expression in our system, but further investigation is needed to clarify the mechanism of the drastic NPC:MSC ratio change.

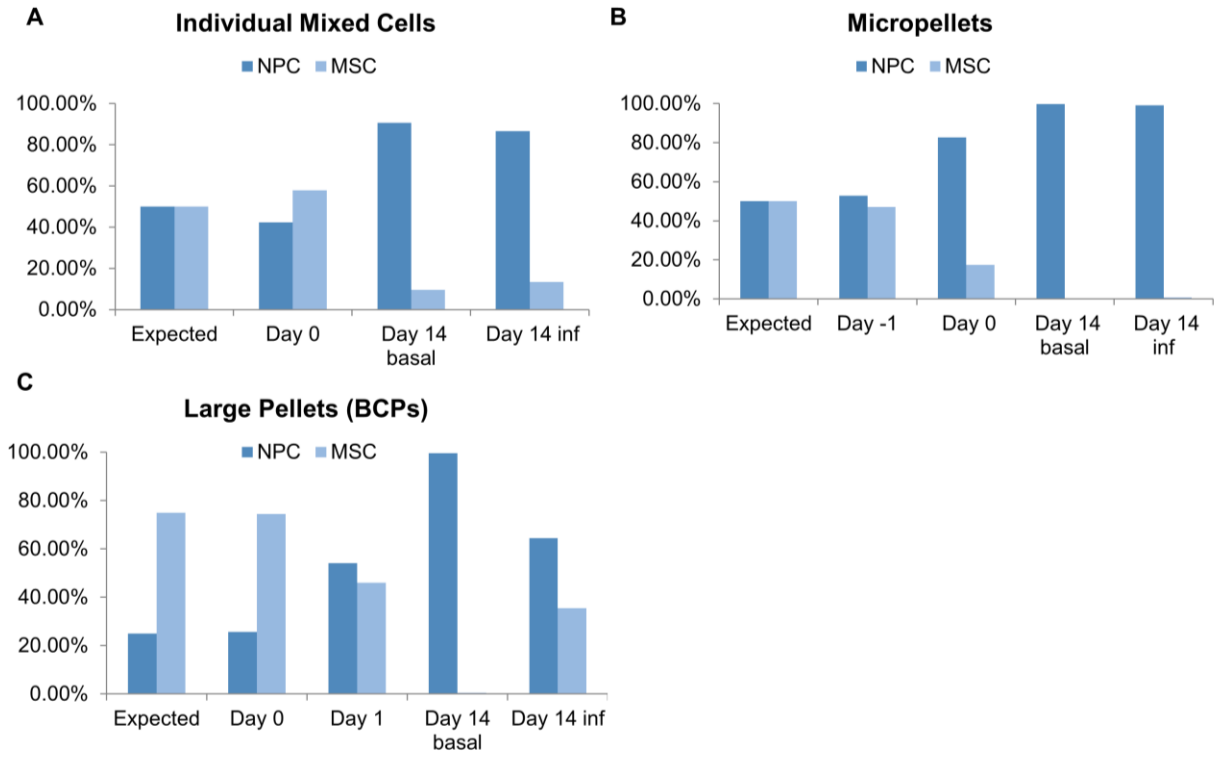

Figure D.1. NPC:MSC ratios calculated from species-specific GAPDH mRNA measurements. The leftmost column of each graph shows the expected NPC:MSC ratio based on initial cell seeding density.

Membrane dye tracking:

After observing dramatic NPC:MSC ratios during the first 24 hours, we used live/dead staining in combination with a far-red membrane dye to track MSC cell fate in coculture micropellets during this timepoint (Figure D.2). Images show only a few dead cells in the micropellet, which appeared to be more centrally located than live cells on the edge of the pellet, and may be part of the MSC core, indicating that MSCs experience cell death. However, the MSC membrane staining was more diffuse than expected, and the number of dead cells visualized would not account for the drastic species-specific mRNA changes we observed. Therefore, additional studies and more replicates are needed to confirm this finding.

We also attempted to stain for more specific proliferation and apoptosis markers using in-situ kits (see Methods section), but observed high background in micropellets for both kits, as well as loss of micropellets during staining and washing steps. Optimization of the micropellet fixation and staining protocol might improve kit performance.

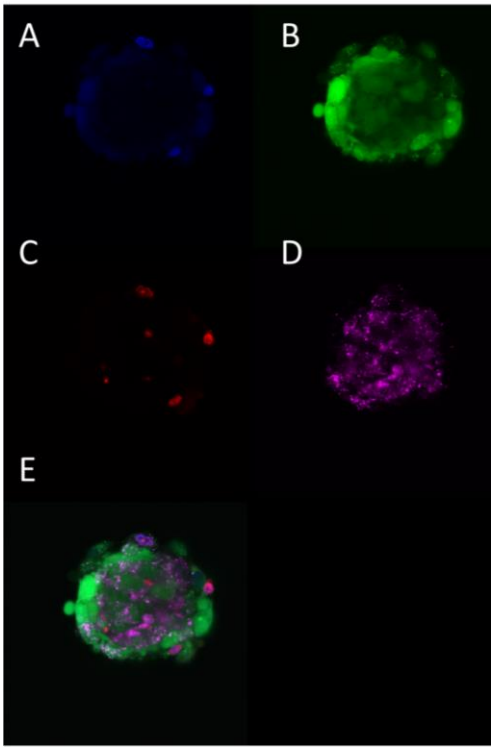

Figure D.2 Cocultured micropellet with live/dead stain and membrane dye after 24 hours of culture, with panels representing a DAPI nuclear stain (A), a calcein stain for live cells (B), an ethidium stain for dead cells (C), a far-red membrane stain used to label MSCs prior to coculture (D), and a composite image (E). All images were taken at 40x magnification.

In a separate experiment, we combined live/dead and membrane staining in coculture diffusion chambers and analyzed a set of test images (Figure D.3). In the analysis, MSCs made up only about 19% of the live cells and about 34% of the dead cells, suggesting that they were more likely than NPCs to undergo cell death. However, this contradicts with viable distance results from Chapter 2, which suggested that MSCs were better able to survive in diffusion-limited conditions. Overall, the analysis also found more total dead cells than live cells, suggesting that perhaps either the interface region we chose was more skewed towards dead cells, or that dead cells were easier to image and detect.

Detected MSCs also only made up approximately 24% of the total cells, which may indicate that our initial cell seeding ratio was not accurate, but could also reflect poor uptake or retention of the far red membrane dye. Other technical problems, such as background staining, a shift in focus when imaging large sections of gel, and choosing parameters for thresholding and cell overlap detection, also contributed to uncertainty regarding our analysis results. Therefore, further investigation is needed to optimize this assay and confirm that our image analysis method is robust. Existing co-localization and co-occurrence image analysis protocols and programs may be useful (*7*, *8*).

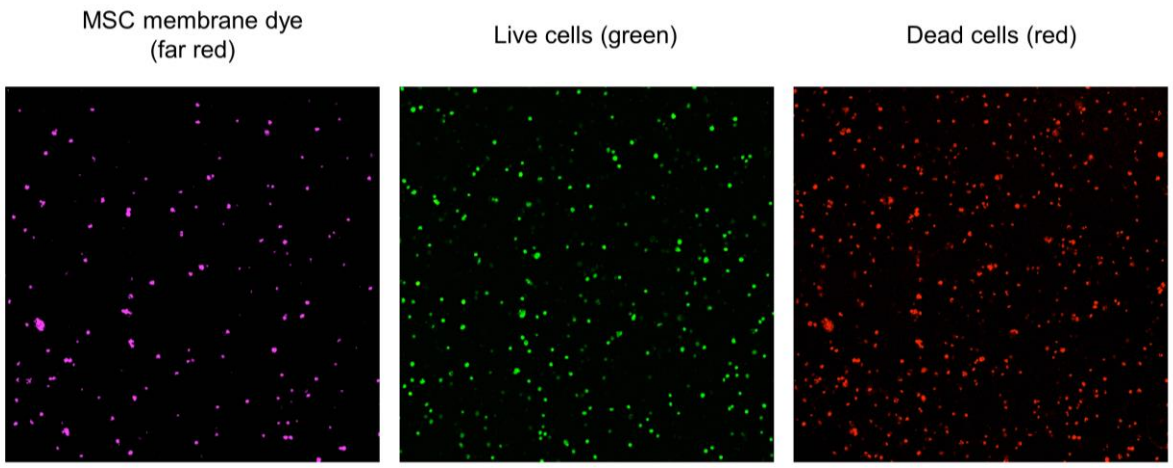

Figure D.3 Coculture diffusion chamber section with live/dead stain and membrane dye. Images were taken at 5x magnification near the live/dead viable distance interface.

D.4 Conclusions

Our initial experiments found some evidence of MSC death in coculture, but the assays must be optimized to improve confidence in these findings. Furthermore, if MSC presence is mostly undetectable after only a few days of culture, this motivates more studies into possible trophic mechanisms through which they affect long-term coculture outcomes.

D.5 References

1. A. A. Allon, K. Butcher, R. A. Schneider, J. C. Lotz, Structured coculture of mesenchymal stem cells and disc cells enhances differentiation and proliferation. *Cells Tissues Organs*. **196**, 99–106 (2012).
2. M. E. Cooke *et al.*, Structured three-dimensional co-culture of mesenchymal stem cells with chondrocytes promotes chondrogenic differentiation without hypertrophy. *Osteoarthritis Cartilage*. **19**, 1210–8 (2011).
3. L. Wu *et al.*, Trophic effects of mesenchymal stem cells increase chondrocyte proliferation and matrix formation. *Tissue Eng. Part A*. **17**, 1425–36 (2011).

4. B. Berg-Johansen, A. J. Fields, E. C. Liebenberg, A. Li, J. C. Lotz, Structure-Function Relationships at the Human Spinal Disc-Vertebra Interface. *J. Orthop. Res.* **Epub ahead** (2017), doi:10.1002/jor.23627.

5. L. Wu, J. Leijten, C. a van Blitterswijk, M. Karperien, Fibroblast growth factor-1 is a mesenchymal stromal cell-secreted factor stimulating proliferation of osteoarthritic chondrocytes in co-culture. *Stem Cells Dev.* **22**, 2356–67 (2013).

6. L. Wu, H.-J. Prins, M. N. Helder, C. A. van Blitterswijk, M. Karperien, Trophic effects of mesenchymal stem cells in chondrocyte co-cultures are independent of culture conditions and cell sources. *Tissue Eng. Part A.* **18**, 1542–51 (2012).

7. K. W. Dunn, M. M. Kamocka, J. H. McDonald, A practical guide to evaluating colocalization in biological microscopy. *AJP Cell Physiol.* **300**, C723–C742 (2011).

8. A. E. Carpenter *et al.*, CellProfiler: image analysis software for identifying and quantifying cell phenotypes. *Genome Biol.* **7**, R100 (2006).

Appendix E: RNA extraction from agarose diffusion chamber constructs for gene expression analysis

E.1 Introduction

Although agarose is a commonly-used hydrogel for cartilage and intervertebral disc tissue engineering experiments, qPCR analysis is a challenge because agarose matrix interferes with quantity and quality of extracted RNA (*1*). In this experiment, we adapted existing RNA extraction protocols to harvest RNA from diffusion chambers made of agarose. We also compared gene expression in different regions of the diffusion chamber using qPCR to determine whether nutrient availability affects gene expression.

E.2 Methods

RNA extraction materials

- Qiagen Buffer QG
- Qiagen RNeasy Mini kit
- Qiagen RNase-free DNase set
- RNA-grade isopropanol

Reagents to prepare

- **RPE buffer**: ensure that ethanol has been added
- **DNase**: resuspend lyophilized DNase with 550 µl RNase-free ddH_2O
- **DNase solution**: for each sample, add 10 µl DNase to 70 µl buffer RDD (included with DNase kit)

RNA Extraction Protocol (adapted from (*2*) and from the RNeasy mini kit protocol)

1. Gently separate the top slide from the diffusion chamber, and wash the agarose gel with PBS.

2. Divide the gel into portions using a sterile scalpel or razorblade and load into Eppendorf tubes (see Figure E.1).

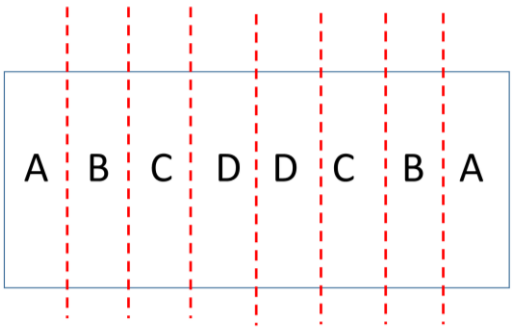

Figure E.1 Diffusion chamber harvesting diagram. We divided each agarose diffusion chamber into sections and pooled groups of two sections that had the same distance from the edge (and therefore similar nutrient constraints.)

3. Incubate at 42°C for 10 min in 750 µl QG buffer. Vortex at least twice during the incubation.
4. Add 125 µl of RNAse-free isopropanol, vortex.
5. Transfer the sample to a pink RNeasy column (in two batches if centrifuging, or the whole sample if using the vacuum manifold) and centrifuge for 15s at RT and 8000 x g. Discard the flow-through.
    - If your volume exceeds 700 µl, apply 700 µl of the sample to the column, spin, discard flow-through, and add the remainder of the sample through the same column for an additional spin and binding step.
6. Add 500 µl of buffer QG, centrifuge at 8000 x g for 15s, and discard flow-through.
7. Move to a new collection tube.
8. Add 350 µl Buffer RW1 to column and spin 15 sec ≥10,000 rpm (8000 x g). Discard flow-through.

9. Add 80 µl DNase solution directly to column, ensuring that no solution sticks to the column walls. Incubate at room temp for 15 min.
10. Add 350 µl Buffer RW1 to column and spin 15 sec ≥10,000 rpm (8000 x g). Discard flow-through.
11. Add 500 µl Buffer RPE to column and spin 15 sec ≥10,000 rpm (8000 x g). Discard flow-through.
12. Add 500 µl Buffer RPE to column and spin 2 min ≥10,000 rpm (8000 x g).
13. Spin 1 min full speed to remove excess liquid from column.
14. Transfer column to 1.5 ml collection tube with cap and add 30 µl RNase-free ddH_2O directly to column. Incubate 1 min at room temperature for ddH_2O to absorb and spin 1 min ≥10,000 rpm (8000 x g) to elute RNA.
    - Save the column in case RNA yield is poor – you can try to elute additional RNA off the column using the initial eluate.
15. RNA is ready to use. Store at -80C and avoid multiple freeze-thaws. Take care to protect RNA from RNase degradation by using clean tips and technique.

After RNA extraction, the RNA was measured on an ND-1000 Nanodrop spectrophotometer and converted to cDNA using iScript reverse transcriptase (BioRad). Gene expression was measured using quantitative reverse transcription PCR with SYBR green master mix (BioRad) using the BioRad CFX96 RealTime Thermal Cycler (see Chapter 2 for primer sequences and qPCR analysis details.) 18s was used as the housekeeping gene, and only 1 replicate was used per sample for this pilot study.

E.3 Results and Future Work

RNA quality and quantity:

When performing RNA extractions with this protocol, we measured concentrations in the range of 0.49 – 32.54 ng/µl. These were generally lower than the recommended concentration for sufficient cDNA synthesis. RNA quality was also poor: 260/280 ratios varied from 1.41 - 2.58 and were generally within the recommended range (> 1.8), but 260/230 ratios ranged from 0.04 – 2.45 and were usually much less than the recommended range (1.8 – 2.2).

The low RNA quantity and quality could be attributable to low cell numbers. We used small sections of agarose for the RNA extraction, which only contained approximately 60,000 cells each. Pilot RNA extractions from 60,000 cells in the absence of agarose also resulted in low RNA concentrations and low 260/230 ratios. However, agarose interference and high cell death (especially in center sections of the chamber) could also negatively impact RNA quality and quantity. Snap-freezing and storing samples at -80°C prior to extraction did not appear to affect RNA quality or quantity.

In the future, using larger gel pieces, for example by dividing the chamber into 6 pieces instead of 8, may improve quality slightly, although we did not see large improvements in pilot tests. RNA extraction kits that are specially designed for small samples may also help, as well as plant RNA extraction kits that reduce interference from polysaccharides (*1*).

Gene expression analysis:

Although RNA quality and quality were low, we standardized concentrations as much as possible before performing reverse transcription and qPCR. qPCR results are shown in Figure E.2. We found that Ct values for all genes, including the housekeeping gene, were higher than recommended, most likely due to low RNA quality and quantity. Also, although 18s mRNA was detected in the center of chambers, which consisted of mostly dead cells, gene expression of aggrecan, HIF-1α, and SLC2A1 was usually undetectable. Due to unreliable RNA quality and

high Ct values, we were unable to draw conclusions about gene expression trends in different cell types and diffusion chamber locations. However, improved RNA quality might lead to more definitive qPCR results. In addition, methods such as fluorescence in situ hybridization (FISH) could provide detailed spatial information about gene expression while requiring much fewer cells for detection.

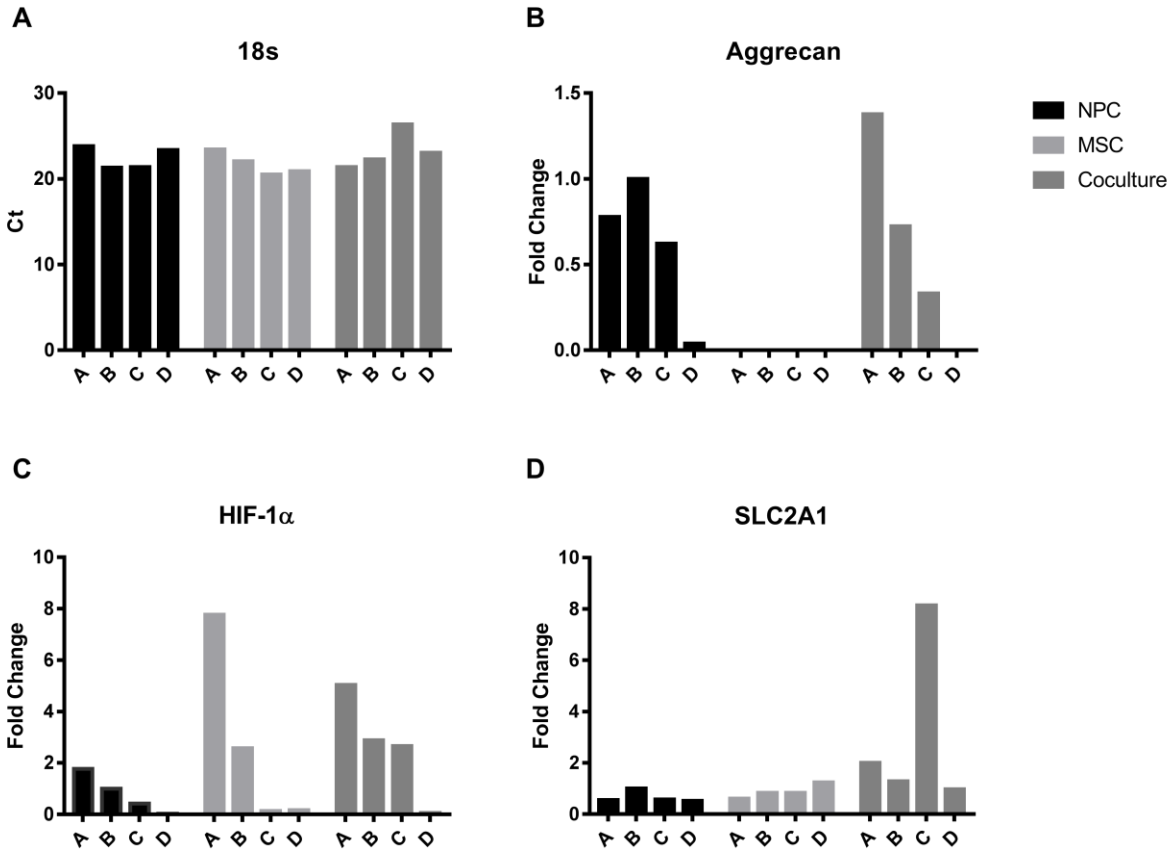

Figure E.2 qPCR results for NPC, MSC, and coculture diffusion chambers divided into regions. Regions are shown in Figure E.1. Panel A shows Ct values from 18s, the housekeeping gene, while panels B, C, and D show fold change results from various tested genes.

E.3 References

1. T. Ogura, A. Tsuchiya, T. Minas, S. Mizuno, Methods of high integrity RNA extraction from cell/agarose construct. *BMC Res. Notes*. **8**, 644 (2015).
2. D. A. Lee, J. Brand, D. Salter, O.-O. Akanji, T. T. Chowdhury, Quantification of mRNA using real-time PCR and Western blot analysis of MAPK events in chondrocyte/agarose constructs. *Methods Mol. Biol.* **695**, 77–97 (2011).

Publishing Agreement

It is the policy of the University to encourage the distribution of all theses, dissertations, and manuscripts. Copies of all UCSF theses, dissertations, and manuscripts will be routed to the library via the Graduate Division. The library will make all theses, dissertations, and manuscripts accessible to the public and will preserve these to the best of their abilities, in perpetuity.

Please sign the following statement:

I hereby grant permission to the Graduate Division of the University of California, San Francisco to release copies of my thesis, dissertation, or manuscript to the Campus Library to provide access and preservation, in whole or in part, in perpetuity.

Author Signature

6-14-17
Date